The Holographic Principle in a Cosmological Setting

The Holographic Principle in a Cosmological Setting

Het Holografische Principe in een Kosmologische Context

(met een samenvatting in het Nederlands)

PROEFSCHRIFT

ter verkrijging van de graad van doctor aan de Universiteit Utrecht op gezag van de Rector Magnificus, Prof. dr. W. H. Gispen, ingevolge het besluit van het College voor Promoties in het openbaar te verdedigen op donderdag 3 april 2003 des middags te 12.45 uur

door

Ivo Lothar Savonije

geboren op 6 april 1975, te Haarlem

PROMOTOR: Prof. dr. E. P. Verlinde

Department of Physics
Princeton University
oud-hoogleraar aan de Universiteit Utrecht

BEOORDELINGSCOMMISSIE: Prof. dr. G. 't Hooft
Prof. dr. R. H. Dijkgraaf
Prof. dr. B. Q. P. J. de Wit
Prof. dr. E. A. Bergshoeff
Prof. dr. J. de Boer

Typeset in Times using LaTeX 2_ε
ISBN 90-393-3320-3

Het in dit proefschrift beschreven onderzoek werd mede mogelijk gemaakt met financiële steun van de Nederlandse Organisatie voor Wetenschappelijk Onderzoek (NWO).

Voor Anneroos

CONTENTS

1

INTRODUCTION

String theory originated in the 1960's as a model for strong interactions. Only after it was replaced by a much more successful theory in this respect, by the name of quantum chromodynamics (QCD), was it reinvented as a theory of quantum gravity. Up to that time, twentieth century physics had borne two extremely successful theories. These are quantum mechanics, which describes physics at the very small scale, and Einstein's theory of general relativity, a theory of gravity providing a description of physics at the largest of scales.

Quantum mechanics or, more precisely, quantum field theory provides a unified description of all but one of the forces known in nature. In the form of the Standard Model it brings together the electromagnetic force with the strong and weak nuclear forces. Moreover, this framework also includes all known elementary particles. The force missing is the gravitational force. The Standard Model is exceptionally successful at describing physics at the energy scales nowadays accessible in particle accelerators. In fact, there exists no experimental data in violation thereof. Nonetheless, the Standard Model will not be the final theory of particle interactions. Besides the absence of interaction with gravity, it exhibits a certain degree of arbitrariness, or at least inelegance, due to the large number of free parameters. This has led to many attempts at formulating a more fundamental theory.

General relativity is the theory of space, time and gravity. It has drastically changed our thinking about each of these concepts. On large scales, where gravity dominates, the theory provides an accurate description of the observed physics. It predicts such remarkable things as the expansion of the universe and the bending of light. Because gravity is such a weak force, it is very difficult to test the theory on small scales. This leaves open the possibility of new gravitational physics appearing at relatively low energy scales.

The two theoretical frameworks of quantum mechanics and general relativity have almost no overlap. There is, as mentioned above, no interaction

with gravity in the Standard Model. In laboratory particle experiments this is not so much of a problem, since gravity is too weak to play a significant role. There are, however, situations in which the gravitational interaction becomes of comparable strength to the particle interactions described by the Standard Model. These include black holes, or spacetime singularities in general, as well as the early universe. For a complete description of these situations, it is then necessary to construct a quantized theory of gravity, combining quantum mechanics with general relativity. However, general relativity is – in the language of quantum field theory – a non renormalizable theory. This means that it becomes useless when covariantly quantized because irremovable infinities appear at high energies, indicating that new physics is likely to play a role there. Hence arises the need for a full-fledged theory of quantum gravity. This new theory must replicate the predictions of quantum mechanics and general relativity in their respective regimes, but in the extreme situations where the two meet it must deviate and provide a natural connection between them. This is where string theory enters the arena.

String theory offers a radical new point of view. The fundamental constituents of the theory are one-dimensional objects rather than point particles. When being considered as a theory of the strong interactions, these so called strings arose as flux tubes between quarks. One of the problems it had as a theory of hadrons was the appearance of a massless spin-2 particle in the string spectrum. After being replaced by QCD, this massless spin-2 particle was reinterpreted as the graviton: the quantum of gravity. In this way, string theory naturally provides a theory of quantum gravity. It also encompasses the Standard Model, reproducing all known particle interactions found in nature. Moreover, it does so in a strongly unified way since all interactions are different manifestations of the same object. The mediators of the forces as well as all elementary particles are simply different vibrational modes of the fundamental string.

String theory contains both open strings, with the topology of a line, and closed strings, which are loops. While matter fields and their Standard Model interactions are described by open strings, closed strings describe the gravitational interactions. The closed string spectrum consists of an infinite tower of states, starting from the massless graviton and ever increasing in mass from there. It is the addition of these massive string modes that softens the divergences encountered at high energies in the covariant quantization of general relativity. String theory in this way provides a consistent perturbative description of the gravitational interaction.

The development of string theory as a theory of quantum gravity is characterized by two important developments known as string revolutions. The first revolution came in the 1980's when spacetime supersymmetry was brought into the theory. Supersymmetry relates bosonic and fermionic degrees of freedom.

Until that time, only the bosonic string had been considered. This theory was troubled by the appearance of a tachyonic state in the string spectrum and by the fact that it could only be formulated consistently in twenty-six spacetime dimensions. The introduction of supersymmetry not only allowed the description to be extended to fermions, it simultaneously rid the theory of the tachyon in a natural way. These superstrings live in ten spacetime dimensions, which is, alas, not as bad as twenty-six. Supersymmetry has not yet been observed in nature. It is, however, most relevant to high energy phenomena and one can imagine that while it is broken at currently accessible energies, it gets restored at higher energies. The questions that remain are how exactly it gets broken and at which energy.

As for the dimensionality of spacetime, it is an everyday fact that we only experience three spatial and one time dimension. There are several proposals as to what happens with the six extra spatial dimensions required for a consistent formulation of superstring theory. The oldest and most generally accepted resolution is that the extra dimensions are compactified on circles with such small radii as to be undetectable in current high energy experiments. More recently, a competing idea has been put forward. It utilizes the difference in energy scales up to which the Standard Model and the gravitational interactions have been experimentally checked. The proposal states that the Standard Model fields are confined to a $3+1$-dimensional hypersurface in ten dimensional spacetime. The gravitational interaction, on the other hand, is free to probe all spacetime dimensions, as it should since it describes the dynamics of spacetime itself. These extra dimensions then only need to be curled up so much as to be consistent with high energy checks of gravity, which as mentioned are much less restrictive then those of the Standard Model. These models, called brane worlds, can naturally be embedded into string theory. The hypersurface is then represented as a D-brane, which is a topological defect to which the endpoints of open strings are confined. Gravity, being represented by closed strings, is not confined to the brane. The interaction of the Standard Model fields on the brane with gravity is described by closed strings breaking open and turning into open strings on the brane. The qualification as a topological defect derives from this process in which the topology of the string changes.

In the years ensuing the first string revolution, several superstring theories were discovered. In total there appeared to be five different theories, which were all defined perturbatively. These are the type IIA, type IIB, type I and two heterotic theories. This situation was unsatisfactory as it caused a certain ambiguity. With five different theories, which is the one that describes nature? During the 1990's relations between these different theories were discovered. These relations are known as dualities and they showed that in fact all five theories are different manifestations of one underlying theory. This important step in the development of superstring theory is referred to as the second string

revolution. Lacking a fundamental coupling constant, the underlying theory is intrinsically non-perturbative. Because of this the theory, known as M-theory, is notoriously difficult to describe. The five superstring theories correspond to perturbative vacua of M-theory.

Through these and more recent developments, such as the discovery by Polchinski [100] of the relevance of D-branes in a non perturbative description of the theory, string theory has evolved into a more mature theory. It is fair to say that string theory is the leading candidate for a theory of quantum gravity. That is not to say that it is the only candidate. Certainly, based on the way string theory was unveiled as a theory of quantum gravity, there is no reason to believe that there would be no other theories waiting to be discovered. The only way of determining the full merit of string theory is then by testing it. While it has already withstood many tests, with many more awaiting, these are without exception of a theoretical nature; largely confirming only the theory's internal – mathematical – consistency. The ultimate test of any theory that strives to describe nature, is to withstand experimentation. The extreme smallness of the corrections predicted by string theory to the theories it replaces makes this very difficult. The natural energy scale of the theory, the Planck scale at which stringy effects become relevant, is many orders of magnitude larger than those attained in modern particle accelerators. To directly test whether the fundamental building blocks of nature look like tiny rubber bands will therefore not be possible any time soon. That said, there is one laboratory where the required energies are realized: the universe itself.

This brings us to the subject of cosmology. Cosmology studies the evolution of the universe, from the putative beginning in a big bang to the vast universe we observe today and onward into the future. Although cosmology has been phenomenally successful in some respects, it fails to answer fundamental questions regarding, *e.g.*, the nature of the initial singularity and the origin of inflation. The formulation of an underlying theory is necessary to approach these basic questions and it seems natural to consider string theory in this respect. This line of research has not proven very successful. String theory, as currently formulated, is not background independent. Each background thus requires its own consistent formulation of the theory and, so far, these have not been found for realistic cosmological backgrounds. Conversely, due to the high energies involved, some of these questions provide the best available testing ground for string theory. The rather limited interaction between the two subjects is therefore surprising. One observation that has recently sparked a change in this is that the current cosmological constant may be nonzero and positive. From a cosmological point of view, this means that the universe is entering a de Sitter phase. On the other hand, it has so far proven impossible to find a de Sitter solution to string theory. This forms an important challenge for string theory and perhaps comes closest to a comparison with nature in any test

so far, although it must be noted that the observation of a positive cosmological constant is still tentative. The issue of finding a de Sitter string solution plays a major role in the second half of this thesis.

The single most important formula around which this thesis revolves is the Bekenstein-Hawking area law

$$S = \frac{A}{4G_{\mathrm{N}}} .$$

This formula expresses the entropy hidden by an event horizon in terms of the area of that horizon in Planck units. The most amazing feature of this formula is its universality. Not only does it apply to black hole and cosmological horizons alike, but also to the black strings and branes found in string theory. From the Bekenstein-Hawking formula derives a fundamental entropy bound. The maximal entropy contained in a certain volume is given by the area of that volume in Planck units. This is known as the holographic principle, originally proposed by 't Hooft [131]. It implies a radical departure from the intuitive notion that the entropy would be proportional to the volume. Moreover, the holographic principle introduces a degree of non locality into any theory of quantum gravity. That it is expected to be a generic feature of any theory of quantum gravity is based on the fact that it derives directly from black hole formation, which limits the amount of mass a region of spacetime can support. It remains to be seen, however, whether this will appear as an effective property or as a manifest underlying principle.

As for string theory, it is not yet clear whether the holographic principle is manifest. In the perturbative picture of string theory we have today, it is only partly realized. As shown by Susskind [125], the perturbative expansion breaks down before the entropy bound of one bit per Planck area is violated. However, one would expect it to be completely explicit only in a fully non perturbative formulation of the theory. Recently, such formulations have become available in certain special cases. Most notably, Maldacena [90] has proposed the AdS/CFT correspondence, relating full, non perturbative string theory on anti-de Sitter backgrounds to conformal field theories living on the boundary of the AdS space. The number of degrees of freedom in this context manifestly obeys the holographic principle, as we will review in this thesis.

Studying the holographic principle in string theory may guide us towards answering important open questions. It has, for example, not been possible so far to find a string description of most realistic black holes and singularities of general relativity. More generally, while string theory is relatively well understood at small coupling, our knowledge of the strongly coupled regime is much more limited. The holographic principle may prove to be a valuable guide in that respect as it becomes more stringent in regions of spacetime that are highly dynamical and strongly gravitating.

The approach that will be taken in this thesis is to consider the compatibility of the holographic principle with cosmological models. This approach may help in the construction of realistic cosmological models within string theory. Since cosmology lacks a fundamental underlying theory, the solutions it offers may seem rather ad hoc. Inflation, for example, clearly offers a solution to the horizon and flatness problems, but different solutions to the same problems are certainly imaginable. How then must we choose between different cosmological models? Assuming that the holographic principle turns out to be of a fundamental nature, one would expect it to be a manifest feature of a cosmological model. This provides a possible way of determining the feasibility of specific cosmological models. Lacking a fundamental theory, one cannot look for an explicit manifestation of the holographic principle as a fundamental principle. Instead, one can consider whether a certain model obeys the entropy bounds that derive from it. These entropy bounds have culminated in a covariant entropy bound as formulated by Bousso [23,24]. This proposal has been tested to be consistent with many situations that are expected to occur in the universe, such as gravitational collapse and inflation.

This thesis is organised as follows. In Chapter 2, a general overview of the concept of holography is given. Its origin in black hole physics is reviewed as well as its most concrete realization in the form of the celebrated AdS/CFT correspondence. In between, several entropy bounds that derive from it are considered.

Chapter 3, largely based on [112], applies those entropy bounds to cosmological models. A striking relation between entropy and energy formulas on the one hand and the equations that govern the cosmological evolution of a radiation dominated FRW universe is reviewed. Subsequently, this is applied to a specific brane world model from which it derives a natural explanation.

In Chapter 4, we return to the subject of holography but now in the specific context of a spacetime with positive curvature, or de Sitter space. Although much less well established than the AdS/CFT correspondence, we review the recent proposal of an analogous dS/CFT correspondence.

Finally, Chapter 5, based on [96,111], provides a new point of view towards quantum gravity in de Sitter space. The problems that plague a formulation thereof are reconsidered within the proposed model.

For a thorough introduction to superstring theory, the reader is referred to the standard textbooks [55,101].

2

HOLOGRAPHY

At first sight, quantum field theories and gravity seem to have little to do with each other. Indeed, it has proven impossible to quantize gravity following the usual perturbative techniques of field theory. On the other hand, string theory naturally provides a quantum theory of gravity. It turns out that these different kinds of theories are intimately related.

In the nineteen seventies, 't Hooft [128] showed that in the limit of large gauge group the diagrammatic expansion of gauge theories looks like that of a free string theory. Although a description in terms of a worldsheet action was not found, this provides a direct connection between gauge theories and string theories. More recently, it was realized that the strings arising from certain conformal gauge theories are exactly the type IIB strings, moving on a curved background which has a boundary at spatial infinity. In a different approach, it was conjectured by 't Hooft [131] and Susskind [125] that any theory of quantum gravity should be dual to a quantum field theory living on the boundary of spacetime. This is called the holographic principle.

A major step forward came in 1995 with the discovery of D-branes by Polchinski [100]. Dp-branes are $p+1$-dimensional hypersurfaces on which open strings can end. The low energy theory of open strings ending on a Dp-brane is U(1) gauge theory in $p+1$ dimensions. If one puts N Dp-branes on top of each other, this generalizes to U(N) gauge theory. On the other hand, by worldsheet duality, the Dp-brane also acts as a source for closed strings, which contain gravitons in their massless spectrum. This dual nature of the D-branes is depicted in Figure 2.6 on page 22.

All of this finally led Maldacena [90] in 1997 to conjecture the celebrated AdS/CFT correspondence, providing an explicit example of a gravity theory on a curved background and its dual field theory. These are type IIB string theory on Anti-de Sitter (AdS) space times a sphere and $\mathcal{N}=4$ SU(N) super Yang-Mills (SYM) theory. This last theory is a conformal field theory (CFT) which lives on the boundary of the AdS space.

We begin in Section 2.1 by discussing the holographic principle and the entropy bounds that can be inferred from it. In Section 2.2 we consider an explicit realization of the holographic principle: the AdS/CFT correspondence. This correspondence is then used to derive a holographic entropy formula for the dual CFT.

2.1 THE HOLOGRAPHIC PRINCIPLE

In a quantum theory of gravity there exists a natural upper limit on the amount of energy that a region of space can contain. Consider, for simplicity, a spherical region. The maximal energy content is then given by the mass of a black hole that fills the region. The important point is that the mass of a black hole in four dimensions is proportional to its horizon radius,

$$M_{\rm BH} = \frac{r_{\rm H}}{2}\,, \tag{2.1}$$

and not to its volume. Since the ratio volume over radius, $V/r \propto r^2$, grows rapidly with r, the bound becomes more stringent as one considers larger volumes. This bound on the mass translates to a bound on the number of degrees of freedom that a region can support. Based on this, 't Hooft [131] and Susskind [125] proposed the holographic principle, which asserts that the number of accessible degrees of freedom in a specified region of space is proportional to the area of its boundary measured in Plank units. This is a radical step away from local field theory, which has degrees of freedom at every scale. Indeed, even when a finite number of degrees of freedom per unit volume is obtained by imposing infra-red (IR) and ultra-violet (UV) cutoffs, the total number is proportional to the volume. This discrepancy lies at the heart of the problems in unifying quantum field theory and gravity.

From the holographic principle, bounds on the entropy in a specified region can be derived. We will discuss these 'holographic entropy bounds' in the remainder of this section. For an extensive review of the holographic principle and the resulting entropy bounds see [21,27].

2.1.1 BLACK HOLE THERMODYNAMICS

Consider the Schwarzschild black hole solution in $D = n+1$ dimensions. The metric takes the form

$$ds^2 = -\left(1 - \frac{\omega_n M}{r^{n-2}}\right) dt^2 + \left(1 - \frac{\omega_n M}{r^{n-2}}\right)^{-1} dr^2 + r^2 d\Omega_{n-1}^2\,, \tag{2.2}$$

where

$$\omega_n \equiv \frac{16\pi G_{\rm N}}{(n-1)\mathrm{Vol}(S^{n-1})}\,, \tag{2.3}$$

$G_{\rm N}$ is the D-dimensional Newton constant, M denotes the mass of the black hole and $d\Omega_{n-1}$ is shorthand for the metric on the n–1-dimensional unit sphere. Focusing on the case $D = 4$ and setting $G_{\rm N} = 1$, the metric reduces to

$$ds^2 = -V(r)\,dt^2 + V(r)^{-1}dr^2 + r^2 d\Omega_2^2\,, \tag{2.4}$$

where

$$V(r) = 1 - \frac{2M}{r}\,. \tag{2.5}$$

The black hole horizon is at $r_{\rm H} = 2M$ and the area of the horizon is

$$A_{\rm H} = 16\pi M^2\,. \tag{2.6}$$

Hawking's area theorem [64] states that the area of a black hole event horizon never decreases with time: $dA_{\rm H} \geqslant 0$. For example, if something drops into a black hole this increases its mass and consequently its horizon area increases as well. The area theorem bears resemblance to the second law of thermodynamics, which states that entropy never decreases with time: $dS \geqslant 0$. However superficial the similarity between the two laws may seem, it turns out to be of a fundamental nature.

There is also the 'no hair theorem' [32,76], which states that a black hole is completely characterized by three quantities: its mass, charge and angular momentum. Since this allows for only a single quantum state, it implies that black holes have zero entropy. Throwing an entropy carrying thermodynamical system into a black hole would then cause entropy to be lost; in violation of the second law of thermodynamics.

As a resolution, Bekenstein [15–17] suggested to associate an entropy to a black hole proportional to its horizon area,

$$S_{\rm BH} = \eta A\,, \tag{2.7}$$

where η is the constant of proportionality. Bekenstein then generalized the second law of thermodynamics to include black hole entropy,

$$dS_{\rm matter} + dS_{\rm BH} \geqslant 0\,. \tag{2.8}$$

Any loss of matter entropy from objects falling into a black hole is compensated for by an increase of the black hole entropy. If the Bekenstein entropy of a black hole is to be interpreted as a thermodynamical entropy, the first law of thermodynamics,

$$dM = T\,dS\,, \tag{2.9}$$

implies that black holes must have a temperature. Classically this is not possible, since a black hole cannot radiate by definition. Hawking [65] showed that black holes do in fact radiate through a quantum process and found that they emit a black body spectrum at a temperature which is a function of the black hole mass. This result establishes the analogy between the laws of thermodynamics and those of black hole dynamics as a true physical principle. It gives an indication that a statistical system perhaps underlies the theory of gravitation.

To calculate the Hawking temperature for a 4-dimensional Schwarzschild black hole, consider the Euclidean version of the metric (2.4),

$$ds_{\text{E}}^2 = V(r)\,d\tau^2 + V(r)^{-1}dr^2 + r^2 d\Omega_2^2\,, \tag{2.10}$$

$$V(r) = 1 - \frac{2M}{r}\,. \tag{2.11}$$

Demanding that the metric be non singular at the horizon gives a periodicity condition for the Euclidean time coordinate τ. The Hawking temperature is then given by the inverse period. In terms of a coordinate $r_\star$ given by

$$r_\star = r + r_{\text{H}} \ln(r - r_{\text{H}})\,, \tag{2.12}$$

the metric becomes

$$ds^2 = V(r)(d\tau^2 + dr_\star^2) + r^2 d\Omega_2^2\,. \tag{2.13}$$

Introduce coordinates $u_\pm$ defined by

$$u_\pm = e^{\frac{2\pi}{\beta}(r_\star \pm i\tau)}\,, \tag{2.14}$$

where β is the periodicity of τ. In terms of these coordinates, the metric takes the form

$$ds^2 = \frac{\beta^2}{4\pi^2} V(r)\, e^{-\frac{4\pi r_\star}{\beta}} du_+ du_-\,. \tag{2.15}$$

Expanding $V(r)$ around $r = r_{\text{H}}$,

$$V(r) \approx (r - r_{\text{H}}) \cdot V'(r_{\text{H}}) \qquad (r \approx r_{\text{H}})\,, \tag{2.16}$$

we see that the metric is regular around $r = r_{\text{H}}$ if

$$e^{\frac{4\pi r_\star}{\beta}} \propto (r - r_{\text{H}})\,, \tag{2.17}$$

or, equivalently, if

$$r_\star \propto \frac{\beta}{4\pi} \ln(r - r_{\text{H}})\,. \tag{2.18}$$

Comparing with (2.12), we see that this requires

$$\beta = 4\pi r_{\text{H}} = 8\pi M \,. \tag{2.19}$$

We conclude that the Hawking temperature equals

$$T_{\text{H}} = \frac{1}{8\pi M} \,. \tag{2.20}$$

By the first law of thermodynamics, this fixes the proportionality constant η in the Bekenstein entropy (2.7). The so called Bekenstein-Hawking entropy of a Schwarzschild black hole in four dimensions is given in Planck units by

$$S_{\text{BH}} = \frac{A}{4} \,. \tag{2.21}$$

Reinstating all dimensionfull parameters, this formula takes the form

$$S_{\text{BH}} = \frac{k_{\text{B}} A_{\text{H}} c^3}{4 G_{\text{N}} \hbar} \,, \tag{2.22}$$

where k_{B} is the Boltzmann constant, c denotes the speed of light and $\hbar$ is the Planck constant.

The laws of black hole thermodynamics are by now well established and it is expected that a quantum theory of gravity will associate $N = e^{A/4}$ microstates with a black hole, as suggested by (2.21). In fact, for a special class of black holes, string theory has succeeded in doing just that [38,92,123]. We will see in Chapter 4 that the Bekenstein-Hawking formula (2.21) applies just as well to the cosmological horizon that is present in the context of de Sitter space. This is exemplary of the universality of this formula, as advocated in the Introduction.

2.1.2 Entropy bounds from black holes

For a system that includes gravity, an entropy bound can be deduced from the Bekenstein-Hawking formula (2.21) together with the generalized second law (2.8). Consider a spherical region of space V. The area of the boundary of V equals A. Start with a thermodynamical system $\mathcal{Q}$, with entropy S, that is completely contained within V. The total energy of the system $\mathcal{Q}$ cannot exceed that of a black hole of area A, since it would then not fit within V.

By collapsing a spherical shell of matter with precisely the right energy onto the system $\mathcal{Q}$, this system can be converted into a black hole that fills the volume V. This process of converting the system into a black hole is called the Susskind process [125]. The entropy of the resulting system is simply that

of a black hole with horizon area A, as given by (2.21). From the generalized second law it follows that the entropy of the original system is bounded by this entropy,

$$S \leqslant S_{\rm BH}\,. \tag{2.23}$$

This is called the spherical entropy bound, and it is an example of a holographic entropy bound. The most stringent form of this bound is obtained by choosing V to be the smallest spherical volume that contains the system $\mathcal{Q}$.

Because of the limited validity of the spherical entropy bound, *e.g.*, it only applies to spherical regions, one would like to try and generalize it. The most natural extension is simply to drop the assumptions under which it is derived. The resulting entropy bound, called the spacelike entropy bound, states that the entropy within any spatial region cannot exceed the area of that region's boundary,

$$S(V) \leqslant \frac{A(V)}{4}\,. \tag{2.24}$$

Besides the fact that many counterexamples to this bound have been found, a crucial difficulty with any entropy bound on a spacelike volume is that the concept of a region and its boundary is not covariant. This makes it impossible to say exactly what the region is on which the entropy is bounded by a given boundary surface. Since a natural covariant notion is that of a lightlike volume, one might try to formulate holographic entropy bounds on such volumes [125]. This leads to covariant 'lightlike entropy bounds'. Before discussing lightlike bounds, in the next section we first discuss an interesting relation between the Einstein equation and the first law of thermodynamics. The derivation of this relation by Jacobson [77] involves an early formulation of the idea to implement the holographic principle via entropy flow through light-sheets.

2.1.3 Thermodynamics and the Einstein equation

The laws of black hole mechanics can be derived from the classical Einstein equation [14]. The discovery of Hawking radiation established the link between these laws and those of thermodynamics. How then did classical general relativity know that horizon area is a sort of entropy?

Jacobson [77] answers this question by deriving the Einstein equation from the proportionality of entropy and horizon area together with the fundamental relation

$$\delta Q = T\,dS \tag{2.25}$$

connecting heat, entropy and temperature. To illustrate the idea, consider a thermodynamical system. Assume that the entropy $S(E, V)$ of the system is given as a function of energy and volume. The first law of thermodynamics,

together with the relation (2.25), yields

$$\delta Q = dE + p\, dV\,, \tag{2.26}$$

where p is the pressure within the system. Differentiating the entropy gives

$$dS = \frac{\partial S}{\partial E}\, dE + \frac{\partial S}{\partial V}\, dV\,. \tag{2.27}$$

From combining these relations, we infer the equation of state

$$p = T\,\frac{\partial S}{\partial V}\,. \tag{2.28}$$

The approach of [77] is to start from the holographic entropy relation and then derive an equation of state *for spacetime* along these lines. This equation takes the form of the Einstein equation.

In order to apply the relation (2.25) to spacetime dynamics, we need appropriate definitions of the appearing quantities. Heat will be defined as energy that flows across a causal horizon. A causal horizon is not necessarily a black hole horizon, it can be simply the boundary of the past of any set. The entropy of the system hidden by the horizon is assumed to be proportional to that horizon's area. The final quantity that has to be identified is the temperature of the system into which the heat is flowing. Jacobson defines this to be the Unruh temperature [134] that is associated with an uniformly accelerated observer hovering just inside the horizon.

For equilibrium thermodynamics to be applicable, construct a system that is instantaneously stationary in the following way. Through any spacetime point p, there exists a spacelike, 2-dimensional surface element $\mathcal{P}$ whose past directed null normal congruence to one side has vanishing expansion and shear in a first order neighbourhood of p. Call the past horizon of such a $\mathcal{P}$ the 'local Rindler horizon of $\mathcal{P}$'. The part of spacetime beyond the Rindler horizon is in local equilibrium at p.

Following [77], we now demonstrate that from the relation (2.25), interpreted in terms of energy flux and area of local Rindler horizons, it follows that gravitational lensing by matter energy affects the causal structure of spacetime in just the right way so that the Einstein equation holds.

We need to make the definitions of heat and temperature more precise. In a neighbourhood of $\mathcal{P}$ spacetime is approximately flat and exhibits the usual Poincaré symmetries. In particular, there exists an approximate Killing field χ^a generating boosts orthogonal to $\mathcal{P}$ and vanishing at $\mathcal{P}$ itself. Like in the familiar Rindler case, the vacuum state is a thermal state with respect to the boost Hamiltonian at temperature

$$T = \frac{\hbar\kappa}{2\pi}\,. \tag{2.29}$$

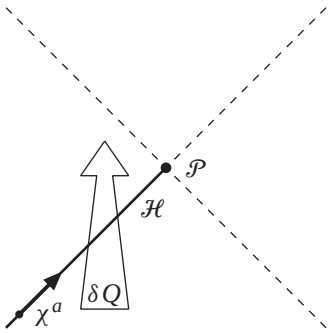

FIGURE 2.1: The heat flow δQ across the local Rindler horizon $\mathcal{H}$ of a two-surface element $\mathcal{P}$, generated by the approximate boost Killing vector χ^a. Every point represents a 2-dimensional space-like surface. Figure adapted from [77].

where κ is the acceleration of the Killing orbit on which χ^a has unit norm. Assuming that all the energy passing through the horizon is carried by matter, the local heat flow is defined by $T_{ab}\,\chi^a$, where T_{ab} is the matter energy-momentum tensor.

Referring to Figure 2.1, consider a local Rindler horizon $\mathcal{H}$ through a spacetime point p. The horizon is generated by the approximate local boost Killing field χ^a. The heat flux through the horizon is given by [77]

$$\delta Q = \int_{\mathcal{H}} T_{ab}\,\chi^a d\Sigma^b\,. \tag{2.30}$$

We can write $\chi^a = -\kappa\lambda k^a$, where k^a is the tangent vector to the horizon generators for an affine parameter λ that vanishes at $\mathcal{P}$ and is negative to the past of $\mathcal{P}$. Then also $d\Sigma^a = k^a d\lambda d\mathcal{A}$, where $d\mathcal{A}$ is the area element on a cross section of the horizon. Inserting these relations into (2.30) puts it in the form

$$\delta Q = -\kappa \int_{\mathcal{H}} \lambda T_{ab} k^a k^b d\lambda d\mathcal{A}\,. \tag{2.31}$$

As mentioned above, it is assumed that the entropy is proportional to the horizon area. The entropy variation associated with a piece of the horizon is then proportional to the variation $\delta\mathcal{A}$ of the cross sectional area of neighbouring horizon generators,

$$dS = \eta\delta\mathcal{A}\,, \tag{2.32}$$

where η is the constant of proportionality and the area variation is given by

$$\delta\mathcal{A} = \int_{\mathcal{H}} \theta d\lambda d\mathcal{A}\,. \tag{2.33}$$

Here, θ denotes the expansion of the horizon generators defined by

$$\theta \equiv \frac{1}{\mathcal{A}} \frac{d\mathcal{A}}{d\lambda} \,. \tag{2.34}$$

The relation $\delta Q = T dS$ relates the energy flux to a change in the horizon area, *i.e.*, to a focusing of the horizon generators. By definition, at $\mathcal{P}$ the local Rindler horizon has vanishing expansion. It follows that the focusing to the past of $\mathcal{P}$ must cause the expansion to vanish there. Moreover, the rate of focusing must be so that the increase of a portion of the horizon will be proportional to the energy flux across it. This translates to a condition on the curvature of spacetime in the following way.

The Raychaudhuri equation

$$\frac{d\theta}{d\lambda} = -\frac{1}{2}\theta^2 - \sigma_{ab}\sigma^{ab} + \omega_{ab}\omega^{ab} - \mathcal{R}_{ab}k^a k^b \tag{2.35}$$

relates the change in expansion along the generators parametrized by λ to the shear σ_{ab}, the twist ω_{ab} and, through the Ricci tensor $\mathcal{R}_{ab}$, the curvature of spacetime. By stationarity of the horizon, θ, σ and ω vanish at $\mathcal{P}$. When integrating (2.35) to find θ near $\mathcal{P}$, the first three terms on the right hand side can thus be neglected as they are are higher order contributions. For sufficiently small λ, this integration yields $\theta = -\lambda \mathcal{R}_{ab}k^a k^b$ and by substituting this into (2.33) one obtains

$$\delta\mathcal{A} = -\int_{\mathcal{H}} \lambda \mathcal{R}_{ab}k^a k^b d\lambda d\mathcal{A} \,. \tag{2.36}$$

From (2.31) and (2.36) we see that

$$\delta Q = T dS = \frac{\hbar\kappa}{2\pi}\eta\delta\mathcal{A} \tag{2.37}$$

can only hold if

$$T_{ab}k^a k^b = \frac{\hbar\eta}{2\pi}\mathcal{R}_{ab}k^a k^b \tag{2.38}$$

for all null vectors k^a. This condition implies that

$$\frac{2\pi}{\hbar\eta}T_{ab} = \mathcal{R}_{ab} + f g_{ab} \tag{2.39}$$

for some function f. The stress-energy tensor T_{ab} is divergence free by local conservation of energy and momentum. It follows by the contracted Bianchi identity that $f = -\mathcal{R}/2 + \Lambda$ for some constant Λ. This leads to the conclusion that the Einstein equations,

$$\mathcal{R}_{ab} - \frac{1}{2}\mathcal{R}g_{ab} + \Lambda g_{ab} = \frac{2\pi}{\hbar\eta}T_{ab} \,, \tag{2.40}$$

hold automatically [77].

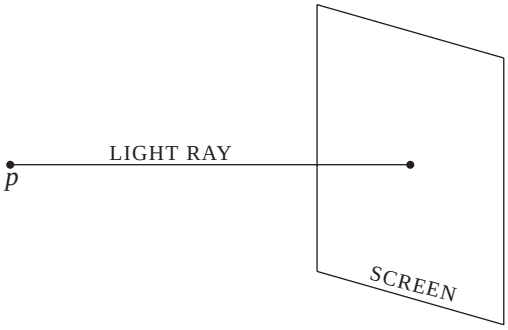

FIGURE 2.2: The spacetime point p is mapped to a holographic screen through a light ray. Figure adapted from [125].

2.1.4 COVARIANT ENTROPY BOUNDS

The most important aspect in which covariant entropy bounds differ from the spherical and spacelike bounds discussed before is that they bound the entropy not in a spatial volume but on a null hypersurface; a so called light-sheet. This formulation via light-sheets is what provides the covariance of the prescription. The most general formulation of a covariant entropy bound is given by Bousso [23,24]. Bousso provides a detailed discussion of the notion of a light-sheet, and how they can be constructed.

To illustrate the idea, we will discuss an early example of a covariant entropy bound, as constructed by Susskind [125]. Consider a 4-dimensional, asymptotically flat spacetime. Asymptotically, we can define Minkowski light cone coordinates X^+, X^-, x^i $(i = 1, 2)$, where X^+ is the light cone time coordinate. Define a light-sheet to be the set of light rays which, in the limit $X^- \to \infty$, have equal X^+. These light rays fill a 3-dimensional lightlike volume and are asymptotically parallel. The complete set of light-sheets, for all X^+ values, fills the entire spacetime (except for points inside black hole horizons).

Assign to a spacetime point p 'holographic coordinates' X^+, x^i, according to the *asymptotic* coordinate values of the light ray that passes through p. In this way, all the points along a light ray are assigned the same holographic coordinates. The value of X^- is thus projected out and for every value of the time coordinate X^+, the x^i parameterize a 2-dimensional surface called a holographic screen. In this way the $3+1$-dimensional theory is mapped onto $2+1$-dimensional screens, as depicted in Figure 2.2.

This mapping defines an entropy density $\sigma(x^i)$ on the screen. The entropy of systems that are swept out by a light-sheet is mapped to part of the screen.

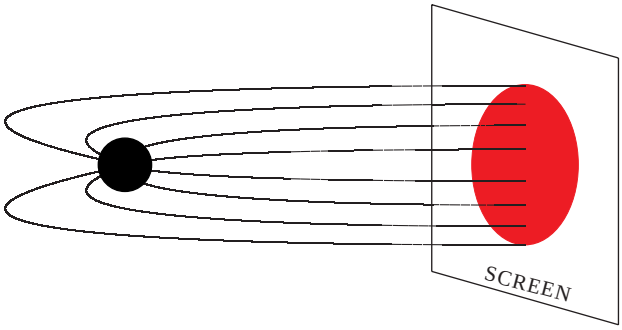

FIGURE 2.3: A black hole horizon is projected through light rays onto a holographic screen. Only lightrays in the plane of the paper are shown. Figure adapted from [125].

In the following we will show that no distribution of energy will ever lead to an entropy density on the screen that exceeds the bound [125]

$$\sigma(x^i) \leqslant \frac{1}{4}\,. \tag{2.41}$$

To start with, consider a black hole. The entropy of a black hole is given in terms of its horizon area by (2.21). We can thus assign an entropy density of $1/4$ to the black hole horizon. By the mapping defined above, the horizon is projected onto a certain area on the holographic screen, as shown in Figure 2.3. To show that the proposed bound (2.41) holds in this case, we must proof that the horizon area is smaller than its image area on the screen. This can be done by applying the Raychaudhuri equation (2.35) in the following way. For a null vector k^a, we have from the Einstein equations that

$$\mathcal{R}_{ab}k^a k^b = 8\pi T_{ab}k^a k^b \qquad (g_{ab}k^a k^b = 0)\,. \tag{2.42}$$

The Raychaudhuri equation (2.35) for the expansion θ of the cross sectional area of neighbouring light rays can then be written as

$$\frac{d\theta}{d\lambda} = -\frac{1}{2}\theta^2 - \sigma_{ab}\sigma^{ab} + \omega_{ab}\omega^{ab} - 8\pi T_{ab}k^a k^b\,, \tag{2.43}$$

where λ is an affine parameter along the light rays. For a surface-orthogonal family of light rays, such as a light-sheet, the twist ω vanishes. Moreover, by the null energy condition, the final term is non positive [67]. We thus see that the right hand side of (2.43) is manifestly non positive. It follows that the expansion θ never increases along the light rays that constitute a light-sheet,

$$\frac{d\theta}{d\lambda} \leqslant 0\,. \tag{2.44}$$

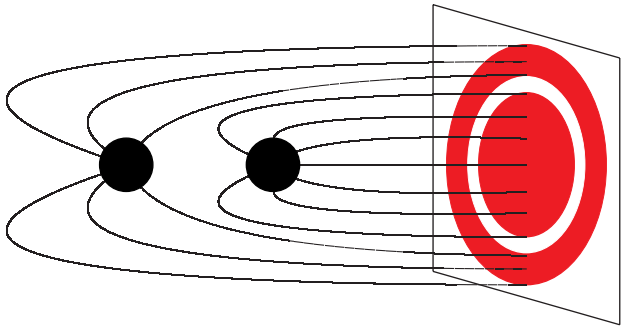

FIGURE 2.4: Projection of a two black hole configuration onto a holographic screen. Figure adapted from [125].

The physical content of this focusing theorem is to say that light is always focused by matter, never diverged.

Since asymptotically, in the flat region, the light rays are parallel, the expansion approaches zero there,

$$\theta \sim 0 \qquad (\lambda \to \infty)\,. \tag{2.45}$$

Hence, θ must be positive along the light rays that map the horizon onto the screen. This implies that the area on the holographic screen to which the horizon is mapped, is larger than the horizon area. The bound (2.41) on the entropy density follows.

One can try to increase the entropy density on the screen by adding matter to the light-sheet between the black hole and the screen. For example, we can add another black hole. However, as depicted in Figure 2.4, the bending of light by matter, together with the focusing theorem (2.44), ensures that the entropy density on the screen does not exceed the bound. These considerations lead to the conjecture [125] that for any entropy carrying system, when mapped to the screen, the entropy density obeys the bound (2.41). This conjecture was generalized by Fischler and Susskind [45] to include more general spacetimes. We will consider this generalization in detail when we discuss cosmological entropy bounds in Section 3.2.

2.2 AdS/CFT

If the holographic principle turns out to be of a fundamental nature, one would expect it to be manifest in a quantum theory of gravity. It is not yet clear

whether this is true for string theory, but backgrounds that provide explicit realizations of holography have recently been found. In this section we consider the most prominent example to date: the AdS/CFT correspondence. The conjecture is that type IIB string theory on backgrounds of the form $\mathrm{AdS}_n \times X^{10-n}$ (where X is a compact manifold) is dual to a superconformal field theory that lives on the boundary of the Anti-de Sitter space. We will focus our attention on the case $\mathrm{AdS}_5 \times S^5$, where the dual field theory is $\mathcal{N} = 4$ SU(N) super Yang-Mills.

The correspondence considered in this section is a realization of the idea that gauge theories might have a dual description in terms of a string theory. This idea originates from 't Hoofts large N limit, which we will review below. The particular relation we consider was motivated by studies of D-branes and black holes in string theory. Before presenting the exact formulation of the correspondence, we will discuss these objects in some detail. We also consider the way the correspondence implements holography. Finally, a holographic entropy formula for the dual CFT is derived in Section 2.2.8.

The correspondence was conjectured by Maldacena [90] and subsequently made precise by Gubser, Klebanov and Polyakov [61] and independently by Witten [144]. For a review, please refer to [2,82].

2.2.1 Classical geometry of AdS

For easy reference in the remainder of the text, let us begin by discussing a few geometrical aspects of Anti-de Sitter space and gathering some useful metrics. For a detailed account of the classical properties of this space please refer to [67].

AdS is the unique vacuum solution to the Einstein equations with maximal symmetry and constant negative curvature. In D spacetime dimensions, it is locally characterized by

$$\mathcal{R}_{\mu\nu} = -\frac{D-1}{L^2} g_{\mu\nu} \,, \tag{2.46}$$

where L is the radius of curvature of AdS, and by the vanishing of the Weyl tensor. The cosmological constant, Λ, is given as a function of L by

$$\Lambda = -\frac{(D-1)(D-2)}{2L^2} \,. \tag{2.47}$$

The whole space is covered by global coordinates, for which the metric becomes

$$ds^2 = L^2 \left(-\cosh^2 r \, dt^2 + dr^2 + \sinh^2 r \, d\Omega^2_{D-2} \right) \,. \tag{2.48}$$

A different coordinate system is defined by the so called Poincaré coordinates. In terms of these coordinates the metric takes the form

$$ds^2 = \frac{L^2}{r^2}dr^2 + \frac{r^2}{L^2}\eta_{\mu\nu}dx^\mu dx^\nu \,. \tag{2.49}$$

A third form of the metric that we will encounter is

$$ds^2 = L^2\frac{\eta_{\mu\nu}dx^\mu dx^\nu + dz^2}{z^2} \,, \tag{2.50}$$

where the boundary of the space is at $z = 0$.

2.2.2 'T HOOFT LARGE N LIMIT

Gauge theories in four dimensions have no dimensionless parameters which can be used as perturbation parameters. SU(N) Yang-Mills theories have, however, an extra parameter: the rank N of the gauge group. It was suggested by 't Hooft [128] that these theories might simplify at large N and have a perturbation expansion in terms of $1/N$. We need to specify how the gauge coupling $g_{\rm YM}$ scales as we take N large. Of particular interest is the limit where $\lambda \equiv g^2_{\rm YM}N$ is kept fixed while one takes $N \to \infty$. This is called the 't Hooft large N limit. The observation made by 't Hooft is that, identifying $1/N$ with the string coupling constant, the Feynman diagram expansion in this limit takes a form similar to that of perturbative closed string theory. Associated with a field theory diagram with V vertices, P propagators and L loops is a coefficient proportional to

$$g^{2(P-V)}_{\rm YM}N^L = (g^2_{\rm YM}N)^{P-V}N^\chi = \lambda^{P-V}N^\chi \,, \tag{2.51}$$

where $\chi = L - P + V$ is the Euler character of the surface corresponding to the diagram. The perturbative expansion of a diagram in the field theory can thus be written as

$$\sum_{\chi,P,V} c_{\chi,P,V}N^\chi\lambda^{P-V} = \sum_\chi N^\chi f_\chi(\lambda) \,, \tag{2.52}$$

where f_χ is some polynomial in λ. In terms of the genus g of a closed oriented surface, $\chi = 2 - 2g$. Thus, each diagram is weighted by a factor N^{2-2g}. In the large N limit, the first order diagrams in this expansion are those of lowest genus. When written in the 't Hooft double line notation, these are the diagrams with the topology of a plane, called planar diagrams, see Figure 2.5. These planar diagrams are in one-to-one correspondence with the lowest order string diagrams and similarly for higher orders. Notice that while the gauge

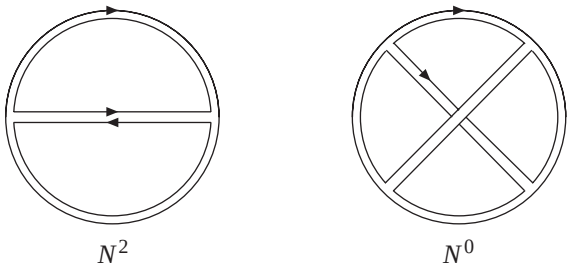

FIGURE 2.5: A planar diagram (left) and a non-planar diagram (right) with the corresponding factors in large N gauge theory.

theory may be strongly coupled, $g_{\rm YM} \gtrsim 1$, the string theory will be weakly coupled when N is large. 't Hooft first suggested the large N limit in the context of QCD, which is a very successful SU(3) gauge theory for the strong interactions. Being asymptotically free, the gauge theory is useful in describing the high energy regime. On the other hand, at low energies, where interesting phenomena like confinement occur, the theory is strongly coupled and it is difficult to extract information. Since the dual string theory will be weakly coupled (the coupling constant is $1/N$, or $1/3$ for QCD), the hope was that that theory would give a usable description of the low energy regime. However, formulation of the string theory dual to QCD in terms of a 2-dimensional worldsheet action remains an open problem.

For two dimensional gauge theories dual string theories have been constructed [57,58,95]. The case of four dimensional gauge theories is more complicated. Recently, however, there has been progress and, for a certain class of gauge theories, dual string theories have been constructed. These are large N superconformal gauge theories. QCD on the other hand is neither conformal nor supersymmetric and it is unclear how to break these symmetries.

2.2.3 D-BRANES

Dp-branes are solitonic solutions to string theory. They are defined as $p+1$-dimensional hypersurfaces on which open strings can end. String theory on a background with D-branes has two types of perturbative excitations: closed and open strings. Closed strings, propagating in the bulk, describe perturbations around the background metric, as they include a graviton mode in their massless spectrum. Open strings, which have their endpoints confined to the branes, describe excitations of the branes. The D-branes are topological defects in the sense that a closed string, when it hits a D-brane, can open up and become an open string living on the brane. Reversely, they must act as a closed

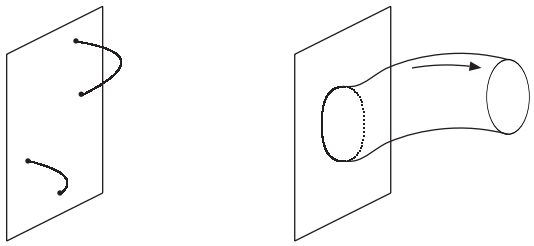

FIGURE 2.6: D-brane as open string boundary condition (left) and as closed string source (right).

string source, as depicted in Figure 2.6. Through the open strings, the D-branes realize gauge theories on their worldvolume. Indeed, the massless spectrum of open strings living on a Dp-brane is that of a maximal supersymmetric U(1) gauge theory in p+1 dimensions. The spectrum contains $9-p$ massless scalars, which are associated with the transverse oscillations of the brane. Putting N Dp-branes on top of each other, the gauge theory generalizes to a U(N) theory. There are then N^2 different kinds of open strings, since the strings can begin and end on any of the branes; see Figure 2.7. The expectation values of the scalars determine the relative separations of the branes in the $9-p$ transverse directions. Turning on all of these expectation values breaks the gauge group to $U(1)^N$. In the current context, we are interested in the case of many coincident D-branes.

Before the discovery of D-branes by Polchinski [100], their low energy description in terms of black p-branes was already known. The p-branes are classical solutions to type IIsupergravity, which is the low energy limit of string theory. The p-brane description provides a second, dual description of D-branes, besides the gauge theoretical description discussed above. The comparison of these two descriptions led to the discovery of the AdS/CFT correspondence.

A stack of N p-branes is a heavy macroscopic object that curves spacetime. It can be described by a classical metric and other background fields, such as the Ramond-Ramond $p+1$ form potential. In the following we will focus on the 3-brane. In this case, the metric takes the form [71]

$$ds^2 = \left(1+\frac{L^4}{r^4}\right)^{-1/2}\left(-dt^2+dx_1^2+dx_2^2+dx_3^2\right) + \left(1+\frac{L^4}{r^4}\right)^{1/2}\left(dr^2+r^2d\Omega_5^2\right), \quad (2.53)$$

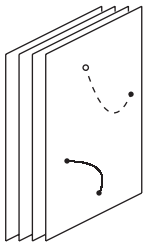

FIGURE 2.7: N D-branes on top of each other. Open strings can begin and end on any of the branes.

where $L^4 = 4\pi g_s l_s^4$ with l_s the characteristic string length and the dilaton is constant. Notice that this metric is everywhere non-singular. The horizon is at $r = 0$. The metric for N 3-branes on top of each other only differs in that

$$L^4 = 4\pi g_s l_s^4 N \,. \tag{2.54}$$

For the classical supergravity description to be valid, the curvature of the geometry of the p-brane has to be small compared to the string scale. This ensures that string corrections are negligible. To suppress string loop corrections, the effective string coupling also needs to be kept small. These requirements can be expressed as

$$1 \ll g_s N < N \,. \tag{2.55}$$

On the other hand, the D-brane description uses the string worldsheet and is thus a good description in string perturbation theory. In the case where there are N D-branes on top of each other, every open string boundary loop ending on the D-branes comes with a factor N times the string coupling. The D-brane description is thus valid in exactly the regime complementary to (2.55), namely when

$$g_s N \ll 1 \,. \tag{2.56}$$

2.2.4 LOW ENERGY LIMIT

The system of string theory on a background of D3-branes can be described by an action of the form

$$S = S_{\text{bulk}} + S_{\text{brane}} + S_{\text{int}} \,. \tag{2.57}$$

Here S_{bulk} describes the 10-dimensional type IIB string theory in the bulk, S_{brane} the $3+1$-dimensional open string gauge theory on the branes and S_{int} the interactions between these two theories. If we consider the system at low energies, *i.e.*, at energies below the string scale $1/l_s$, only the massless modes

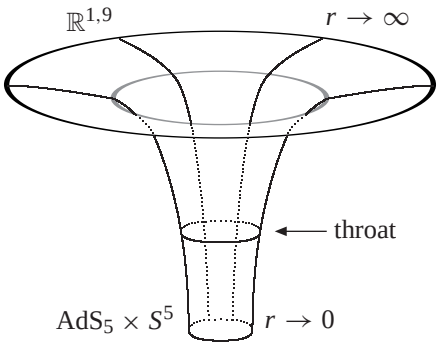

FIGURE 2.8: D3-brane geometry as interpolation between flat 10-dimensional Minkowski space and $\mathrm{AdS}_5 \times S^5$.

can be excited. In this limit the theory on the branes reduces to the low energy effective theory, which is pure $\mathcal{N}=4$ U(N) SYM [143] and the bulk theory becomes free supergravity on a Minkowski background. Moreover, S_{int} vanishes and the theory on the branes decouples from the theory in the bulk.

We can also consider the low energy limit in the dual supergravity p-brane description. From the perspective of an observer at infinity, there are two types of low energy excitations. There are the massless modes propagating in the bulk region. Since the metric (2.53) becomes flat at large r, these describe supergravity in flat space. On the other hand, since g_{tt} in (2.53) depends on r, objects close to the horizon appear red-shifted by a factor

$$\left(1+\frac{L^4}{r^4}\right)^{-1/4} \sim \frac{r}{L} \qquad (r \to 0) \tag{2.58}$$

to an observer at infinity. Thus, *any excitation* becomes a low energy excitation as it is brought close to the horizon. The metric in the near-horizon regime takes the form

$$ds^2 = \frac{r^2}{L^2}\left(-dt^2+dx_1^2+dx_2^2+dx_3^2\right)+L^2\frac{dr^2}{r^2}+L^2 d\Omega_5^2\,. \tag{2.59}$$

Comparing to (2.49) we see that this is the metric of $\mathrm{AdS}_5 \times S^5$, where both components have equal radius L. The metric (2.53) thus interpolates between flat space and $\mathrm{AdS}_5 \times S^5$. Figure 2.8 illustrates this separation into two regions. It depicts how the radius of the 5-sphere becomes constant as r becomes small. Both geometries, which are thought to be exact string theory vacua, are separated by an infinitely long 'throat'. The two types of excitations

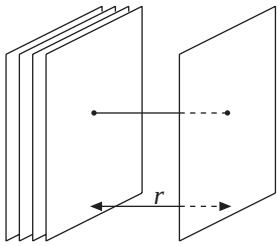

FIGURE 2.9: Open string stretched between a stack of D-branes and a probe brane.

decouple, because the low energy absorption cross section is proportional to $\omega^3 L^8$ [62,81], where ω is the energy. More intuitively, this happens because the wavelength of low energy bulk excitations becomes much larger than the typical size of the brane and, reversely, because it becomes increasingly difficult for the excitations near $r = 0$ to escape the gravitational well and propagate into the asymptotic region. We conclude that the low energy theory from the p-brane perspective consists of two decoupled regimes: free supergravity in 10-dimensional Minkowski space and string theory on the near horizon geometry of $AdS_5 \times S^5$.

2.2.5 MALDACENA'S CONJECTURE

In this section we formulate the precise AdS/CFT conjecture, as proposed by Maldacena, and present some initial motivation for it. In both dual descriptions discussed above, the theory far from the branes is string theory (or supergravity) on Minkowski space. The theory near the branes is, however, not the same in both cases: it is a gauge theory in one case, string theory on $AdS_5 \times S^5$ in the other. This led Maldacena [90] to conjecture that $\mathcal{N} = 4$ U(N) SYM is dual to type IIB superstring theory on $AdS_5 \times S^5$.

As motivation for the conjecture, note that the near horizon limit is equivalent to the low energy limit. Indeed, in taking the low energy limit, $l_s \to 0$, it is natural to keep fixed the energy of an open string stretched between a stack of D-branes and a probe brane, as in Figure 2.9. The energy of such a string is r/l_s^2. In order to keep this fixed, one needs to take $r \to 0$, which is the near horizon limit. Additionally, consider a massless particle incident from the asymptotic region. In the D-brane description, this will be absorbed by the D-branes and cause an excitation of the gauge theory. In the geometric description, it will tunnel into to throat region and cause an excitation there. The fact that the absorption cross sections for these dual processes are equal [81] provides strong

motivation for the conjecture.

As final motivation, consider the symmetry groups. The YM theory is conformal. Its symmetry group is the conformal group in four dimensions, SO(2, 4), times the R-symmetry group SU(4). This group is isomorphic to the symmetry group of $AdS_5 \times S^5$, which is SO(2, 4) for AdS_5 and SO(6) for S^5. Taking into account the supersymmetry, the isometry group of $AdS_5 \times S^5$ is SU(2, 2|4), which is exactly the superconformal group in four dimensions.

It is important to note that, because of the redshift (2.58), the entire spectrum of string excitations becomes low energy in the near horizon region. Indeed, we have taken the low energy limit in such a way, keeping r/l_s^2 fixed, that the energies of objects in the throat remain fixed in string units. The near horizon low energy spectrum is thus that of the full type IIB string theory.

2.2.6 The correspondence between fields and operators

Shortly after the AdS/CFT conjecture was made, a precise correspondence between gauge theory observables and those of supergravity was proposed in [61,144]. The basic idea is to identify the correlation functions in the conformal field theory with the dependence of the supergravity action on the asymptotic behaviour near the boundary of AdS.

Because of scale invariance, there is no notion of asymptotic states or of an S-matrix in conformal field theory. The natural objects to consider are then operators. Consider an operator $\mathcal{O}$ in $\mathcal{N} = 4$ super Yang-Mills which changes the value of the coupling constant g_{YM}. Since the gauge coupling is related to the string coupling by [42,100]

$$4\pi g_s = g_{\text{YM}}^2 \,, \tag{2.60}$$

this causes the string coupling to change. In turn, the string coupling is related to the expectation value of the dilaton ϕ. This expectation value depends on the boundary value for the dilaton. We see that changing the gauge coupling is related to changing the boundary value of the dilaton. By adding a term $\int d^4x\, \phi_0(\vec{x})\mathcal{O}(\vec{x})$ to the Lagrangian, we can change the boundary condition on the dilaton to $\phi(\vec{x}, z)|_{z=0} = \phi_0(\vec{x})$, in the coordinates (2.50). It then seems natural to identify [61,144]

$$\left\langle e^{\int d^4x\, \phi_0(\vec{x})\mathcal{O}(\vec{x})} \right\rangle_{\text{CFT}} = \mathcal{Z}_S\big[\phi(\vec{x}, z)|_{z=0} = \phi_0(\vec{x})\big] \,. \tag{2.61}$$

The left hand side of this equation denotes the generating functional of correlation functions in the CFT and the right hand side the supergravity (or string) partition function with the boundary condition that the field ϕ approaches the

value ϕ_0 on the boundary. In this way, the operators of the CFT are in one to one correspondence with the string theory fields. This is true not only for the scalar fields but for any field, including tensor and fermion fields. For example, the stress tensor of the boundary field theory corresponds to the graviton in the bulk.

The AdS/CFT correspondence is a strong/weak coupling duality in that it relates the strong coupling regime of one theory to the weak coupling regime of the dual theory. This complicates direct tests of the conjecture in which a certain quantity is calculated in both theories and compared. Nevertheless the correspondence has been tested extensively, *e.g.*, through comparison of certain correlation functions that do not depend on the coupling [34,49,70]. Based on these tests, it is fair to say that the AdS/CFT conjecture is by now well established and is beyond being a mere conjecture.

2.2.7 AdS/CFT and holography

The AdS/CFT correspondence provides an explicit realization of holography. It allows one to describe the 5-dimensional bulk physics in terms of a 4-dimensional conformal field theory, which can be thought of as living on the boundary* of the AdS space. There is, however, an important aspect of the holographic principle that we have not yet addressed. Namely, the holographic theory should contain a finite number of degrees of freedom per Planck area. In the case at hand, the holographic theory, being a conformal theory, in fact has degrees of freedom at arbitrarily small scales. Also, the area of the boundary of AdS space is infinite. In order to perform a sensible counting of degrees of freedom, we need to regulate both the boundary area and the UV degrees of freedom of the gauge theory. In the following we will see that we can do both with a single regulator.

The number of degrees of freedom can be regulated by imposing an ultraviolet, or short distance cutoff δ. Let us consider the bulk interpretation of such a cutoff. Close to the boundary of AdS we can use the metric (2.50), in which the boundary is at $z = 0$. The AdS isometry (in Euclidean coordinates) corresponding to a rescaling of the boundary is then given by

$$\begin{aligned} x^i &\to \lambda x^i \,, \\ z &\to \lambda z \,. \end{aligned} \tag{2.62}$$

*It may seem that the boundary of $AdS_5 \times S^5$ is not 4-dimensional, but 9-dimensional instead. However, from the metric (2.59) on this space, we see that in approaching the boundary (at $r = \infty$) four of the dimensions blow up, while the S^5 remains constant. In order to obtain a finite metric on the boundary we will need to multiply by a factor that goes to zero at the boundary. Effectively, we are then left with a 4-dimensional boundary.

The scale size of objects in the boundary CFT thus corresponds to the radial coordinate, z, of AdS. This can also be seen directly in the AdS space. Consider a volume $\mathcal{V}$ near the center of AdS. Using an AdS isometry, map the volume to a coordinate distance ϵ from the boundary. The volume will have scaled to a coordinate size $\epsilon\mathcal{V}$. In this way, the scale size becomes a spatial dimension. This implies that a UV cutoff in the boundary at a length scale δ corresponds in the bulk theory to a IR cutoff at

$$z \leftrightarrow \delta \,. \tag{2.63}$$

This relation between the bulk and boundary theories is called the UV/IR connection [127]. In Chapter 4 we will see that it is not a peculiarity of the AdS/CFT correspondence and also appears in a conjectured holographic duality of de Sitter space.

We can now proceed and calculate the entropy of the boundary theory. Assume that each independent quantum field has one degree of freedom per cutoff volume δ^3. Write the metric of AdS as

$$ds^2 = L^2 \left[-\left(\frac{1+r^2}{1-r^2}\right)^2 dt^2 + \frac{4}{(1-r^2)^2}(dr^2 + r^2 d\Omega_3^2) \right] . \tag{2.64}$$

In these coordinates the radial coordinate is denoted by r and the boundary is at $r = 1$. The regulated boundary is at $r = 1 - \delta$, where $\delta \ll 1$. Consider $\mathcal{N} = 4$ SYM on a three-sphere with unit radius. The number of degrees of freedom of a U(N) theory is of order N^2. Since the volume of the three-sphere in terms of the cutoff δ is of order δ^{-3}, the total number of degrees of freedom is

$$N_{\text{d.o.f.}} = \frac{N^2}{\delta^3} \,. \tag{2.65}$$

The area of the regulated sphere is $A \approx {}^{L^3}\!/_{\delta^3}$. Using (2.54), we can write

$$N_{\text{d.o.f.}} = \frac{AL^5}{l_s^8 g_s^2} \,. \tag{2.66}$$

In terms of the 5-dimensional Newton constant, $G_5 = l_s^8 g_s^2 L^{-5}$, this takes the form [127]

$$N_{\text{d.o.f.}} = \frac{A}{G_5} \,. \tag{2.67}$$

We see that, after suitable regularization, the SYM boundary theory provides a holographic theory including the information density bound.

Since in AdS space the volume and area of any region scale in the same way,[†]

$$\frac{A}{V} \sim \frac{1}{L} \qquad (V \to \infty)\,, \tag{2.68}$$

one might ask how strong a statement it is to say that gravity in AdS is holographic. Indeed, for any field theory in AdS it holds true that the number of degrees of freedom is proportional to the boundary area. Compare this to the case of flat space where

$$\frac{A}{V} \sim 0 \qquad (V \to \infty)\,. \tag{2.69}$$

However, in the case at hand there is another parameter: the AdS length scale L. In the boundary theory it corresponds to the rank of the gauge group, N. We can then consider AdS spaces with different radii and observe whether the number of degrees of freedom goes like the volume or the area. This is relevant, since the volume and area depend differently on L. Combining (2.66) and (2.68), which for $\mathrm{AdS}_5 \times S^5$ takes the form $V = AL^6$, gives [127]

$$\frac{N_{\text{d.o.f.}}}{V} = \frac{1}{L l_s^8 g_s^2}\,. \tag{2.70}$$

From this we see that, as L becomes large, the number of degrees of freedom per unit volume goes to zero. In this sense, then, the holographic bound is similarly restrictive as in flat space.

2.2.8 The Cardy-Verlinde formula

The AdS/CFT correspondence can be applied to the situation where there is a black hole present in Anti-de Sitter space. Like black holes in asymptotically flat space, these solutions have thermodynamic properties including a characteristic temperature and an entropy equal to one quarter of the area of the event horizon in Planck units [68]. It was argued by Witten [145] that this temperature and entropy, as well as the mass of the black hole can be identified with the temperature, entropy and energy of a CFT at high temperatures.

Consider an Anti-de Sitter Schwarzschild black hole in $D+1$ dimensions, the metric is given by

$$ds^2 = -\left(1 + \frac{r^2}{L^2} - \frac{\omega_D M}{r^{D-2}}\right) dt^2 + \left(1 + \frac{r^2}{L^2} - \frac{\omega_D M}{r^{D-2}}\right)^{-1} dr^2 + r^2 d\Omega_{D-1}^2\,, \tag{2.71}$$

[†]Note that L, the curvature radius of the AdS space, is a constant.

where

$$\omega_D = \frac{16\pi G_{\rm N}}{(D-1)\mathrm{Vol}(S^{D-1})}\,, \tag{2.72}$$

cf. (2.2). Here, $G_{\rm N}$ denotes the D+1-dimensional Newton constant and L is the radius of curvature of the AdS spacetime. The radius of the black hole horizon is $r_{\rm H}$, with $r_{\rm H}$ the largest solution of the equation

$$1 + \frac{r^2}{L^2} - \frac{\omega_D M}{r^{D-2}} = 0\,. \tag{2.73}$$

The dual CFT lives on the $D = n+1$ dimensional boundary of the AdS Schwarzschild spacetime, with topology $\mathbb{R}\times S^n$.

As shown in [145], the energy and entropy of the black hole (2.71) are given by

$$E = M = \frac{(D-1)(r_{\rm H}L^{-2} + r_{\rm H}^{-1})V}{16\pi G_{\rm N}} \tag{2.74}$$

and

$$S = \frac{V}{4G_{\rm N}}\,, \tag{2.75}$$

where V is the horizon volume,

$$V = r_{\rm H}^{D-1}\mathrm{Vol}(S^{D-1})\,. \tag{2.76}$$

For future purpose, rescale these formulas so that the CFT lives on a sphere with radius equal to that of the black hole horizon. Moreover, eliminate the D+1-dimensional Newton constant using its relation with the central charge, c, of the CFT,

$$\frac{1}{4G_{\rm N}} = \frac{c}{12}\frac{1}{L^n}\,. \tag{2.77}$$

Since the entropy is dimensionless it does not scale. Using the substitution for $G_{\rm N}$ we can write it as

$$S = \frac{c}{12}\frac{V}{L^n}\,. \tag{2.78}$$

The energy does scale and this introduces a factor $L/r_{\rm H}$ as compared to (2.74), which can then be written as

$$E = \frac{c}{12}\frac{n}{4\pi L}\left(1 + \frac{L^2}{r_{\rm H}^2}\right)\frac{V}{L^n}\,. \tag{2.79}$$

The temperature of the black hole can be deduced from the metric (2.71) in the same way as for the asymptotically flat case, *cf.* (2.10)-(2.20). The temperature of the CFT living on a sphere of radius $r_{\rm H}$ then follows after the appropriate

rescaling. Alternatively, it follows from the first law of thermodynamics and is given by

$$T = \frac{1}{4\pi L}\left[(n+1) + (n-1)\frac{L^2}{r_{\rm H}^2}\right] . \tag{2.80}$$

Based on the above formulas for the entropy and energy of the dual CFT, Verlinde [137] constructed a formula for the entropy reminiscent of the Cardy formula for the entropy of a 1+1-dimensional CFT. Note that the energy (2.79) exhibits an extensive, but also a sub-extensive term,

$$E = E_{\rm E} + \frac{1}{2}E_{\rm C} , \tag{2.81}$$

where $E_{\rm E}$ and $E_{\rm C}$ denote the extensive part and the sub-extensive part, respectively. The factor $1/2$ is introduced for later convenience. As we will derive in more detail in the next chapter, the sub-extensive term is given by [137]

$$E_{\rm C} = \frac{c}{12}\frac{n}{2\pi r_{\rm H}}\frac{V}{L^{n-1}r_{\rm H}} \tag{2.82}$$

and is called the Casimir energy. Although the Casimir effect is usually discussed at zero temperature [33], a similar effect occurs at finite temperature. It results from finite size effects in the quantum fluctuations of the CFT and disappears in the infinite volume limit. Substituting for c and L leads to a unique expression for the entropy [137],

$$S = \frac{2\pi r_{\rm H}}{n}\sqrt{E_{\rm C}(2E - E_{\rm C})} . \tag{2.83}$$

This formula has become known as the Cardy-Verlinde formula. Indeed, substituting

$$\begin{aligned} E\, r_{\rm H} &= L_0 , \\ E_{\rm C}\, r_{\rm H} &= \frac{c}{12} , \end{aligned} \tag{2.84}$$

the formula (2.83) reduces to the Cardy formula. It is rather surprising that the Cardy formula can so easily be generalized to higher dimensions, since the standard derivation, based on modular invariance, only works in $1+1$ dimensions. These formulas will play an important role in Chapter 3 and the required substitutions (2.84) will be clarified there. In the derivation above it is assumed that $r_{\rm H} \gg L$. For future purpose we note that within this parameter range the Casimir energy $E_{\rm C}$ is smaller than the total energy E.

3

Energy and Entropy in a Radiation Dominated FRW Universe

In this chapter, we study the holographic principle in the context of a radiation dominated FRW universe. The radiation is represented by a strongly coupled CFT with an AdS-dual description. A surprising merger between the applicable entropy and energy formulas and the equations that govern the cosmological evolution will be discussed. Subsequently, we introduce a Randall-Sundrum type brane world model in the background of an AdS-Schwarzschild geometry. The merger derives a natural explanation from this model, as it occurs exactly when the brane crosses the black hole horizon. The treatise is based on [112].

3.1 Introduction

In the previous chapter the foundations of the holographic principle were discussed. To further elucidate the holographic principle and the entropy bounds that are derived from it, we now study a closed, radiation dominated standard Friedmann-Robertson-Walker (FRW) cosmology. Keeping the spacetime dimension $D = n+1$ general, the metric takes the form

$$ds^2 = -dt^2 + a^2(t)d\Omega_n^2\,, \tag{3.1}$$

where $a(t)$ represents the radius of the universe at time t. The spatial sections of this closed metric are n-spheres with finite volume

$$V = \mathrm{Vol}(S^n)\, a^n\,. \tag{3.2}$$

The radiation can be described by an interacting CFT. More usually, radiation is described by free, or weakly interacting, massless particles. The number of species of such particles corresponds to the central charge c of this CFT. The

case of interest to us is of a CFT with a very large central charge. As was shown in Section 2.2.8, the entropy of such a CFT, at least for CFT's that have an AdS dual, is given by the Cardy-Verlinde formula (2.83).

In Section 3.3, we discuss a relation between the entropy formulas for the CFT and the FRW equations which was first considered by Verlinde [137]. This relation provides a deep and fundamental connection between the holographic principle, the CFT entropy formulas and the gravitational evolution of the radiation dominated FRW universe. Setting the cosmological constant to zero, the FRW equations take the form

$$H^2 = \frac{16\pi G_{\rm N}}{n(n-1)}\frac{E}{V} - \frac{1}{a^2}\,, \tag{3.3}$$

$$\dot{H} = -\frac{8\pi G_{\rm N}}{n-1}\left(\frac{E}{V}+p\right) + \frac{1}{a^2}\,, \tag{3.4}$$

where $H \equiv \dot{a}/a$ is the Hubble constant and the dot denotes differentiation with respect to the time t. For convenience, we write the FRW equations in terms of the total energy E and entropy S, instead of their respective densities, $\rho = E/V$ and $s = S/V$, as is more usual.

The first law of thermodynamics states that

$$d(\rho a^n) = -p\,d(a^n)\,. \tag{3.5}$$

Dividing by dt and evaluating, we obtain

$$\dot{\rho} = -n(\rho + p)H\,. \tag{3.6}$$

Together with the equation of state for radiation, $p = \rho/n$, this implies that ρ and p drop off in the usual fashion as $a^{-(n+1)}$. It follows that the cosmological evolution will be that of a standard closed radiation dominated FRW universe. Starting from a big bang, the universe expands until it reaches its maximal size. Subsequently, it re-collapses to end in a big crunch. In this respect nothing special happens. However, as observed by Verlinde [137], an interesting merger occurs when one compares the holographic entropy bound with the entropy formulas for the CFT. At the point where the bound is saturated, the FRW equations merge together with the entropy formulas for the CFT to give one set of equations. The role of the entropy bounds is illustrated by the substitutions [137]

$$2\pi L_0 \Rightarrow \frac{2\pi}{n} E a\,, \tag{3.7}$$

$$2\pi\frac{c}{12} \Rightarrow (n-1)\frac{V}{4G_{\rm N}a} \tag{3.8}$$

and

$$S \Rightarrow (n-1)\frac{HV}{4G_{\mathrm{N}}}\,, \tag{3.9}$$

which, as one easily checks, turn the Cardy-Verlinde formula (2.83) into the Friedmann equation (3.3). As we will discuss in detail below, each of these substitutions correspond to a cosmological entropy bound. In this way the merger becomes a natural consequence of the holographic principle.

In Section 3.2 we introduce several cosmological entropy bounds, including three corresponding to each of the equations (3.7)-(3.9). In Section 3.3 we introduce the cosmological Casimir bound and show that the FRW equations and the entropy formulas are exactly matched when the bound is saturated. After a general discussion of brane world scenarios in Section 3.4, we consider the merger from the viewpoint of a brane world scenario in Section 3.5. A brane of constant tension is considered in the background of an AdS-Schwarzschild black hole. The idea is to use the AdS/CFT correspondence where the brane takes the place of the boundary. The Hawking temperature of the AdS-Schwarzschild geometry, measured with respect to time on the brane, can be interpreted as the temperature of the CFT to which the bulk is dual through the AdS/CFT correspondence. The induced geometry on the brane is shown to be that of a radiation dominated FRW universe. The entropy and energy formulas derived in the preceding sections can then be applied to this spacetime. It is shown that the moments at which the merger between the different sets of equations occurs play a special role in this scenario: they are the moments at which the brane crosses the horizon of the bulk black hole. That one obtains a radiation dominated universe in this way can be understood from the CFT perspective. All CFT's have the same equation of state up to numerical factors, so the FRW equations take the same form as they do in the radiation dominated era of our universe. We conclude and summarize in Section 3.6.

3.2 Cosmological entropy bounds

The holographic entropy bound in the form (2.23) cannot directly be applied to closed cosmological models. This is because a closed universe does not have a boundary. Furthermore, the argumentation leading to (2.23) assumes that it is possible to form a black hole that fills the entire volume. This is not true in a cosmological setting, because the expansion rate H of the universe as well as the given value of the total energy E restrict the maximal size a black hole can have. Moreover, in standard cosmology, it is usually assumed that in the late universe the entropy density is constant in comoving coordinates. This implies that one can violate the bound (2.23) by choosing a large enough volume, since

in this case the entropy clearly grows like the volume. In this section, we discuss modifications of the holographic bound designed to circumvent these difficulties.

3.2.1 The Fischler-Susskind bound

The first cosmological entropy bound we consider is a generalization, by Fischler and Susskind [45], to more general spacetimes of the covariant bound discussed in Section 2.1.4. Consider a flat $n+1$-dimensional Robertson-Walker cosmology; the metric has the form

$$ds^2 = -dt^2 + a^2(t)\, dx^i dx_i \qquad (i = 1, \ldots, n)\,. \tag{3.10}$$

The usual cosmological assumptions of homogeneity, isotropy and, in the late universe, constant entropy density in comoving coordinates are made. Consider a spherical spatial region V with coordinate radius ℓ and boundary A. The lightlike surface L is formed by past lightrays from A towards the center of V. There are three situations, depending on whether ℓ is larger, smaller or equal to the cosmological horizon $a_{\rm C}$. When $\ell < a_{\rm C}$, the surface L forms a light cone with its tip in the future of the singularity at $t = 0$. For $\ell = a_{\rm C}$, L is a light cone with its tip at $t = 0$. Finally, in the case $\ell > a_{\rm C}$, the surface is a truncated cone. These situations are indicated in Figure 3.1. Consider the entropy that passes through L. For the first two cases this entropy is the same as the entropy in the interior of V (or less, as entropy increases after it crosses L). In the last case it is less than the entropy in V. The Fischler-Susskind holographic entropy bound states that the entropy passing through L never exceeds the area of the boundary surface A,

$$S(L) \leqslant \frac{A}{4}\,. \tag{3.11}$$

For the homogeneous case, this corresponds to the following condition: the entropy contained within a volume of coordinate size $a_{\rm C}$ should not exceed the area of the horizon in Planck units. In terms of the constant comoving entropy density σ, this condition takes the form

$$\sigma a_{\rm C}^n \leqslant (a \cdot a_{\rm C})^{n-1}\,, \tag{3.12}$$

with everything measured in Planck units. Comparing to the bound discussed in Section 2.1.4, we see that A now plays the role of holographic screen.

Both $a_{\rm C}$ and a depend on time and the bound (3.12) should hold at all times. At the current time, the entropy of the observable universe is of order 10^{86}, while the horizon size is of order 10^{60}. By substituting these numbers and $n = 3$ in (3.12), one easily checks that the bound holds for the observable

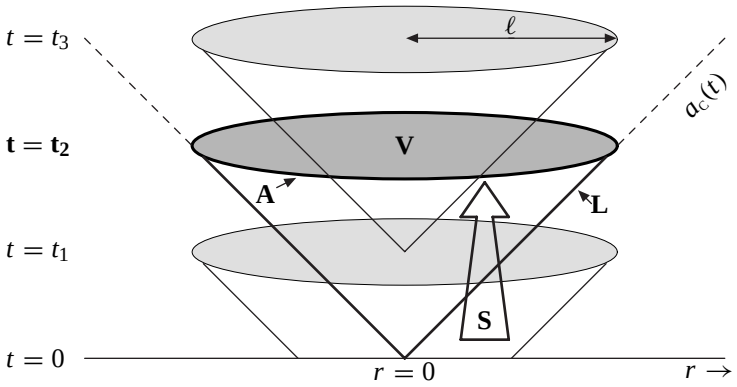

FIGURE 3.1: Spherical spatial volumes with coordinate radius ℓ are shown at times $t = t_1,\ t_2,\ t_3$. The big bang is at $t = 0$. For the volume **V** at $t = t_2$, the construction is shown in boldface. The arrow **S** denotes the entropy flow through the lightsheet **L** corresponding to the volume **V** with boundary **A**. The cosmological horizon $a_c(t)$ is indicated by the dotted lines for $t > t_2$. The lightsheet **L** coincides with the cosmological horizon for $t \leqslant t_2$.

universe at this moment. Indeed, the entropy to area ratio, $\rho = S/A$, is of order

$$\rho(t_0) \approx 10^{-34}\,, \tag{3.13}$$

where t_0 is *now*. It is interesting to consider whether the bound will continue to hold in the future. Assuming that $a(t) \propto t^p$, the horizon size is given by

$$a_c(t) = \int_0^t \frac{dt}{a(t)} \propto t^{1-p}\,. \tag{3.14}$$

From this we deduce that (3.12) will continue to hold if

$$p > \frac{1}{n}\,, \tag{3.15}$$

setting a lower bound for the expansion rate.

Looking backwards in time, standard estimates give an entropy to area ratio at the time of decoupling, $t = t_d$, which is about 10^6 times larger than the current ratio,

$$\rho(t_d) \approx 10^{-28}\,. \tag{3.16}$$

During the preceding, radiation dominated era, the time dependence of ρ is given by

$$\rho(t) \propto 10^{-28}\sqrt{\frac{t_d}{t}} \approx \frac{1}{\sqrt{t}}\,, \tag{3.17}$$

where in the last step we used that $t_d \approx 10^{56}$ in Planck units. We see that the entropy in the universe is as large as it can be with (3.12) holding all the way back to the Planck time.

The above construction makes clear the advantage of bounding entropy on lightsheets instead of spatial volumes in a cosmological setting. Since the spatial entropy density σ is constant and uniform, if we choose V big enough the entropy in V will exceed its area A, as noted above. However, the lightsheet associated with V does not grow proportional to V. If V becomes larger than the cosmological horizon, the lightsheet is truncated by the big bang. This means that part of the entropy in V never passed through L. Taking into account only the entropy that did pass through L, this does scale like the area A.

The Fischler-Susskind bound applies to flat and open universes, but fails for closed and recollapsing universes. Bousso [23,24] has proposed a refinement of the bound that applies in arbitrary spacetimes. To any surface A, with arbitrary shape, topology and location, are associated at least two (and at most four) well defined lightsheets. The bound (3.11) is then argued to apply to each lightsheet independently. With certain assumptions on the relation between entropy density and energy density, this bound was proven to hold [46]. We will refer to this bound as the Fischler-Susskind-Bousso or FSB bound and say a bit more about how it is defined in Section 4.4.3, where we use it to define the apparent horizon.

3.2.2 The Bekenstein bound

Bekenstein [18–20] was the first to propose a bound on the entropy of a macroscopic system. Assuming that the system has limited self-gravity, Bekenstein argued that its entropy must be bounded by (a multiple of) the energy and the linear dimension of the system. The assumption of limited self-energy means that the gravitational self-energy of the system is small compared to the total energy E. Applying this bound in the present context of a closed radiation dominated FRW universe with radius a, it takes the form [137]

$$S \leqslant S_B \,, \tag{3.18}$$

where the Bekenstein entropy S_B is defined by

$$S_B \equiv \frac{2\pi}{n} E a \,. \tag{3.19}$$

The assumption of limited self-gravity requires that the Hubble radius H^{-1} is larger than the radius a of the universe,

$$Ha \leqslant 1 \,. \tag{3.20}$$

As noted in the introduction to this chapter, $\rho \propto a^{-(n+1)}$ for a radiation dominated universe. Hence, the energy behaves as $E \propto a^{-1}$. Comparing to (3.19), we see that this means that the Bekenstein entropy is constant during the evolution, providing the entropy S does not change.

3.2.3 THE COSMOLOGICAL BEKENSTEIN-HAWKING BOUND

In a strongly self-gravitating universe, *i.e.* for

$$Ha \geqslant 1\,, \tag{3.21}$$

the possibility of black hole formation has to be taken into account. One can try to generalize the idea of a space filling black hole to a cosmological context, despite the difficulties mentioned at the beginning of this section. For a closed universe, the closest one can come to the expression (2.21) is perhaps [137]

$$S_{\mathrm{BH}}^{\mathrm{c}} \equiv (n-1)\frac{V}{4a}\,. \tag{3.22}$$

This expression grows like an area, as appropriate for a black hole, motivating the identification of $S_{\mathrm{BH}}^{\mathrm{c}}$ as the Bekenstein-Hawking entropy of a universe filling black hole. The corresponding entropy bound takes the form

$$S \leqslant S_{\mathrm{BH}}^{\mathrm{c}}\,. \tag{3.23}$$

From the Friedmann equation (3.3) one derives that

$$Ha \lessgtr 1 \qquad \Leftrightarrow \qquad S_{\mathrm{B}} \lessgtr S_{\mathrm{BH}}^{\mathrm{c}}\,. \tag{3.24}$$

Therefore, the appropriate bound is also the most stringent in its respective regime of validity. However the cosmological Bekenstein-Hawking bound breaks down, as expected, since it assumes the existence of arbitrarily large black holes and is irreconcilable with a finite homogeneous entropy density. In the next section, we will use the cosmological Bekenstein-Hawking entropy rather as a bound on the sub-extensive component of the entropy. This sub-extensive contribution is associated with a corresponding sub-extensive term E_{C} in the energy, *cf.* (2.81).

3.2.4 THE HUBBLE BOUND

Since arbitrarily large black holes are not possible, one can instead use black holes of maximal size to obtain an entropy bound for the universe. This idea of filling the universe with black holes the size of the Hubble horizon is pursued

in [79,135] and leads to the Hubble bound. A black hole filling a Hubble volume $V_{\rm H}$ has entropy approximately equal to

$$S \approx \frac{HV_{\rm H}}{4}\,. \tag{3.25}$$

The number of such black holes that will fit in the universe is given by

$$N_{\rm H} = \frac{V}{V_{\rm H}}\,, \tag{3.26}$$

where V is the volume of the universe. Multiplying these expressions leads to an upper bound on the total entropy S given by a multiple of $HV/4$. The precise prefactor was determined in [137], using a local formulation of the FSB bound. The Hubble bound then takes the form

$$S \leqslant S_{\rm H}\,, \tag{3.27}$$

where the Hubble entropy $S_{\rm H}$ is defined by

$$S_{\rm H} \equiv (n-1)\frac{HV}{4}\,. \tag{3.28}$$

The Hubble bound is only valid for strongly self-gravitating systems, *i.e.* for $Ha \geqslant 1$.

3.3 The cosmological Casimir bound

We consider a new cosmological entropy bound that was first proposed by Verlinde in [137]. This bound is equivalent to the Hubble bound in the strongly gravitating phase, but unlike the Hubble bound remains valid in the phase of weak self-gravity. A surprising merger between the FRW equations that govern the gravitational evolution and the CFT formulas for the entropy and Casimir energy occurs when the bound is saturated.

3.3.1 Energy and entropy formulas for the CFT

We begin by discussing the entropy of the CFT that describes the radiation in the FRW universe. In cosmology it is usually assumed that the total entropy S and energy E are purely extensive quantities. This means for the energy, as a function of entropy and volume, that $E(\lambda S, \lambda V) = \lambda E(S, V)$. From this relation one can derive the Euler relation in the following way. Differentiate with respect to λ and put $\lambda = 1$. This gives

$$E = V\left(\frac{\partial E}{\partial V}\right)_{\rm S} + S\left(\frac{\partial E}{\partial S}\right)_{\rm V}\,. \tag{3.29}$$

Using the first law of thermodynamics, $dE = TdS - pdV$, one can express the derivatives as

$$\left(\frac{\partial E}{\partial V}\right)_{\mathrm{S}} = -p\,, \qquad \left(\frac{\partial E}{\partial S}\right)_{\mathrm{V}} = T\,. \tag{3.30}$$

Substituting these in (3.29) gives the Euler relation,

$$TS = E + pV\,. \tag{3.31}$$

As shown in Section 2.2.8 for a CFT with an AdS dual, the energy and entropy of a CFT with a large central charge are in fact not purely extensive. In a finite volume there is a non-extensive Casimir contribution to the energy proportional to c, the central charge. The Casimir energy can be defined as the violation of the Euler relation (3.31),

$$E_{\mathrm{C}} \equiv n(E + pV - TS)\,, \tag{3.32}$$

where the factor n is inserted for later convenience. The Casimir energy is again a function of the entropy and volume, but it will scale sub-extensively. From general considerations, the first correction to the extensive part of the energy should scale like

$$E_{\mathrm{C}}(\lambda S, \lambda V) = \lambda^{1-\frac{2}{n}} E_{\mathrm{C}}(S, V)\,. \tag{3.33}$$

The total energy can again be written as a sum of an extensive and a sub-extensive term, *cf.* (2.81),

$$E(S, V) = E_{\mathrm{E}}(S, V) + \frac{1}{2} E_{\mathrm{C}}(S, V)\,. \tag{3.34}$$

The product Ea is independent of the volume V by conformal invariance, thus depending only on the entropy S. This holds for both terms in the energy expression (3.34). From the known (sub-)extensive behaviour of E_{E} and E_{C}, we derive the general expressions [137],

$$E_{\mathrm{E}} = \frac{c_1}{4\pi a} S^{1+\frac{1}{n}}\,, \qquad E_{\mathrm{C}} = \frac{c_2}{2\pi a} S^{1-\frac{1}{n}}\,, \tag{3.35}$$

where the positive constants c_1 and c_2 are independent of a and S. The factors of 2π and 4π are put in for later convenience. Using these expressions, the entropy can be written as

$$S = \frac{2\pi a}{\sqrt{c_1 c_2}} \sqrt{E_{\mathrm{C}}(2E - E_{\mathrm{C}})}\,. \tag{3.36}$$

This is almost the same as the Cardy-Verlinde formula (2.83) we derived before for a CFT which has an AdS dual. Comparing the two, we conclude that $\sqrt{c_1 c_2} = n$ for such a CFT. From now on we will simply assume that $\sqrt{c_1 c_2} = n$ for the CFT we consider.

Given the energy E, the entropy formula (2.83) has a maximal value,

$$S \leqslant \frac{2\pi}{n} E a \,. \tag{3.37}$$

This is exactly the Bekenstein bound (3.18). The bound is saturated when the Casimir energy $E_{\rm C}$ is equal to the total energy E. In principle $E_{\rm C}$ could also become larger than E, with the entropy S again decreasing. However, as noted in Section 2.2.8, this does not happen in the parameter range for which (2.83) is valid. This leads us to assume that

$$E_{\rm C} \leqslant E \,. \tag{3.38}$$

3.3.2 A BOUND ON THE CASIMIR ENERGY

As expressed in (3.24), at the transition point where the universe goes from the strongly to the weakly self-gravitating phase, the Bekenstein entropy $S_{\rm B}$ is equal to the cosmological Bekenstein-Hawking entropy $S^{\rm c}_{\rm BH}$. Given the radius a, define the cosmological Bekenstein-Hawking energy, $E^{\rm c}_{\rm BH}$, to be the value of the energy at which this transition occurs,

$$\frac{2\pi}{n} E^{\rm c}_{\rm BH} a \equiv (n-1)\frac{V}{4a} \,. \tag{3.39}$$

Similar to the interpretation of the cosmological Bekenstein-Hawking entropy as the entropy of a universe filling black hole, the energy $E^{\rm c}_{\rm BH}$ can be interpreted as the energy required to form such a black hole. It is easy to check that

$$Ha \lessgtr 1 \qquad \Leftrightarrow \qquad E \lessgtr E^{\rm c}_{\rm BH} \,, \tag{3.40}$$

providing a new criterium for distinguishing between a weakly or strongly self-gravitating universe.

The physical content of the new cosmological bound proposed in [137] is that the sub-extensive Casimir contribution $E_{\rm C}$ to the total energy by itself does not suffice to form a universe filling black hole. This corresponds to a bound

$$E_{\rm C} \leqslant E^{\rm c}_{\rm BH} \,. \tag{3.41}$$

This bound is universally valid, both in the strongly and the weakly self-gravitating phases of the evolution. As we will show next, in a strongly gravitating

universe it is equivalent to the Hubble bound, while in a weakly gravitating universe it is equivalent to the Bekenstein bound. Since it is formulated in terms of the cosmological Bekenstein-Hawking entropy, which can be interpreted as the energy of a universe-filling black hole, it is a purely holographic bound. Moreover, as we will see, when the bound is saturated the laws of general relativity and quantum field theory merge in a miraculous way, giving a strong indication that they have a common origin in a more fundamental unified theory. We will refer to this bound as the cosmological Casimir entropy bound.

3.3.3 A COSMOLOGICAL CARDY FORMULA

In order to prove that the cosmological Casimir bound is equivalent to the Hubble bound and the Bekenstein bound in the strongly and weakly gravitating phases respectively, write the Friedmann equation as an expression for the Hubble entropy $S_{\rm H}$ in terms of the energy E, the radius a and the cosmological Bekenstein-Hawking energy $E^{\rm c}_{\rm BH}$. This leads to the unique expression

$$S_{\rm H} = \frac{2\pi}{n} a \sqrt{E^{\rm c}_{\rm BH}(2E - E^{\rm c}_{\rm BH})}\,. \tag{3.42}$$

This looks suspiciously like the Cardy-Verlinde entropy formula for a CFT, (2.83), except the entropy is replaced by the Hubble entropy and the Casimir energy by the cosmological Bekenstein-Hawking energy. It seems as if, somehow, the Friedmann equation knows about the Cardy-Verlinde formula.

From (3.40) we have that in the strongly gravitating phase, $Ha \geqslant 1$, the energy satisfies $E \geqslant E^{\rm c}_{\rm BH}$. Furthermore, we always assume that $E_{\rm C} \leqslant E$, *cf.* (3.38). The Cardy-Verlinde entropy is a monotonically increasing function of $E_{\rm C}$ in this range. Therefore, while the cosmological Casimir bound (3.41) is satisfied, or more specifically in the range

$$E_{\rm C} \leqslant E^{\rm c}_{\rm BH} \leqslant E\,, \tag{3.43}$$

it reaches its maximum when $E_{\rm C} = E^{\rm c}_{\rm BH}$. This is exactly when the Cardy-Verlinde formula turns into the cosmological Cardy formula (3.42) for $S_{\rm H}$. Therefore, we conclude that $S_{\rm H}$ is the maximal entropy that can be reached when $Ha \geqslant 1$, so that the Casimir bound is indeed equivalent to the Hubble bound in this regime. In the weakly self-gravitating phase, when $E \leqslant E^{\rm c}_{\rm BH}$, the maximum is reached earlier, namely for $E_{\rm C} = E$. Comparing (2.83) and (3.19), we conclude that the maximal entropy is in that case given by the Bekenstein entropy $S_{\rm B}$, proving the equivalence to the Bekenstein bound in this regime.

3.3.4 A LIMITING TEMPERATURE

We have seen that the Friedmann equation becomes identical to the Cardy-Verlinde formula when the cosmological Casimir bound (3.41) is saturated. We will now show that also the second FRW equation has a counterpart in the CFT. This leads to a constraint on the temperature T.

The second FRW equation can be written as a relation between $E^{\rm c}_{\rm BH}$ and $S_{\rm H}$. This relation takes the form

$$E^{\rm c}_{\rm BH} = n(E + pV - T_{\rm H} S_{\rm H})\,, \tag{3.44}$$

where

$$T_{\rm H} \equiv -\frac{\dot{H}}{2\pi H}\,. \tag{3.45}$$

Assume that the universe is in the strongly self-gravitating phase, $Ha \geqslant 1$, so that $H \neq 0$ and $T_{\rm H}$ is well defined. Note that $T_{\rm H} > 0$ since in a radiation dominated universe the expansion is always slowing down, so that $\dot{H} < 0$. We have seen that in the strong gravity regime the Casimir entropy bound is equivalent to the Hubble bound,

$$E_{\rm C} \leqslant E^{\rm c}_{\rm BH} \quad \Leftrightarrow \quad S \leqslant S_{\rm H} \qquad (Ha \geqslant 1)\,. \tag{3.46}$$

From comparing (3.44) and (3.32), the defining relation for the Casimir energy $E_{\rm C}$, we see that the temperature T is bounded from below by $T_{\rm H}$,

$$T \leqslant T_{\rm H} \qquad (Ha \geqslant 1)\,. \tag{3.47}$$

When the Casimir bound is saturated all inequalities turn into equalities. The Cardy-Verlinde formula and the defining Euler relation for the Casimir energy in that case exactly match the Friedmann equation for the Hubble constant and the second FRW equation for the cosmological Bekenstein-Hawking energy. This matching is summarized in Table 3.2 on page 61.

3.3.5 TIME DEPENDENCE OF THE ENTROPY BOUNDS

In order to elucidate the time dependence of the cosmological entropy bounds discussed in Section 3.2, write the Friedmann equation in terms of the Hubble-, Bekenstein- and cosmological Bekenstein-Hawking entropies. This leads to the expression [137]

$$S_{\rm H}^2 + (S_{\rm B} - S^{\rm c}_{\rm BH})^2 = S_{\rm B}^2\,. \tag{3.48}$$

This is the same as the square of (3.42), where we have replaced the energies by entropies through the defining relations (3.19) and (3.39). By representing each entropy appearing in this equation by a line with length proportional to

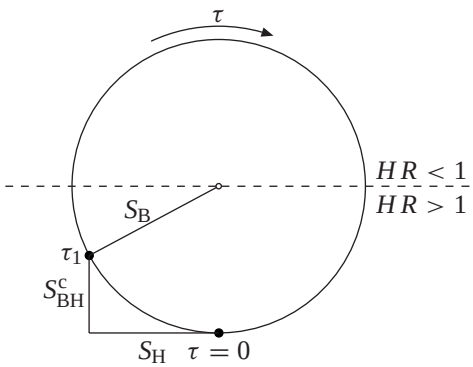

FIGURE 3.2: Diagram depicting the time dependence of the entropy bounds discussed in the text. The diagram represents one cosmological cycle of the standard FRW model. Time runs clockwise along the circle once. The evolution starts at $\tau = 0$ with a big bang and eventually ends, after one revolution, with a big crunch. In between, the universe reaches its largest size at the moment diagonally across from $\tau = 0$. The values of $S_{\rm BH}$ and $S_{\rm H}$ at $\tau = \tau_1$ are indicated as well as the time independent value of $S_{\rm B}$. The dashed line divides the eras when the universe is strongly ($Ha > 1$) or weakly ($Ha < 1$) self-gravitating. Figure adapted from [137].

its value, this relation allows all three to fit nicely together as in Figure 3.2. The circular form of the diagram reflects the fact that $S_{\rm B}$ is constant during the cosmological evolution.

In the same way as for the Bekenstein and the cosmological Bekenstein-Hawking energies, one can associate an entropy to the Casimir energy $E_{\rm C}$. This entropy, defined as

$$S_{\rm C} \equiv \frac{2\pi}{n} E_{\rm C} a \,, \tag{3.49}$$

represents the non-extensive part of the total entropy. As a function of energy and volume it scales like

$$S_{\rm C}(\lambda E, \lambda V) = \lambda^{1-\frac{1}{n}} S_{\rm C} \,, \tag{3.50}$$

i.e. like an area, suggesting that it may have a holographic interpretation. The cosmological Casimir bound, (3.38), can now be reformulated as an entropy bound,

$$S_{\rm C} \leqslant S^{\rm c}_{\rm BH} \,. \tag{3.51}$$

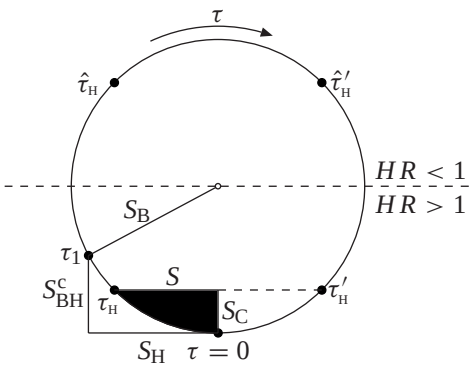

FIGURE 3.3: The entropy S and Casimir entropy $S_{\rm C}$ fill part of the cosmological entropy diagram. If the Bekenstein bound $S \leqslant S_{\rm B}$ holds at one moment, it will continue to hold as long as the total entropy S does not change. The Hubble bound $S \leqslant S_{\rm H}$ restricts the range of τ in the regime $Ha > 1$ to $\tau_{\rm H} \leqslant \tau \leqslant \tau_{\rm H'}$ and is violated in the regime $Ha < 1$ for $\hat{\tau}_{\rm H} \leqslant \tau \leqslant \hat{\tau}'_{\rm H}$. The Casimir bound $S_{\rm C} \leqslant S^{\rm c}_{\rm BH}$ is equivalent to the Hubble bound for $Ha > 1$ and remains valid for $Ha < 1$. Figure adapted from [137].

The total entropy S and the Casimir entropy $S_{\rm C}$ can be naturally incorporated into Figure 3.2. Rewrite the Cardy-Verlinde formula (2.83) as a relation between the entropy S and its super- and sub-extensive counterparts $S_{\rm B}$ and $S_{\rm C}$. One easily checks that it takes the form

$$S^2 + (S_{\rm B} - S_{\rm C})^2 = S_{\rm B}^2 \,. \tag{3.52}$$

This relation has exactly the same form as (3.48). The only difference is that the role of the Hubble entropy and the cosmological Bekenstein-Hawking entropy are taken over by the total entropy and the Casimir entropy. The diagram incorporating S and $S_{\rm C}$ is depicted in Figure 3.3. From this diagram one easily determines the relation between the Casimir bound and the Hubble bound. It is clear that when $Ha > 1$, that is in the strongly self-gravitating phase, the two bounds are equivalent. When the Casimir bound is saturated, $S_{\rm C} = S^{\rm c}_{\rm BH}$, the Hubble bound is also saturated, $S = S_{\rm H}$. The converse statement is not true, as can also easily be seen from Figure 3.3. Indeed, there are two moments in the weakly self-gravitating phase, $Ha < 1$, where $S = S_{\rm H}$, but $S_{\rm C} \neq S^{\rm c}_{\rm BH}$, namely $\tau = \hat{\tau}_{\rm H}, \hat{\tau}'_{\rm H}$. This can be seen as an indication that the cosmological Casimir bound may well be a truly fundamental bound [137]. In preparation for the model that we will introduce in Section 3.5, we now introduce the concept of 'brane worlds'.

3.4 BRANE WORLDS

An interesting new perspective on the merger between the energy and entropy formulas and the equations that govern the cosmological evolution of the above described FRW universe can be obtained from a brane world model. Before discussing the specific model we consider in the next section, we first introduce the general concept of brane worlds.

The accuracy to which the standard model interactions have been tested seems to rule out the possibility of large extra dimensions* beyond the familiar $3+1$ that we observe in everyday life. The standard model has been tested to almost the weak scale, or at least the theoretically predicted value of the weak scale, 10^{-19} m. Gravity, on the other hand, has only been tested up to scales of about 10^{-4} m [72]. This allows for the intriguing possibility that our universe is realized as a D3-brane in a higher dimensional spacetime. The standard model gauge group would be realized on the D-brane worldvolume [22,37, 124] and thus be confined to $3+1$ dimensions, while gravity propagates in all dimensions as it is the dynamics of spacetime itself. Such scenarios are called brane worlds [3,78,108].

In this section, we begin by discussing some technical points regarding the Einstein equations in the context of stress-energy that is localized on a hypersurface, or brane. We then discuss the two brane world models due to Randall and Sundrum [103,104]; in the next section we will use a similar model. Brane worlds have received a lot of attention recently, for a review see [41,47].

3.4.1 ISRAEL MATCHING CONDITIONS

Consider a $d = n+1$-dimensional hypersurface located at coordinate $x^D = 0$ in a $D = d+1$-dimensional bulk spacetime. We assume that the energy content is confined to the codimension one hypersurface, so that the stress-energy tensor takes the form

$$T_{MN} = g^{\mu}_{\text{M}} g^{\nu}_{\text{N}} \hat{T}_{\mu\nu} \delta(x^D) \,, \tag{3.53}$$

where g_{MN} is the bulk metric and M, N take values $1, \ldots, D$ while μ, ν take values $1, \ldots, d$. One can solve the Einstein equations,

$$\mathcal{R}_{MN} - \frac{1}{2}\mathcal{R} g_{\text{MN}} + \Lambda g_{\text{MN}} = 8\pi T_{MN} \,, \tag{3.54}$$

with this ansatz for T_{MN}. For the bulk spacetime the solution is an Einstein space, where

$$\mathcal{R}_{MN} = \frac{2\Lambda}{(d-1)} g_{\text{MN}} \,. \tag{3.55}$$

*In fact, we define 'large' in this way: too large to agree with current experimental data in the conventional framework.

In addition, one finds conditions on the extrinsic curvature $\mathcal{K}_{\mu\nu}$ of the hypersurface, defined by

$$\mathcal{K}_{\mu\nu} \equiv \nabla_\mu n_\nu \,, \tag{3.56}$$

where n^μ is the outward pointing unit normal to the hypersurface. These matching conditions were derived by Israel [75] and take the form

$$\lim_{\epsilon\downarrow 0}\left[\mathcal{K}_{\mu\nu}\right]_{x^D=-\epsilon}^{x^D=\epsilon} = \left(\hat{T}_{\mu\nu} - \frac{1}{d-1} g_{\mu\nu} g^{\alpha\beta}\hat{T}_{\alpha\beta}\right)\Big|_{x^D=0} \,. \tag{3.57}$$

The physical content of this equation is that the extrinsic curvature jumps discontinuously across an energy-momentum carrying codimension one hypersurface. If the spacetime ends at the hypersurface, *i.e.*, when the hypersurface is an energy-momentum carrying boundary, the corresponding extrinsic curvature term disappears and (3.57) becomes a boundary condition on the normal derivative of the metric.

3.4.2 Gibbons-Hawking boundary term

The Einstein equations (3.54) follow by variation from the Einstein-Hilbert action,

$$S_{\rm EH} = \int d^D x \,\sqrt{g}\,(\mathcal{R} - 2\Lambda) \,, \tag{3.58}$$

where g is the absolute value of the determinant of the metric $g_{\rm MN}$. One might expect then that (3.55) and (3.57) could be directly derived from stationarity of the sum of the bulk Einstein-Hilbert and the brane actions,

$$S_{\rm EH} + S_{\rm brane} = \int d^D x \,\sqrt{g}\,(\mathcal{R} - 2\Lambda) + \int_{\mathcal{M}} d^d x \,\mathcal{L}_{\rm b} \,, \tag{3.59}$$

where $\mathcal{M}$ denotes the hypersurface and the brane Lagrangian $\mathcal{L}_{\rm b}$ contains only the matter degrees of freedom and intrinsic curvature terms of the brane. However, this is not the case. Every action that differs from the Einstein-Hilbert action (3.58) by a complete divergence yields the Einstein equations (3.54). But once the brane action is added, as in (3.59), the difference in surface terms between different bulk actions becomes relevant, because the presence of energy-momentum on the brane may spoil the continuity of the surface terms across the brane, implying a numerical difference between the different bulk actions. Therefore, not every bulk action that yields the Einstein equations will yield (3.55) and (3.57) when $S_{\rm brane}$ is added to it. In particular, the Einstein-Hilbert action does not. This can be remedied by adding a Gibbons-Hawking boundary term [52] to (3.59). The appropriate boundary term is given by

$$S_{\rm GH} = -\int_{\mathcal{M}} d^d x \,\sqrt{\hat{g}}\,\mathcal{K} \,, \tag{3.60}$$

where $\mathcal{K} \equiv \mathcal{K}^{\mu}_{\mu}$ is the trace of the extrinsic curvature and $\hat{g}$ denotes the determinant of the induced metric $\hat{g}_{\mu\nu}$ on the brane. Adding this term leads to a well defined variational problem that indeed yields the Einstein condition (3.55) in the bulk and the matching condition (3.57) on the brane.

3.4.3 RANDALL-SUNDRUM MODELS

Randall and Sundrum (RS) [103,104] have proposed two interesting brane world models. Both contain D3-branes in a 5-dimensional background, *i.e.* with one extra dimension. The background geometry of the first scenario (RS1), with two branes, is given by

$$ds^2 = e^{-2kr_c|\phi|}\eta_{\mu\nu}dx^{\mu}dx^{\nu} + r_c^2\, d\phi^2\,. \tag{3.61}$$

As we will show below, this is a slice of AdS_5. The extra dimension, parameterized by ϕ with range $-\pi \leqslant \phi \leqslant \pi$, has the form of an orbifolded circle of radius r_c. The two branes are located at the orbifold fixed points $\phi = 0, \pi$. The 5-dimensional Planck mass M_5 and cosmological constant Λ enter through the constant k,

$$k = \sqrt{\frac{-\Lambda}{24M_5^3}}\,. \tag{3.62}$$

The geometry (3.61) belongs to the class of warped compactifications, in which the higher dimensional geometry is sensitive to the position of the branes. This backreaction on the geometry is caused by the non vanishing of the vacuum energies on the branes, generated by quantum fluctuations in the absence of supersymmetry. The lack of supersymmetry makes it difficult to embed the RS-scenarios into string theory. As was shown by Randall and Sundrum, the effective 4-dimensional mass scales depend on the 5-dimensional mass scales through the warp-factor $e^{-2kr_c|\phi|}$. The relation between them thus will depend on the location in the extra dimension. This allows for large 4-dimensional mass hierarchies to arise from from a fundamental 5-dimensional theory without large hierarchies. The mass parameters of the 5-dimensional theory are taken to be of order the observed Planck scale, $M_{\text{Planck}} \approx 10^{19}\,\text{GeV}$. A general analysis shows that for every massive field the effective mass receives a rescaling

$$m_{\text{eff}} = e^{-kr_c\pi}m_0\,. \tag{3.63}$$

When $kr_c \sim 10$, the exponential factor in (3.63) becomes such that Planck scale masses effectively become of order a TeV. This provides a possible explanation for the large hierarchy between the observed Planck and weak scales, referred to as the gauge hierarchy problem. However, it is replaced by a finetuning of

the compactification radius r_c. Several scenarios for how this radius can be naturally stabilized have been proposed, see for example [54].

The second Randall-Sundrum scenario (RS2) is a single brane modification of the first scenario. The brane located at $\phi = \pi$ is removed from the setup by sending it off to infinity through the decompactification limit $r_c \to \infty$. One is then left with a semi-infinite fifth dimension, now parametrized by z. The metric takes the form

$$ds^2 = e^{-2k|z|}\eta_{\mu\nu}dx^\mu dx^\nu + dz^2\,, \tag{3.64}$$

where we have set $r_c = 1$ through a rescaling of z. At first sight, one might expect the usual problems of large extra dimensions to reappear. In particular, it seems likely that gravity would now be five dimensional. However, calculating the 4-dimensional Planck mass in the RS1 scenario gives

$$M^2_{\text{Planck}} = M_5^3 r_c \int_{-\pi}^{\pi} d\phi\, e^{-2kr_c|\phi|} = \frac{M_5^3}{k}(1 - e^{-2kr_c\pi})\,. \tag{3.65}$$

The important observation is that, in the decompactification limit $r_c \to \infty$, the effective Planck mass remains finite. This means that the graviton zero mode is normalizable and yields a four dimensional Newton's law on the brane located at $z = 0$. Gravity is thus effectively localized on the brane, despite the large extra dimension.

To finish this section, we consider the relation between the holographic principle and the Randall-Sundrum scenarios. There is a particularly concrete connection with the AdS/CFT correspondence, see for example [97,105]. To make this connection explicit, note from (3.62) that the RS solution only makes sense when the bulk cosmological constant Λ is smaller than zero. This suggests that the geometry might look like that of AdS_5. To see that this is indeed the case, write the metric (3.64) in terms of the coordinate

$$u \equiv \frac{\text{sgn}(z)}{k}(e^{k|z|} - 1)\,, \tag{3.66}$$

putting it in the form

$$ds^2 = \frac{1}{(1 + k|u|)^2}\eta_{\mu\nu}dx^\mu dx^\nu + du^2\,. \tag{3.67}$$

On the other hand, recall the AdS_5 metric in Poincaré coordinates,

$$ds^2 = \frac{L^2}{r^2}dr^2 + \frac{r^2}{L^2}\eta_{\mu\nu}dx^\mu dx^\nu\,. \tag{2.49}$$

In terms of a coordinate U, defined trough

$$r \equiv \frac{L^2}{U + L}\,, \qquad (-L < r < \infty)\,, \tag{3.68}$$

this can be written as

$$ds^2 = \frac{1}{(1+\frac{U}{L})^2}\eta_{\mu\nu}dx^\mu dx^\nu + dU^2\,. \tag{3.69}$$

Comparing this with (3.67), we see that the Randall-Sundrum geometry is indeed (part of) an AdS_5 space. The curvature radius of this AdS_5 space is given by $1/k$ and it is only a slice of the full space, since it is cut off at $u = 0$. From (3.68) we see that this cutoff corresponds to $r = L$. Since $r \to \infty$ corresponds to the boundary of AdS, the brane cuts away the region between $r = L$ and the boundary. The brane can thus be interpreted as a IR gravity cutoff. In terms of the AdS/CFT correspondence and in particular the UV/IR connection encountered in Section 2.2.7, this means that the field theory dual to the RS2 scenario is a CFT with a UV cutoff given by k. Note that the cutoff breaks conformal invariance. The conformal anomaly then induces a coupling, through the energy momentum tensor, of the field theory to gravity. In the dual picture, it is these interactions that cause corrections to the 4-dimensional Newton law. The generality of the appearance of gravitational degrees of freedom in the boundary theory, when the radial AdS coordinate is compactified (or semi infinite as in this case), is addressed in [139].

3.5 CFT AND ENTROPY ON THE BRANE

The relation between the entropy, Casimir energy and temperature of the CFT and their cosmological counterparts discussed in Section 3.3 has a very natural explanation from a RS2-type brane world scenario along the lines of [60]. In this section, we will study a brane with fixed tension in the background of an Anti-de Sitter black hole. In this description, the radius of the universe is identified with the distance of the brane to the center of the black hole. At the big bang, the brane originates from the past singularity. At some finite radius, determined by the energy of the black hole, the brane crosses the horizon. It keeps moving away from the black hole, until it reaches a maximum distance and then it falls back into the AdS-black hole. The special moment when the brane crosses the horizon precisely corresponds to the moment when the cosmological entropy bounds are saturated.

We begin by presenting the brane description of a CFT-dominated cosmology in Section 3.5.1. The dimension $d = n+1$ of the brane-universe will be taken to be arbitrary, but its relation with the dimension $D = d+1$ of the AdS space is of course fixed. In Section 3.5.2 we argue that the radiation on the brane can be identified with the CFT dual to the AdS-space and use this fact to fix the normalization of Newton's constant and derive the FRW equations. The entropy density and temperature of the CFT at the moment that the brane

crosses the horizon are calculated in Section 3.5.3. We find that these quantities have a simple expression in terms of the Hubble constant and its time-derivative. In Section 3.5.4 we derive the entropy formulas for the CFT and show the correspondence with the FRW equations. Finally, in Section 3.5.5, we discuss the setup in a Euclidean context.

3.5.1 BRANE COSMOLOGY

We consider a $d = n + 1$ dimensional brane with a constant tension in the background of an $D = d + 1$ dimensional AdS-Schwarzschild black hole. Following the AdS/CFT prescription we regard the brane as the boundary of the AdS-geometry. An important difference is, however, that now the location and the metric on the boundary are, at least partly, dynamical. The movement of the brane is described by the boundary action

$$\mathcal{L}_{\rm b} = \frac{\kappa}{8\pi G_{\rm N}^D}\int_{\mathcal{M}} d^d x\,\sqrt{\hat{g}} - \frac{1}{8\pi G_{\rm N}^D}\int_{\mathcal{M}} d^d x\,\sqrt{\hat{g}}\;\mathcal{K}\,. \tag{3.70}$$

Here κ is a parameter related to the tension of the brane, $\hat{g}$ is the determinant of the induced metric, $\mathcal{M}$ denotes the surface of the brane and we have reinstated the D-dimensional bulk Newton's constant, $G_{\rm N}^D$. The matter Lagrangian for the brane thus consists of only a constant tension term. The appearance of the last term in (3.70), the Gibbons-Hawking boundary term, is explained in Section 3.4.2. Varying the action corresponding to (3.70) gives an equation of motion for the brane that takes the form

$$\mathcal{K}_{\mu\nu} - \mathcal{K}\hat{g}_{\mu\nu} = -\kappa\hat{g}_{\mu\nu}\,, \tag{3.71}$$

where $\mathcal{K}$ denotes the trace of $\mathcal{K}_{\mu\nu}$, the extrinsic curvature defined in (3.56). Taking the trace of this equation leads to

$$\mathcal{K}_{\mu\nu} = \frac{\kappa}{n}\,\hat{g}_{\mu\nu}\,, \tag{3.72}$$

implying that $\mathcal{M}$ is a surface of constant extrinsic curvature.

The bulk action is given by the D-dimensional Einstein action with cosmological term. The AdS-Schwarzschild metric provides a solution of the bulk equations of motion and can be written in the form

$$ds_{\rm b}^2 = \frac{1}{h(a)}da^2 - h(a)dt^2 + a^2 d\Omega_n^2\,, \tag{3.73}$$

where

$$h(a) = \frac{a^2}{R^2} + 1 - \frac{\omega_{n+1}M}{a^{n-1}} \tag{3.74}$$

and R denotes the curvature radius of AdS. The constant

$$\omega_{n+1} = \frac{16\pi G_{\rm N}^D}{n\mathrm{Vol}(S^n)} \tag{3.75}$$

is chosen such that M is the mass of the black hole as measured by an observer who uses t as his time coordinate, *cf.* (2.2).

Our aim is to find the spherically symmetric solutions corresponding to a homogeneous and isotropic induced metric on the brane. Let us parameterize the location of the brane by giving a as a function of the AdS-time t. Equivalently, we may introduce a new time parameter τ and specify the functions

$$a = a(\tau),\ t = t(\tau)\,. \tag{3.76}$$

We will choose the time parameter τ such that the following relation is satisfied,

$$\frac{1}{h(a)}\left(\frac{da}{d\tau}\right)^2 - h(a)\left(\frac{dt}{d\tau}\right)^2 = -1. \tag{3.77}$$

This condition ensures that the induced metric on the brane takes the standard Robertson-Walker form,

$$ds_d^2 = -d\tau^2 + a^2(\tau)d\Omega_n^2\,. \tag{3.78}$$

We note that the size of the $n+1$-dimensional universe is determined by the radial distance, a, from the center of the black hole.

The extrinsic curvature, $\mathcal{K}_{\mu\nu}$, of the brane can be straightforwardly calculated and expressed in term of the functions $a(\tau)$ and $t(\tau)$. One then finds that the equation of motion (3.72) translates into

$$\frac{dt}{d\tau} = \frac{\kappa a}{h(a)}. \tag{3.79}$$

In the following we will tune the $n+1$-dimensional cosmological constant to zero by setting $\kappa = 1/L$. Combining (3.79) with (3.77) leads to an equation that looks suspiciously like the Friedmann equation for a radiation dominated universe,

$$H^2 = -\frac{1}{a^2} + \frac{\omega_{n+1}M}{a^{n+1}}. \tag{3.80}$$

In this equation $H \equiv \dot{a}/a$ is the Hubble constant and the dot denotes differentiation with respect to the cosmological time τ. For future purpose, we also give the equation for the time derivative of H,

$$\dot{H} = \frac{1}{a^2} - \frac{(n+1)}{2}\frac{\omega_{n+1}M}{a^{n+1}}, \tag{3.81}$$

which is obtained by differentiating (3.80).

3.5.2 CFT ON THE BRANE

We now want to identify the equation of motion (3.80) with the d-dimensional Friedmann equation. In particular, we will argue that the radiation can be identified with the finite temperature CFT that is dual to the AdS-geometry. To do so, we interpret the last term on the r.h.s. as the contribution of the energy density ρ of the CFT times the d-dimensional Newton constant $G_{\rm N}^d$. In the brane world scenario the relation between the Newton constant $G_{\rm N}^D$ in the bulk and the Newton constant $G_{\rm N}^d$ on the brane is given by

$$G_{\rm N}^D = \frac{G_{\rm N}^d R}{(n-1)}. \tag{3.82}$$

One possible way to derive this fact is to add a small amount of stress energy on the brane and determine how it effects the equation of motion. This same relation is, as we will discuss, also consistent with the identification of the radiation with the dual CFT.

In [145] it was argued that the energy, entropy and temperature of a CFT at high temperatures can be identified with the mass, entropy and Hawking temperature of the AdS black hole [68]. The CFT lives on a spacetime which, after Euclidean continuation, has the topology of $S^1 \times S^n$ and whose geometry is identified with the asymptotic boundary of the Euclidean AdS-black hole. We remind the reader that the standard GKPW prescription [61,144] of the AdS/CFT correspondence [90] only fixes the conformal class of the CFT metric. It thus specifies only the ratio of the radius of the n-sphere to the Hawking temperature but does not fix the overall scale of the boundary metric. One is therefore free to re-scale the metric as one wishes. It is important to note, however, that such a rescaling does also affect the energy and temperature of the CFT.

To make this more precise, let us consider the asymptotic form of the AdS-Schwarzschild metric (3.73). We have

$$\lim_{a\to\infty}\left(\frac{L^2}{a^2}\, ds_{\rm b}^2\right) = -dt^2 + L^2 d\Omega_n^2\,, \tag{3.83}$$

from which we see that the CFT time is equal to the AdS time t only when the radius of the spatial sphere is set equal to R. Therefore, if we want the sphere to have a radius equal to say a, the CFT time will be equal to at/L. The same factor a/L then appears in the relation between the energy E and the black hole mass M. One thus finds that the energy for a CFT on a sphere with radius a, of volume

$$V = a^n \mathrm{Vol}(S^n)\,, \tag{3.84}$$

is given by

$$E = M\frac{L}{a}\,. \tag{3.85}$$

Note that the total energy E is not constant during the cosmological expansion, but decreases like a^{-1}. This is consistent with the fact that for a CFT the energy density,

$$\rho = \frac{E}{V}\,, \tag{3.86}$$

scales like $a^{-(n+1)}$. Inserting the relation (3.85) combined with (3.82) into the equation of motion (3.80) leads to

$$H^2 = -\frac{1}{a^2} + \frac{16\pi G_{\rm N}^d}{n(n-1)}\rho\,. \tag{3.87}$$

This is the standard Friedmann equation with the appropriate normalization for both terms. By differentiating once with respect to τ and using the fact that $\dot{\rho} = nH(\rho + p)$, one derives the second FRW equation,

$$\dot{H} = \frac{1}{a^2} - \frac{8\pi G_{\rm N}^d}{(n-1)}\,(\rho + p)\,, \tag{3.88}$$

which is equivalent to (3.81). An observer on the brane, who knows nothing about the AdS-bulk gravity, just notices the normal cosmological expansion. The brane description contains more information, since it also knows about the size of the AdS-black hole.

The movement of the brane in the AdS-black hole background is depicted in a Penrose diagram of the spacetime in Figure 3.4. The diagram represents the full geodesically complete black hole geometry including the asymptotic region $a \to \infty$. If one wants to take the brane as the real boundary, one has to cut away the part to the right of the brane. We see that the brane indeed starts inside the black hole at the past singularity and then, as it expands, moves away from $a = 0$. At late times the opposite happens. The points where the brane crosses the black hole horizon will play a central role in the following discussion and have been marked in the figure. These moments are clearly distinguished from the AdS-perspective, even though nothing special happens from the viewpoint of the induced geometry on the brane. So what do these moments mean for an observer on the brane?

3.5.3 Entropy and temperature at the horizon

Let us now consider the points at which the brane crosses the horizon. The horizon of the AdS-black hole is located at radius $a = a_{\rm H}$, where $a_{\rm H}$ is the

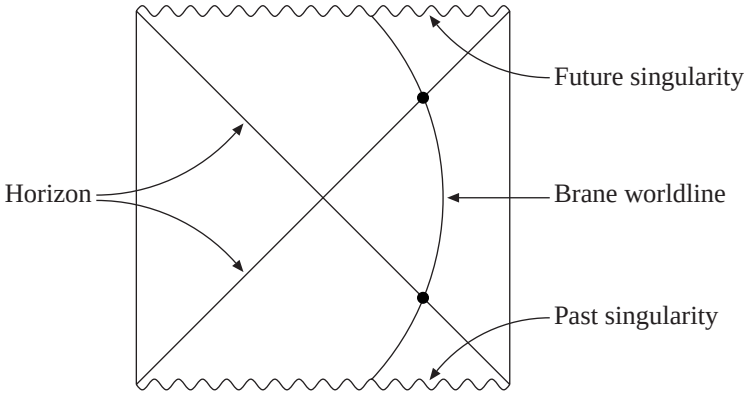

FIGURE 3.4: Penrose diagram of an AdS_{n+2}-Schwarzschild black hole with the trajectory of the brane. The brane originates in the past singularity, expands to a certain size and subsequently falls into the future singularity as it re-collapses. The dots indicate the moments when the brane crosses the black hole horizon.

largest solution to the equation $h(a) = 0$, *i.e.*

$$\frac{a_{\rm H}^2}{L^2} + 1 - \frac{\omega_{n+1} M}{a_{\rm H}^{n-1}} = 0\,. \tag{3.89}$$

From this equation and the equation of motion (3.80), one immediately concludes that the Hubble constant at the horizon obeys

$$H^2 = \frac{1}{L^2}\,, \tag{3.90}$$

and hence $H = \pm 1/L$ depending on whether the brane is expanding or contracting.

Next, let us consider the entropy density. According to [145], the entropy of the CFT is equal to the Bekenstein-Hawking entropy of the AdS-black hole, which is given by the area of the horizon measured in bulk Planckian units. The total entropy may thus be expressed as

$$S = \frac{V_{\rm H}}{4G_{\rm N}^D}\,, \tag{3.91}$$

where $V_{\rm H}$ is the area of the horizon,

$$V_{\rm H} = a_{\rm H}^n \mathrm{Vol}(S^n)\,. \tag{3.92}$$

Note that the area of an n-sphere in AdS equals the volume of the corresponding spatial section for an observer on the brane. The total entropy S is constant during the cosmological evolution but the entropy density,

$$s = \frac{S}{V}\,, \tag{3.93}$$

of course varies with time. It equals

$$s = (n-1)\frac{a_{\rm H}^n}{4G_{\rm N}^d L a^n}\,, \tag{3.94}$$

where we made use of the relation (3.82). What makes the moments that the brane crosses the horizon special is that the entropy density is given by a simple multiple of the Hubble constant H. At the horizon $V = V_{\rm H}$ and hence the entropy density on the brane is $s = 1/4G_{\rm N}^D$. Now, using the relation (3.82) and the fact that $H = 1/L$ one finds that the entropy density equals

$$s = (n-1)\frac{H}{4G_{\rm N}^d} \qquad (a = a_{\rm H})\,. \tag{3.95}$$

The significance of this relation will be further discussed below.

Also the temperature turns out to have a special value at the horizon. The Hawking temperature measured by an observer who uses t as his time coordinate is [60,145]

$$T_{\rm H} = \frac{h'(a_{\rm H})}{4\pi}\,, \tag{3.96}$$

where the prime denotes differentiation with respect to a. Since the CFT time differs from t by a factor a/L the CFT-temperature T will differ from the Hawking temperature $T_{\rm H}$ by the same a-dependent factor,

$$T = T_{\rm H}\frac{L}{a}\,. \tag{3.97}$$

Using the explicit form of $h'(a_{\rm H})$ and using the fact that $h(a_{\rm H}) = 0$, we eventually find

$$T = \frac{1}{4\pi a}\left[(n+1)\frac{a_{\rm H}}{L} + (n-1)\frac{L}{a_{\rm H}}\right]. \tag{3.98}$$

Now, from the derivation of the brane equation of motion, it follows that the quantities H^2 and $-h(a)/a^2$ only differ by a constant and therefore, at the horizon where $h(a_{\rm H}) = 0$, we have that $\dot{H} = -h'(a_{\rm H})/2a_{\rm H}$. This can be used to show that the temperature at the horizon may be expressed in the Hubble constant H and its time derivative $\dot{H}$ as

$$T = -\frac{\dot{H}}{2\pi H} \qquad (a = a_{\rm H})\,, \tag{3.99}$$

cf. (3.45).

3.5.4 Entropy formulas and FRW equations

The above relations between the entropy density and temperature on the one hand, and the Hubble constant, its time derivative and Newton's constant on the other are valid only when the brane crosses the horizon. However, since the entropy density, temperature and energy density all vary in a precisely prescribed manner as a function of the radius a, these relations imply a set of entropy formulas that remain valid at all times.

Before making this point clear, let us first briefly discuss some basic thermodynamics. The first law of thermodynamics,

$$TdS = dE + pdV\,, \tag{3.100}$$

can after some straightforward manipulations be rewritten in terms of the entropy and energy densities s and ρ as

$$Tds = d\rho + n(\rho + p - Ts)\frac{da}{a}\,, \tag{3.101}$$

where we used that $dV = {}^{nVda}/_{a}$. The combination $(\rho + p - Ts)$ is in most standard textbooks on cosmology [84,140] assumed to vanish, which is equivalent to saying that the entropy and energy are purely extensive. But let us now compute it for the CFT. The energy density is given by

$$\rho = \frac{ML}{a^{n+1}\mathrm{Vol}(S^n)}\,. \tag{3.102}$$

For our purpose, it is convenient to rewrite ρ in terms of the horizon radius $a_{\rm H}$ using $h(a_{\rm H}) = 0$. This gives

$$\rho = \frac{na_{\rm H}^n}{16\pi G_{\rm N}^D a^{n+1}}\left(\frac{L}{a_{\rm H}} + \frac{a_{\rm H}}{L}\right)\,. \tag{3.103}$$

The pressure follows from ρ through the equation of state $p = {}^{\rho}/_{n}$. Combined with (3.94) and (3.98), one gets

$$\frac{n}{2}(\rho + p - Ts) = \frac{\gamma}{a^2}\,, \tag{3.104}$$

where the quantity γ is given by

$$\gamma = \frac{n(n-1)a_{\rm H}^{n-1}}{16\pi G_{\rm N}^d a^{n-1}}\,. \tag{3.105}$$

Equation (3.104) may be regarded as the definition of γ. Physically one can think of γ as describing the response of the energy density under variations of

the radius a or, more precisely, the spatial curvature $1/a^2$. It thus represents the geometrical Casimir part of the energy density.

We are now ready to present the main entropy formula for CFT's which have an AdS dual. The Cardy-Verlinde formula was already derived in Section 2.2.8 and expressed in terms of the total energy and entropy. Here we will give the local version in terms of densities. From the given expressions for the entropy density s, energy density ρ and γ, one finds that s may be expressed as

$$s^2 = \left(\frac{4\pi}{n}\right)^2 \gamma \left(\rho - \frac{\gamma}{a^2}\right) . \tag{3.106}$$

As noted in Section 2.2.8, this formula resembles the Cardy formula for a CFT in $1+1$ dimensions, but is valid for all spatial dimensions n.

The formulas (3.104) and (3.106) are valid at all times. It will be interesting, however, to study these formulas at the special time when the brane crosses the horizon. First we note that at that time the Casimir quantity γ equals

$$\gamma = \frac{n(n-1)}{16\pi G_{\rm N}^d} \qquad (a = a_{\rm H}) . \tag{3.107}$$

Let us now consider the entropy formula (3.106). By making the identifications (3.95) and (3.107) one sees that this formula exactly reproduces the Friedmann equation! Similarly, one finds that equation (3.104) reduces to the second FRW equation for $\dot{H}$ by making the same substitutions for s and γ and replacing the temperature T by the r.h.s. of (3.99). In fact, the equations (3.104) and (3.106) are equations of state of the CFT and in principle have an interpretation that is independent of gravity or cosmology. It seems therefore rather surprising that the Friedmann equation knows about the thermodynamic properties of the CFT.

3.5.5 Euclidean brane cosmology

In principle one can use the present setup to calculate the correlation functions of operators in the CFT/FRW cosmology, in particular the stress energy tensor, using the same methods as in the standard AdS/CFT setup. This would for example give information about fluctuations in the energy density in the early universe. As described above, the brane starts out as a point in the past singularity of the black hole. The presence of this singularity may lead to problems in performing these calculations in Minkowski signature. On the gravity side a singularity is associated with the UV properties of the theory, *i.e.* to very high energies. However, through the UV/IR-connection [127] known from AdS/CFT, on the field theory side this in fact corresponds to the IR, *i.e.* to very low energies. As it is the CFT that describes the matter in the universe,

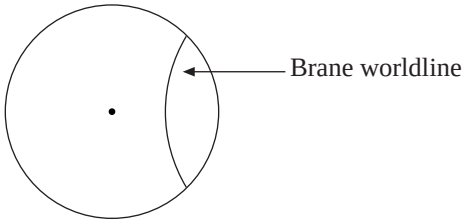

FIGURE 3.5: Diagram of Euclidean AdS_{n+2}-Schwarzschild with the trajectory of the brane. The horizon is represented by the dot in the middle of the diagram; only the region $a \geq a_{\text{H}}$ is drawn. The brane originates at spatial infinity, collapses to a certain minimal size and subsequently re-expands. It remains outside of the black hole horizon during the entire evolution.

this seems strange since conventionally one associates the UV with the early universe.

To calculate correlation functions one can circumvent this problem by analytically continuing to the Euclidean setup. So let us briefly discuss how to describe the Euclidean FRW universe as a brane in an Euclidean AdS-Schwarzschild background. Going through the calculation in a similar way as performed above, one arrives at the following Friedmann equation

$$H_{\text{E}}^2 = \frac{1}{a^2} - \frac{16\pi G_{\text{N}}^d}{n(n-1)}\rho\,. \tag{3.108}$$

From this one easily deduces that the universe, when regarded in Euclidean time, undergoes a reverse evolution, starting out very big, collapsing to a minimal size and subsequently re-expanding. This is depicted in figure 3.5. From the CFT point of view, this means that the universe starts in the far UV, then cools down to a certain minimum temperature after which it re-heats. Note that in this case, the brane does not cross the horizon at all.

3.6 SUMMARY AND CONCLUSION

The main purpose of this chapter has been to apply the holographic principle to a study of the entropy bounds that hold in a radiation dominated universe. This radiation was represented as an interacting CFT with large central charge. This led to the appearance of a fundamental relation between the entropy formulas for the CFT and the FRW equations that govern the cosmological evolution. It is very surprising that the CFT appears to know about the holographic entropy

bounds and the FRW equations appear to know about the entropy formulas for the CFT. The bounds that hold in the early universe on the temperature, entropy and Casimir energy are summarized in Table 3.1 [137].

CFT-bound	FRW-definition
$T \geqslant T_{\rm H}$	$T_{\rm H} \equiv -\frac{\dot{H}}{2\pi H}$
$S \leqslant S_{\rm H}$	$S_{\rm H} \equiv (n-1)\frac{HV}{4}$
$E_{\rm C} \leqslant E^{\rm c}_{\rm BH}$	$E^{\rm c}_{\rm BH} \equiv n(n-1)\frac{V}{8\pi a^2}$

TABLE 3.1: Summary of cosmological bounds.

The matching of the Cardy-Verlinde formula for the CFT and the Euler relation for the Casimir energy with the Friedmann equations written in terms of the quantities listed in Table 3.1, is summarized in Table 3.2 [137].

CFT-formula	FRW-equation
$S = \frac{2\pi a}{n}\sqrt{E_{\rm C}(2E - E_{\rm C})}$	$S_{\rm H} = \frac{2\pi a}{n}\sqrt{E_{\rm BH}(2E - E_{\rm BH})}$
$E_{\rm C} \equiv n(E + pV - TS)$	$E^{\rm c}_{\rm BH} = n(E + pV - T_{\rm H}S_{\rm H})$

TABLE 3.2: Matching between the CFT-formulas and the FRW-equations.

The presented relation between the FRW equations and the entropy formulas precisely holds at the transition point, when the cosmological entropy bounds are saturated. As discussed in Section 3.5, the moments at which the merger occurs play a special role from a brane world perspective. Indeed, they are precisely the moments when the brane crosses the black hole horizon. It was suggested that the values for s and T on the horizon should be regarded as bounds on these respective quantities. Although we still have no proof of this,

note the following. At the moment when the brane crosses the horizon, the quantity γ is essentially equal to the inverse Newton's constant. This means that the response of the energy density to a variation of the curvature is comparable to that of the Einstein action itself. Namely, from (3.104) and (3.107) one finds

$$a\left(\frac{\partial\rho}{\partial a}\right)_s = \frac{-n(n-1)}{8\pi G_{\rm N}^d a^2} \qquad (a = a_{\rm H})\,. \tag{3.109}$$

The right hand side also gives the contribution of the spatial curvature in the equation of motion. Clearly, when this is the case one should reconsider the validity of the usual formulation of gravity, since quantum effects (the Casimir energy density) are of the same order as the spatial curvature. This suggests that a classical description of the geometry of the universe may no longer be well defined and one has to go over to a different, more fundamental formulation of the theory. We have indeed noticed that, at the transition points, the laws that govern the gravitational evolution and the entropy and energy expressions for the CFT, that describes the radiation, merge in a surprising way. This indicates that both sets of equations have a common origin in a single underlying fundamental theory.

We have put the (effective) cosmological constant to zero, since only in that case everything works so nicely. It should be possible to include a cosmological constant, but this complicates the analysis. In particular, one needs to replace H in Hubble entropy bound by

$$\sqrt{H^2 - \frac{\Lambda}{n}}\,. \tag{3.110}$$

We lack a complete understanding of the case $\Lambda \neq 0$ at this time.

4

HOLOGRAPHY IN DE SITTER SPACE

More or less satisfying formulations of holography and, more generally, quantum gravity in Minkowski and Anti-de Sitter space have been obtained. Having thus addressed flat and negatively curved spaces, a natural next step would be to consider positively curved space, or de Sitter space. This case, however, has proven to be particularly difficult and a full description of quantum gravity in de Sitter space is still lacking. With recent observational data [98,106,113] indicating that the universe may be entering a de Sitter phase, this issue has taken on added significance.

Naturally, this has led to a lot of interest in the subject and in this chapter we will review some recent developments, focusing on the formulation of the holographic principle in de Sitter space. Of particular importance is the issue of finding a de Sitter solution to string theory. This would be an important step forward, but attempts in this direction have failed so far. Nonetheless, analogous to the well established AdS/CFT correspondence discussed in Section 2.2, progress has been made in formulating a similar correspondence in the de Sitter case.

We begin this chapter, in Section 4.1, by discussing the classical geometry of de Sitter space. Next, in Section 4.2, we discuss the notions of energy and entropy in a de Sitter context. In Section 4.3, we consider the recently proposed dS/CFT correspondence. Finally, in Section 4.4, we consider an interesting scenario in which the evolution of the universe corresponds to an RG-flow in the dual CFT. We consider a c-theorem in this context and its relation to the size of the apparent horizon in de Sitter space. Detailed accounts of the classical properties of this space can be found in [67,118]; observational constraints and theoretical approaches to the cosmological constant are reviewed in [31,141].

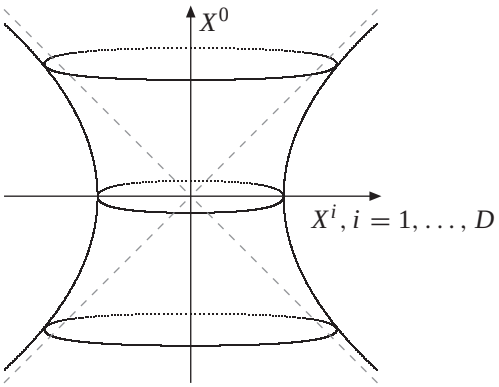

FIGURE 4.1: De Sitter space realized as a hyperboloid in flat Minkowski space.

4.1 CLASSICAL GEOMETRY OF DE SITTER SPACE

Pure de Sitter space is the unique vacuum solution to the Einstein equations with maximal symmetry and constant positive curvature. In $D = n+1$ space-time dimensions, it is locally characterized by

$$\mathcal{R}_{\mu\nu} = \frac{D-1}{R^2} g_{\mu\nu} \,, \tag{4.1}$$

where R is the radius of curvature of de Sitter space, and by the vanishing of the Weyl tensor. The cosmological constant, Λ, is given as a function of R by

$$\Lambda = \frac{(D-1)(D-2)}{2R^2} \,. \tag{4.2}$$

It is convenient to think of de Sitter space as a hypersurface embedded in $D+1$-dimensional flat Minkowski space. The embedding equation is

$$-X_0^2 + X_1^2 + \ldots + X_D^2 = R^2 \tag{4.3}$$

and the resulting timelike hyperboloid is depicted in Figure 4.1. The embedding equation (4.3) makes manifest the $O(1, D)$ isometry group of de Sitter space. The de Sitter metric is the induced metric from the flat Minkowski metric on the embedding space. In this way several coordinate systems can be obtained.

Frequently used are the so called global coordinates, in terms of which the metric takes the form

$$ds^2 = -dT^2 + R^2 \cosh^2 T/R \, d\Omega_n^2 \,. \tag{4.4}$$

The time coordinate T takes values $-\infty < T < \infty$. In these coordinates, which cover all of the hyperboloid shown in Figure 4.1, de Sitter space starts out as an infinitely large n-sphere at $T = -\infty$. Subsequently, it shrinks and reaches its minimal radius R at $T = 0$, after which it re-expands. Note that the global time coordinate T does not define a Killing vector. The appearance of a cosmological horizon is not manifest in these coordinates. Before discussing other useful coordinate systems for de Sitter space, we first consider its Penrose diagram.

4.1.1 Penrose diagram of de Sitter space

To elucidate the causal structure of de Sitter space, it is useful to construct the corresponding Penrose diagram. Through the coordinate transformation

$$\cosh T/R = \frac{1}{\cos \tau/R}\,, \tag{4.5}$$

put the metric (4.4) in the form

$$ds^2 = \frac{1}{\cos^2 \tau/R}(-d\tau^2 + R^2 d\Omega_n^2)\,. \tag{4.6}$$

The range of the new time coordinate τ is $-\pi/2 < \tau/R < \pi/2$. Without affecting the causal structure, we can perform a conformal transformation, bringing the metric to the from

$$d\hat{s}^2 = \cos^2 \tau/R\, ds^2 = -d\tau^2 + R^2 d\Omega_n^2\,. \tag{4.7}$$

This can also be written as

$$d\hat{s}^2 = -d\tau^2 + R^2 \left(d\theta^2 + \sin^2\theta\, d\Omega_{n-1}^2\right)\,, \tag{4.8}$$

where θ is a polar angle with range $0 \leqslant \theta \leqslant \pi$. This leads to the square Penrose diagram depicted in Figure 4.2, where every point is a $n-1$-dimensional sphere with radius $R\sin\theta$. The equal time slices in global coordinates correspond simply to horizontal lines in the Penrose diagram. From the diagram it is clear that no observer can ever see all of de Sitter space. An observer on the south pole can see, as he approaches $\mathcal{I}^+$, all events that happened in regions I and III. Similarly, he can send signals to events in regions I and IV. In the intersection of these, *i.e.* in region I, he can send signals to as well as receive signals from all events; this we call his causal diamond, or static patch. Region II, the causal diamond of an observer on the north pole, remains completely inaccessible to the observer on the south pole.

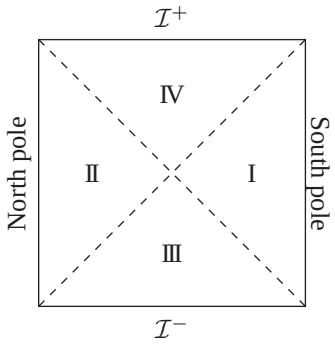

FIGURE 4.2: Penrose diagram of de Sitter space. Every point represents an S^{D-2}, except the north and south poles which are points. A horizontal slice forms an S^{D-1}. The dashed lines indicate the past and future horizons of an observer on the south pole. The asymptotic past and future, indicated by $\mathcal{I}^-$ and $\mathcal{I}^+$ respectively, correspond to $\tau = \pm\pi/2$. The diagram is divided into four regions, as explained in the text.

Another way to see that the Penrose diagram must be square is the following. Consider where a light ray that originates from the south pole at $\mathcal{I}^-$ ends up on $\mathcal{I}^+$. Choosing the ray such that it only moves in the θ-direction selected in (4.8), we have from (4.4) that

$$dT^2 = R^2 \cosh^2 T/R \, d\theta^2 \,. \tag{4.9}$$

The distance the light ray will travel in the θ-direction before it reaches $\mathcal{I}^+$ is therefore given by

$$\Delta\theta \equiv \int_{-\infty}^{\infty} dT \frac{d\theta}{dT} = \int_{-\infty}^{\infty} dT \frac{1}{R \cosh T/R} = \pi \,. \tag{4.10}$$

We see that it will exactly reach the north pole, independent of the value of R, *i.e.*, independent of the cosmological constant Λ. It is interesting to consider what happens when one perturbs de Sitter space by adding some energy density to it. Like in Chapter 3, let us consider a radiation dominated FRW cosmology with radiation density ρ, but now with a positive cosmological constant. The Friedmann equation (3.3) becomes

$$H^2 = \frac{16\pi G_{\rm N}}{n(n-1)}\rho - \frac{1}{a^2} + \frac{2\Lambda}{n(n-1)} \,, \tag{4.11}$$

while the second Friedmann equation (3.4) remains unchanged. The metric

takes the general form

$$ds^2 = -dt^2 + a^2(t)\, d\Omega_n^2 \,. \tag{4.12}$$

For the spacetime to be of the de Sitter form (4.4) at late times, ρ cannot be larger than a certain critical value. For larger values of ρ the spacetime will collapse to form a black hole instead of re-expanding. We will give a general definition of the notion 'asymptotically de Sitter' in Section 4.3.1. Precisely at the critical radiation density, the space will asymptote to its smallest radius and subsequently remain static instead of re-expanding. This final state is of course unstable as small perturbations will cause the space to either collapse to a black hole or to start expanding. The critical value for ρ and the minimal radius $a_{\rm c}$ are given by

$$\rho_{\rm c} = \frac{2\Lambda}{8\pi G_{\rm N}} \left(\frac{R_{\rm c}}{a}\right)^{n+1} , \tag{4.13}$$

$$a_{\rm c} = \sqrt{\frac{n(n-1)^2}{2\Lambda(n+1)}} \,. \tag{4.14}$$

Now take the radiation density to be a fraction of this critical density,

$$\rho = \alpha \rho_{\rm c} \,, \tag{4.15}$$

where $0 \leqslant \alpha \leqslant 1$. Solving (4.11) for $a(t)$ gives (henceforth setting $n = 3$)

$$a^2(t) = \frac{R^2}{2} \left(1 + \sqrt{1-\alpha}\, \cosh 2t/R\right) . \tag{4.16}$$

Using the identity $\cosh 2x = 2\cosh^2 x - 1$, we see that for $\alpha = 0$ this reduces to the pure de Sitter case (4.4), as expected. On the other hand, the critical case $\alpha = 1$ does not behave as described above. Instead, that behaviour corresponds to the particular solution

$$a^2(t) = \frac{R^2}{2} \left(1 + \frac{1}{3} e^{-\frac{2t}{R}}\right) . \tag{4.17}$$

For completeness, we also note the general solution, valid for any value of α,

$$a^2(t') = \frac{R^2}{2} \left[1 + \frac{1}{3} e^{-\frac{2t'}{R}} + \frac{3}{4}(1-\alpha) e^{\frac{2t'}{R}}\right] , \tag{4.18}$$

where the new time coordinate t' is defined by

$$t' = t + \frac{R}{4} \ln\left[\frac{9}{4}(1-\alpha)\right] . \tag{4.19}$$

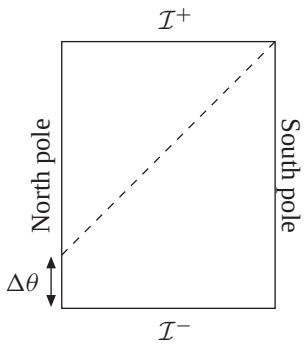

FIGURE 4.3: Rectangular Penrose diagram corresponding to perturbed de Sitter space. The past horizon of an observer on the south pole is indicated. The amount by which the diagram deviates from being square, the extra vertical length $\Delta\theta$, is proportional to the perturbation, *i.e.*, to the radiation density ρ in the case considered.

Using the solution (4.16), we can now repeat the calculation (4.10) for $\Delta\theta$. Since again the result is independent of Λ, we put $R \equiv 1$. This leads to the expression

$$\Delta\theta = \int_{-\infty}^{\infty} dt \left(\frac{2}{1+\sqrt{1-\alpha}\cosh 2t} \right)^{\frac{1}{2}} . \tag{4.20}$$

Expanding for small α gives

$$\lim_{\alpha\to 0} \Delta\theta = \int_{-\infty}^{\infty} dt \left[\frac{1}{\cosh t} + \alpha \frac{\cosh 2t}{8\cosh^3 t} + \mathcal{O}(\alpha^2) \right] , \tag{4.21}$$

$$= \pi + \alpha \frac{3\pi}{16} + \mathcal{O}(\alpha^2) . \tag{4.22}$$

We thus find that in this case the light ray overshoots the antipodal point by some amount proportional to the energy density. This causes the Penrose diagram to become rectangular in shape, as shown in Figure 4.3. It was shown by Gao and Wald [50] that the same thing happens for general perturbations of de Sitter space. These 'tall' de Sitter spaces were considered in [87]. It is important to realize that this elongation of the Penrose diagram has drastic consequences for the causal structure of the spacetime. For example, an observer can now receive information from everywhere on $\mathcal{I}^-$ at a finite time, *i.e.*, before he reaches $\mathcal{I}^+$. These changes in the causal structure present a severe challenge to the antipodal identification considered in the next chapter. We will comment on this in Section 5.7.

4.1.2 COORDINATE SYSTEMS

A coordinate set that is especially well adapted to describe a specific observer are the static coordinates. In these coordinates, the metric takes the form

$$ds^2 = -\left(1 - \frac{r^2}{R^2}\right) dt^2 + \frac{dr^2}{1 - \frac{r^2}{R^2}} + r^2 d\Omega_{n-1}^2 \,. \tag{4.23}$$

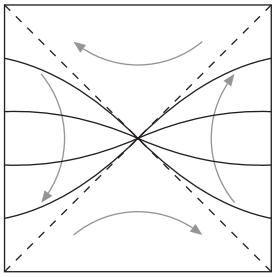

FIGURE 4.4: Equal time slices in static coordinates.

The cosmological horizon is at $r_{\rm C} = R$ and $\partial/\partial t$ now is a Killing vector, although not globally timelike. Constructing these coordinates for an observer at the south pole, $r = 0$ corresponds to the south pole and the corresponding causal diamond (region I in Figure 4.2) has $0 \leqslant r \leqslant R$. The Killing vector $\partial/\partial t$ is timelike in region I, making it a suitable generator of time evolution for this observer. But in regions III and IV, this vector becomes spacelike. In region II, it is again timelike, but it is directed in the opposite direction from region I, *i.e.* towards the past. The lack of a globally timelike Killing vector in de Sitter space affects the notions of entropy and energy as well as complicates the quantization of fields on this background. The equal time slices in the northern and southern causal diamonds are shown in Figure 4.4, where also the direction of the Killing field $\partial/\partial t$ is indicated.

Another coordinate set, which we will encounter often, covers only half of de Sitter space. These are the planar coordinates appropriate for a big bang (or big crunch) de Sitter model. The metric takes the form

$$ds^2 = -dt^2 + e^{\pm\frac{2t}{R}} dx_i dx^i \,, \tag{4.24}$$

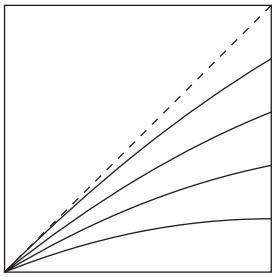

FIGURE 4.5: Equal time slices in planar coordinates.

and, when applied to the south pole and depending on the sign in the exponential, covers either regions I and III or I and IV. These coordinates derive their name from the fact that the equal time slices, as depicted in Figure 4.5 for the combined regions I and III, are flat n-planes.

For future purpose, we introduce the Schwarzschild-de Sitter solution. In $D = n+1$ dimensions, the line element in static coordinates takes the form

$$ds^2 = -F(r)\, dt^2 + F^{-1}(r)\, dr^2 + r^2 d\Omega_{n-1}^2 \,, \tag{4.25}$$

$$F(r) = 1 - \frac{2M}{r^{d-2}} - \frac{r^2}{R^2} \,. \tag{4.26}$$

De Sitter space cannot support arbitrarily large black holes. In fact, the size of any object in de Sitter space is limited by the cosmological horizon. Putting a black hole in de Sitter space gives rise to a second horizon, namely a black hole horizon besides the cosmological horizon. Their locations, denoted respectively by r_{BH} and r_C, are the positive roots of the equation $F(r) = 0$. The bound on the size of the black hole can then be expressed as $r_C \geqslant r_{BH}$. This limits the mass of the black hole to be within the range $0 \leqslant M \leqslant M_{\max}$, where

$$M_{\max} = \frac{1}{D-1}\left(\frac{(D-3)(D-2)}{2\Lambda}\right)^{\frac{D-3}{2}} . \tag{4.27}$$

When $M = M_{\max}$, the black hole horizon coincides with the cosmological horizon.

4.2 Energy and Entropy

In a gravitational background there is no local notion of energy. However, the total energy can generally be defined, using an asymptotically timelike Killing vector. Since there exists no globally timelike Killing vector in de Sitter space, one cannot define a Hamiltonian in this way. Due to the spatial compactness, de Sitter space cannot support conserved Noether charges like mass and angular momentum. The only asymptotic regions within de Sitter space are temporal past and future infinity. An alternative definition of mass, using the Brown-York stress tensor, is given in [8].

In the absence of a Hamiltonian, there is no global notion of time-evolution. Indeed, we have seen above that the most natural timelike Killing vector to define the evolution of an observer, points towards the past in part of de Sitter space. Thus, a particle moving forward in time with respect to one observer, would be conceived as moving backwards in time by a second observer; that is, if he were able to see it. Note, however, that these different regions are causally disconnected. These considerations will play an important role in the next chapter.

4.2.1 Entropy

One of the most enigmatic features of de Sitter space is its entropy [10]. That de Sitter space has a finite entropy may be expected, based on the appearance of a horizon in pure de Sitter. This horizon is, however, qualitatively different from a black hole horizon. The position of the horizon is observer dependent and, because of this, it is not entirely clear which concepts about black holes carry over to de Sitter space. In fact, the de Sitter cosmological horizon looks in many ways like the Rindler horizon in Minkowksi space.

It was, however, shown by Gibbons and Hawking [53] that entropy and temperature can be ascribed to the cosmological horizon just as in the black hole case. Indeed, an observer in de Sitter space will observe a background of thermal radiation coming from the cosmological horizon that surrounds him.* The area of the horizon is then a measure of the information hidden by it from the observer. By absorbing this thermal radiation, the observer can presumably gain knowledge on what lies beyond the horizon; thus causing the horizon to shrink. Indeed, in pure – or empty – de Sitter space the horizon size is maximal.

The radius of the cosmological horizon in D-dimensional de Sitter space, as described by the metric (4.23), is given by

$$r_{\mathrm{C}} = R = \sqrt{\frac{(D-1)(D-2)}{2\Lambda}} \overset{(D=4)}{=} \sqrt{\frac{3}{\Lambda}}\,. \tag{4.28}$$

The horizon area then becomes

$$A_{\mathrm{C}} = \frac{2\pi^{\frac{n}{2}}}{\Gamma(\frac{n}{2})}\left(\frac{(D-1)(D-2)}{2\Lambda}\right)^{\frac{D-2}{2}} \overset{(D=4)}{=} \frac{12\pi}{\Lambda}\,, \tag{4.29}$$

where Γ denotes the Euler Gamma function. The corresponding Bekenstein-Hawking entropy equals

$$S_{\mathrm{dS}} = \frac{A_{\mathrm{C}}}{4G_{\mathrm{N}}}\,, \tag{4.30}$$

as usual. From the metric one can also deduce the Hawking temperature of the black hole by demanding it to be regular across the horizon. This leads to

$$T_{\mathrm{H}} = \frac{1}{4\pi}\sqrt{\frac{8\Lambda}{(D-1)(D-2)}} \overset{(D=4)}{=} \frac{1}{\pi}\sqrt{\frac{\Lambda}{12}}\,. \tag{4.31}$$

The values for the 4-dimensional case agree with those given in [53].

It is natural to interpret the Bekenstein-Hawking entropy for de Sitter space as the logarithm of the number of quantum states necessary to describe such a universe [12]. This is similar to the interpretation of the Bekenstein-Hawking entropy for a black hole, as discussed in Section 2.1.1, and extends the analogy between the two cases. More precisely, the Hilbert space of quantum gravity in asymptotically de Sitter space has finite dimension $\mathcal{N}$, in terms of which the entropy is given by

$$S_{\mathrm{dS}} = \ln \mathcal{N}\,, \tag{4.32}$$

cf. (4.30). Since in the presence of gravity the metric fluctuates, we need to speak of *asymptotically* de Sitter space. Keep in mind, however, that the only asymptopia are in the past and future; there is no spatial infinity.

*Note the necessity of an observer dependent notion of particles.

It is the finiteness of the entropy (4.30), and hence of the dimensionality of the Hilbert space, that leads to conceptual problems. It appears to be irreconcilable, for example, with the fact that at early times de Sitter space has very large volume. One can impose boundary conditions that have entropy larger than (4.32), where $\mathcal{N}$ is fixed by the value of the cosmological constant. However, these initial conditions will not evolve into a spacetime that is again de Sitter in the future. Said differently, the Einstein equations ensure that the FSB bound, the generalized Fischler-Susskind bound discussed in Section 3.2.1, is not violated.

Another important implication of a finite dimensional Hilbert space is that the de Sitter symmetry group, $O(D,1)$, cannot act on it [142]. Indeed, $O(D,1)$ is non compact and does not have (nontrivial) finite-dimensional unitary representations. In fact, one should not expect the full de Sitter group to act on the Hilbert space. The symmetry generators can be expressed as surface terms at infinity and, as we have seen before, de Sitter space cannot support such conserved charges. Hence, the de Sitter generators are zero. Any quantum gravity theory on de Sitter space will thus not have the full de Sitter isometry group that is the symmetry group of classical de Sitter space. The elliptical modification of de Sitter space that is the subject of Chapter 5 suggests that the relevant group is actually the compact subgroup $\mathrm{SO}(D-1)$ of the full isometry group. This allows for unitary representations related to the de Sitter entropy, as discussed in Section 5.5.4.

4.2.2 Bounds from the cosmological horizon

As noted above, the cosmological horizon in de Sitter space attains its maximal size for pure de Sitter. Thus, pure de Sitter constitutes a state of maximal entropy for universes with a positive cosmological constant that tend towards pure de Sitter in the future, as can be understood in the following way. The exponential expansion of space will cause anything present within a cosmological horizon to be swept out of it, eventually leaving pure de Sitter. From the second law of thermodynamics we infer that entropy must have increased in the process. The generic final stage of such evolution being pure de Sitter, this must constitute a state of maximal entropy. By Bousso's [25] proof of the so called N-bound this is generalized to include *any* universe with positive cosmological constant, not necessarily asymptoting to pure de Sitter in the future; see also [8,89].

In Section 2.1.2, we derived entropy bounds from studying the dynamics of black hole horizons. Similarly, entropy bounds can be derived from the cosmological horizon in de Sitter space. Consider a matter system, including possibly black holes, with entropy S_{m} in asymptotically de Sitter space. By above arguments, the system is surrounded by a cosmological horizon with

area

$$A'_{\rm C} < A_{\rm C}\,, \tag{4.33}$$

where $A_{\rm C}$ is the horizon area in pure de Sitter given by (4.29). The total entropy then equals

$$S_{\rm total} = S_{\rm m} + \frac{A'_{\rm C}}{4}\,. \tag{4.34}$$

From the point of view of an observer, the entire matter system will at some point pass through the horizon, as the final state is pure de Sitter space. In this process, the matter entropy $S_{\rm m}$ is lost, while the Bekenstein-Hawking entropy of the cosmological horizon increases by an amount

$$\Delta S_{\rm dS} = \frac{1}{4}(A_{\rm C} - A'_{\rm C})\,. \tag{4.35}$$

The generalized second law (2.8), with black hole entropy generalized to cosmological horizons, implies that the total entropy must not decrease, *i.e.*

$$\Delta S_{\rm dS} \geqslant S_{\rm m}\,. \tag{4.36}$$

This gives a bound on the matter entropy,

$$S_{\rm m} \leqslant \frac{1}{4}(A_{\rm C} - A'_{\rm C})\,, \tag{4.37}$$

called the D-bound [25] on matter systems in asymptotically de Sitter space. Its relation to the Bekenstein bound is considered in [26].

As an example, let us check the D-bound for a black hole in de Sitter, as described by the Schwarzschild-de Sitter solution (4.25). For concreteness, we take $D = 4$, so that the metric reduces to

$$ds^2 = -F(r)\,dt^2 + F^{-1}(r)\,dr^2 + r^2 d\Omega_2^2\,, \tag{4.38}$$

$$F(r) = 1 - \frac{2M}{r} - \frac{r^2}{R^2}\,, \tag{4.39}$$

and $M_{\rm max} = 1/3\sqrt{\Lambda}$. For $M < M_{\rm max}$, there are two horizons, whose locations are given by the positive roots of $F(r)$ and depend on the mass. These are the cosmological horizon, $r_{\rm C}$, and the black hole horizon, $r_{\rm BH}$, where $r_{\rm C} < r_{\rm BH}$. For $M = 0$, corresponding to pure de Sitter, there is only a cosmological horizon, no black hole horizon. For $M = M_{\rm max}$, the two horizons coincide. It is easy to see that in between these two values of the mass, the black hole radius *increases* monotonically, while the cosmological radius *decreases* monotonically. This confirms the relation (4.33) for the case of a black hole in de Sitter space. More precisely, the entropy of Schwarzschild-de Sitter is given by

$$S_{\rm SdS} = \pi(r_{\rm BH}^2 + r_{\rm C}^2) \tag{4.40}$$

and the D-bound, (4.37), states that

$$S_{\rm SdS} \leqslant \pi R^2 \,. \tag{4.41}$$

Note, that the cosmological horizon for pure de Sitter equals the radius of curvature, $r_{\rm C} = R$. Solving the cubic equation $F(r) = 0$ for its positive roots, gives for small M [26]

$$S_{\rm SdS} = \pi R^2 \left(1 - \frac{2M}{R}\right) + \mathcal{O}(M^2) \,. \tag{4.42}$$

This is a monotonically decreasing function of M, as expected. For the maximum value of the mass, $M = M_{\rm max}$, one finds $S_{\rm SdS} = \frac{2}{3}\pi R^2$ showing that the D-bound, in the form (4.41), holds.

4.2.3 De Sitter space in string theory

A logical step towards deriving the entropy and thermodynamic properties of de Sitter space from a microscopic description, would be to embed the space as a solution of string theory. As mentioned in Section 2.1.1, this approach has been successfully employed in deriving a microscopic description of a certain class of black holes. So far, various attempts at finding a de Sitter solution of string theory have failed. One of the main conclusions of this chapter and the next, will be that, in searching for a string theory embedding, the global perspective on de Sitter space may not be the correct one to take. In Chapter 5, we will consider a partial view which may be more appropriate. We will now discuss several of the obstacles encountered.

First of all, there is the issue of the finiteness of the de Sitter entropy, (4.30). In four dimensions, the entropy equals $S_{\rm dS} = 3\pi/\Lambda$. The number of degrees of freedom necessary to describe such a universe is

$$\mathcal{N} = e^{\frac{3\pi}{\Lambda}} \,, \tag{4.43}$$

which for the currently observed value of the cosmological constant is very large, but finite. Conversely, this means that a quantum theory of gravity with finite dimensional Hilbert space of dimension $\mathcal{N}$, for consistency requires a cosmological constant $\Lambda = 3\pi/\ln N$. As argued by Banks [12], this means that the cosmological constant, Λ, should not be viewed as a derived quantity, but instead as a fundamental input parameter. This leads to the proposal that universes with positive cosmological constant are described by a fundamental theory with a finite number of degrees of freedom. A consequence of the finiteness of $\mathcal{N}$ is that string theory, having an infinite dimensional Hilbert space, does not seem appropriate to describe de Sitter space. Banks [12] also connects

the finiteness of $\mathcal{N}$ with the breaking of supersymmetry; an issue that we will discuss next.

It is easy to see that there cannot be unbroken supersymmetry in de Sitter space. This is simply because there exist no superalgebra extensions of the de Sitter symmetry algebra. In [99] a de Sitter superalgebra was constructed, but it results in a Lagrangian that leads to a gauge field with the wrong sign kinetic term. The absence of a superalgebra is related to the fact that there is no positive conserved energy in de Sitter space. If there were to be nonzero supercharges $\mathcal{Q}$, which we can assume to be Hermitian, then these would anti-commute to give the Hamiltonian [142],

$$\sum \{\mathcal{Q}, \mathcal{Q}^*\} = \mathcal{H}\,. \tag{4.44}$$

Lacking a Hamiltonian, this is clearly impossible. Instead, the supercharges of the de Sitter superalgebra constructed in [99] square to zero. Since superstring theory is naturally supersymmetric, the lack of supersymmetry in de Sitter space complicates the issue of finding a de Sitter string solution. Indeed, a 'no go' theorem was proven in [91], stating that de Sitter space cannot arise from a conventional compactification of string theory. Attempts to find de Sitter solutions in a non-standard way include [35,74,116].

Finally, consider the issue of observables [44,69] and that of the construction of an S-matrix in de Sitter space. In quantum field theory, asymptotic incoming and outgoing states are properly defined only in the asymptotic regions of spacetime. But for de Sitter space these regions are spacelike and there is no single observer who can determine the states both at past infinity as well as at future infinity. Consequently, the matrix elements of S-like matrices in de Sitter space are not measurable quantities; they are mere meta-observables, rather than observables. When one considers quantum gravity in asymptotically de Sitter space, the situation becomes even more serious. As has been pointed out by Witten, the only available pairing between in-states and out-states, CPT, is used to obtain an inner product for the Hilbert space [142]. There then does not seem to be an additional pairing between in- and out-states that could be used to arrive at an S-matrix. As the conventional formulation of string theory is based on the existence of an S-matrix, the lack of an analogue in de Sitter space heightens the difficulty of finding a relevant string solution.

An approach analogous to that which was successfully employed in the AdS/CFT [7,102] case is taken in [119]. Employing the only available asymptotic regions, the infinite past and future, standard S-matrix elements are constructed despite their unobservable character. These are then used to relate correlation functions on de Sitter space to those of a proposed dual CFT; this is the subject of the next section. After re-addressing the issue of defining an S-matrix for de Sitter space in Section 5.5.2, we come back to that of finding a string realization in Section 5.6.

4.3 THE dS/CFT CORRESPONDENCE

In line with the AdS/CFT correspondence, it is natural to look for a similar duality in the case of quantum gravity in de Sitter space. Indeed, one might expect such a relation to exist, since de Sitter space can be obtained from Anti-de Sitter by analytic continuation. However, unlike the AdS case, there is no known realization of quantum gravity in de Sitter space. Nonetheless, following the approach of Brown and Henneaux [29] in the AdS_3/CFT_2 case, Strominger [121] formulated a tentative holographic duality relating quantum gravity in de Sitter space to a Euclidean CFT on a sphere of one lower dimension. This approach requires no input from string theory.

The duality thus constructed for de Sitter space exhibits many similarities, but also many differences with the AdS/CFT correspondence [93]. An important difference is that the boundary of de Sitter space not only is spatial, it also consists of two disconnected parts. This complicates the question as to where the dual CFT would live. Strominger employs the fact that, at least for pure de Sitter, the two boundary parts are causally connected, to arrive at a single CFT on a single sphere.

In this section, we consider the proposed dS/CFT correspondence in three spacetime dimensions. Although the correspondence should apply in general dimension, the 3-dimensional case is especially rich because of the infinite dimensionality of the 2-dimensional conformal group. In a sense this makes the 3-dimensional case the most restrictive regarding the properties of the dual theory; allowing for the most definite statements. In this section we set the radius of curvature of de Sitter space equal to one, $R \equiv 1$.

4.3.1 ASYMPTOTIC SYMMETRIES

The asymptotic symmetry group of de Sitter constitutes those nontrivial[†] diffeomorphisms that preserve the boundary conditions on the asymptotic metric, *i.e.*, the metric at $\mathcal{I}^{\pm}$. So, we need to specify the appropriate boundary conditions for what we would call 'asymptotically de Sitter space'. An elegant way to do this is by using the Brown-York stress tensor [30], defined as

$$T_{ij} \equiv \frac{2}{\sqrt{-\gamma}} \frac{\delta S_{\rm cl}}{\delta \gamma^{ij}} \,, \tag{4.45}$$

where γ_{ij} is the induced metric on the boundary and $S_{\rm cl}$ denotes the action evaluated at a classical solution. Though similar in definition to the usual stress-energy tensor, T_{ij} characterizes the entire system, including contributions from

[†]Nontrivial in the sense that the transformation does not annihilate physical states.

both the gravitational field and, if present, matter fields. The bulk diffeomorphisms are generated by appropriate moments of this tensor, which lives on the boundary of the spacetime. We can then take as definition of an asymptotically de Sitter spacetime one for which the Brown-York stress tensor, and hence all symmetry generators, is finite.

The Brown-York tensor, (4.45), evaluated for the boundary $\mathcal{I}^-$ of de Sitter space in general dimension, takes the form [83]

$$T_{ij} = \frac{1}{4G_{\rm N}}\left[\mathcal{K}_{ij} - \mathcal{K}\gamma_{ij} - (D-2)\gamma_{ij} - \frac{\mathcal{G}_{ij}}{(D-3)}\right], \tag{4.46}$$

where $\mathcal{K}_{ij}$ is the extrinsic curvature, as defined in (3.56), and $\mathcal{G}_{ij}$ denotes the boundary Einstein tensor. For $D = 3$ this reduces to

$$T_{ij} = \frac{1}{4G_{\rm N}}[\mathcal{K}_{ij} - (\mathcal{K}+1)\gamma_{ij}], \tag{4.47}$$

which is identically equal to zero in planar coordinates (4.24). However, calculating (4.47) for perturbed de Sitter, with metric

$$ds^2 = g_{\mu\nu} + h_{\mu\nu}, \tag{4.48}$$

gives [118]

$$T_{zz} = \frac{1}{4G_{\rm N}}\left(h_{zz} - \partial_z h_{tz} + \frac{1}{2}\partial_t h_{zz}\right) + \mathcal{O}(h^2), \tag{4.49}$$

$$T_{z\bar{z}} = \frac{1}{4G_{\rm N}}\left[\frac{1}{4}e^{-2t}h_{tt} - h_{z\bar{z}} + \frac{1}{2}\left(\partial_{\bar{z}}h_{tz} + \partial_z h_{t\bar{z}} - \partial_t h_{z\bar{z}}\right)\right] + \mathcal{O}(h^2). \tag{4.50}$$

Imposing the condition that the Brown-York tensor remains finite, one obtains the boundary conditions

$$g_{z\bar{z}} = \frac{e^{-2t}}{2} + \mathcal{O}(1), \tag{4.51}$$

$$g_{tt} = -1 + \mathcal{O}(e^{2t}), \tag{4.52}$$

$$g_{zz} = \mathcal{O}(1), \tag{4.53}$$

$$g_{tz} = \mathcal{O}(1). \tag{4.54}$$

These boundary conditions define what is meant by 'asymptotic de Sitter'. The asymptotic symmetry group hence consists of those diffeomorphisms that leave (4.51)-(4.54) invariant. The most general form of a diffeomorphism that does so, is given by [118]

$$\zeta = U\partial_z + \frac{1}{2}U'\partial_t + \mathcal{O}(e^{2t}) + \text{complex conjugate}, \tag{4.55}$$

where $U(z)$ is holomorphic in z. We can identify what these transformations are and, at the same time, find the central charge of the boundary theory, by acting with the diffeomorphism (4.55) on the Brown-York tensor,

$$\delta_\zeta T_{zz} = -U\partial T_{zz} - 2U' T_{zz} - \frac{1}{8G_{\rm N}} U''' \,. \tag{4.56}$$

The first two terms are those one expects for a conformal field of weight two under a conformal transformation. The third term, identified as the anomalous Schwarzian derivative term, corresponds to a central charge (restoring R) [121]

$$c_2 = \frac{3R}{2G_{\rm N}} \,. \tag{4.57}$$

Here the subscript 2 refers to the dimensionality of the boundary theory, but note that both $G_{\rm N}$ and R apply to the 3-dimensional bulk. We thus identify (4.55) as a conformal transformation in two dimensions and, since $U(z)$ is general, the asymptotic symmetry group of dS_3 as the conformal group of the Euclidean plane. It is important to note that is not possible to construct a diffeomorphism analogous to (4.55) for the case of global coordinates. This is because evolution in the global time T is not part of any of the de Sitter isometries. Hence, it is impossible to associate evolution in the global time coordinate with conformal transformations of the boundary. This strongly suggests that the global perspective is not the relevant one when considering holography – and thus quantum gravity – in de Sitter space.

4.3.2 THE CORRESPONDENCE

Having found that the symmetry group of the boundary $\mathcal{I}^-$ is the Euclidean conformal group, it is to be expected that gravity correlators restricted to the boundary transform as in a 2-dimensional Euclidean CFT. Indeed, this is what one finds for massive scalar fields with mass m. The solutions to the wave equation these fields obey, which near the boundary takes the form

$$m^2\phi = \nabla^2\phi \sim -\partial_t^2\phi + 2\partial_t\phi \qquad (t \to -\infty) \,, \tag{4.58}$$

asymptotically behave as

$$\phi \sim e^{h_\pm t} \qquad (t \to -\infty) \,, \tag{4.59}$$

where

$$h_\pm = 1 \pm \sqrt{1 - m^2} \,. \tag{4.60}$$

For masses in the range

$$0 \leqslant m^2 \leqslant 1 \,, \tag{4.61}$$

$h_\pm$ are real and positive, while $h_- \leqslant h_+$. Picking the minus sign in (4.59),[‡] the imposed boundary condition has the form

$$\lim_{t\to-\infty} \phi(z,\bar{z},t) = e^{h_- t}\phi_-(z,\bar{z})\,. \tag{4.62}$$

Analogous to the AdS/CFT correspondence, the proposed dS/CFT correspondence associates to ϕ_- a dual operator in the boundary CFT, $\mathcal{O}_\phi$, of dimension h_+. The two point function of this dual operator has the form [121]

$$\langle \mathcal{O}_\phi(z,\bar{z})\mathcal{O}_\phi(v,\bar{v})\rangle \propto \frac{1}{|z-v|^{2h_+}}\,. \tag{4.63}$$

Outside of the range (4.61), *i.e.* for $m^2 > 1$, the conformal weights $h_\pm$ are no longer real, signalling that the dual CFT is not unitary. Albeit there are no a priori reasons that the CFT needs to be unitary, this might mean that consistent theories of quantum gravity on de Sitter space have no (stable) scalars with masses greater than one.

So far, we have only considered the combined regions I and III of Figure 4.2 on page 66, with a single boundary $\mathcal{I}^-$. When taking into account the full space, one might expect two separate CFT's, living on disconnected spaces, to be necessary to describe the complete bulk dynamics. However, the two boundaries are causally connected. As we showed in Section 4.1, a light ray that originates from a certain point on $\mathcal{I}^-$, will arrive at the antipodal point on the sphere at $\mathcal{I}^+$. A singularity of a correlator between a point on $\mathcal{I}^-$ and a point on $\mathcal{I}^+$ can only occur if the two points are null separated. Through the singularity structure of the Green's function on de Sitter space, such a correlation is related to one between the point on $\mathcal{I}^-$ and the antipode of the point on $\mathcal{I}^+$, also on $\mathcal{I}^-$. The insertion of a gravity operator on $\mathcal{I}^+$ then effectively corresponds to inserting the dual CFT operator at the antipodal point on $\mathcal{I}^-$. We are thus left with a single CFT on a single sphere. The antipodal relation in de Sitter space will be the main theme of Chapter 5 and we will consider the singularity structure of the Green's function in more detail in Section 5.2.1.

Everything in this section generalizes to higher dimensions. The proposed correspondence can then be summarized in terms of bulk and boundary correlation functions as

$$\begin{aligned}\langle \phi(x_1^-)\cdots\phi(x_i^-)\phi(y_1^+)\cdots\phi(y_j^+)\rangle_{dS_D} \\ \leftrightarrow \langle \mathcal{O}_\phi(x_1)\cdots\mathcal{O}_\phi(x_i)\mathcal{O}_\phi(\bar{y}_1)\cdots\mathcal{O}_\phi(\bar{y}_j)\rangle_{S^{D-1}}\,.\end{aligned} \tag{4.64}$$

Here, x_i^- and y_i^+ are points on $\mathcal{I}^-$ and $\mathcal{I}^+$, respectively. On the right hand side, all points are on the sphere on which the dual CFT lives, denoted by

[‡]We only consider the leading behaviour, ignoring the subleading term proportional to $e^{h_+ t}$.

S^{D-1}, and the bar denotes the antipode on that sphere. Note that the fields ϕ with argument on $\mathcal{I}^-$ in (4.64) obey the boundary condition (4.62), while those with argument on $\mathcal{I}^+$ obey the corresponding boundary condition appropriate in the $t \to \infty$ limit.

4.4 RG FLOW

Recall how the conformal transformations of the boundary arise from bulk diffeomorphisms. Looking at the diffeomorphism ζ, (4.55), we see that the first term generates a holomorphic diffeomorphism of the plane. In terms of the metric in planar coordinates, (4.24), this can be compensated for by a shift in t, as generated by the second term of (4.55). On the plane, this shift corresponds to a Weyl transformation. Together these transformations constitute the conformal transformations on the plane and, hence, on the boundary. A special class of these are the simple time shifts corresponding to scalings of the boundary. This is reminiscent of the AdS case where radial shifts correspond to scalings in the boundary metric, as is clear from the metric (2.49). In that case, renormalization group (RG) flow corresponds to radial flow of the bulk solutions [6,11,39]. For de Sitter, one might then expect RG flow of the putative dual theory to correspond – perhaps more naturally – to time evolution in the bulk [8,87,122].

4.4.1 INFLATION

An interesting RG scenario in de Sitter space was recently suggested by Strominger [122]. As opposed to Section 4.3, where we considered three spacetime dimensions because it was the most explicit case, we now focus on four dimensions since the current model is aimed at describing the real world. RG flows similar to the one we will discuss here were considered in [8].

As we have mentioned, recent astronomical observations suggest that the universe is currently entering a de Sitter phase. It is a much older idea that there has also been a temporary de Sitter phase in the early universe, referred to as 'inflation' [4,63,88]. Such a period of rapid expansion solves important cosmological issues like the flatness and horizon problems; see [84] for a review of early universe physics. Following Strominger [122], we assume that the metric is well-approximated by the flat Robertson-Walker big bang form

$$ds^2 = -dt^2 + a^2(t)\, dx_i dx^i \,, \tag{4.65}$$

where $a(t)$ is the scale factor of the universe. In the early and late universe, the

scale factor behaves as

$$\frac{\dot{a}}{a} \to H_{\pm} \qquad (t \to \pm\infty)\,, \tag{4.66}$$

so that the metric takes the 4-dimensional planar de Sitter form

$$ds^2 = -dt^2 + e^{2H_{\pm}t} dx_i dx^i \qquad (t \to \pm\infty)\,. \tag{4.67}$$

Here, $H_{\pm}$ denotes the Hubble constant during the de Sitter phase either in the early or late universe. Comparing to (4.24), note that

$$H_{\pm} = \frac{1}{R} \tag{4.68}$$

in terms of the curvature radius of the appropriate de Sitter space. During the inflationary period, the cosmological constant is conjectured to have been about one hundred orders of magnitude larger than that currently observed. In terms of the Hubble constant, we have $H_{-} \approx 10^{24}\,\mathrm{cm}^{-1}$ versus $H_{+} \approx 10^{-28}\,\mathrm{cm}^{-1}$.

As noted at the beginning of this section, the de Sitter metric (4.67) is invariant under a time translation accompanied by an appropriate scaling of the plane; namely under the transformation

$$t \to t + \lambda\,, \qquad x^i \to e^{-\lambda H_{\pm}} x^i\,. \tag{4.69}$$

This expresses that time evolution in the bulk generates scale transformations in the boundary theory. Moreover, we conclude from the behaviour (4.69) that early times in the bulk correspond to the IR regime of the boundary theory, while late times correspond to the UV regime. This is the de Sitter variant of the UV/IR correspondence discussed in Section 2.2.7. Note that a similar relation is not to be expected when taking the global perspective on de Sitter space. In that case, there is no monotonic relation between time and evolution from UV to IR in the bulk. Indeed, both early and late times would correspond to IR, while intermediate times would correspond to UV. This gives yet another indication that the global perspective is not the correct one when considering quantum gravity on de Sitter space.

In between the two de Sitter phases, the universe as described by (4.65) will have looked very different from (4.67) and likely will not have exhibited invariance under (4.69). There is thus no reason to expect the bulk gravity theory to be dual to a conformal theory on the boundary during that stage. An elegant interpretation is suggested by a similar situation encountered in AdS [48,59]. Radial[§] translations in the bulk of AdS correspond to RG flow in the boundary theory. Viewing the universe as a perturbed de Sitter space,

[§]Keep in mind that the radial and time directions are interchanged when going from AdS to dS.

the conformal invariance of the boundary theory is broken by insertion of the operators dual to the bulk perturbations. This way, the boundary theory is perturbed away from its UV conformal fixed point and ends up, by the RG flow, in an IR fixed point. Note that in this interpretation the RG flow runs opposite to the bulk time, since the universe actually starts out in the IR.

The above model has been applied in [86] to cosmic microwave background anisotropies. A simple dictionary between the holographic approach of the model just discussed and the standard inflationary model is constructed. Despite the very different inputs the two models give similar predictions.

4.4.2 *c*-FUNCTION

Let us consider the boundary theory in the RG flow model discussed above in a bit more detail. On dimensional grounds, the generalization of the central charge (4.57) to higher dimensions takes the form

$$c_{\text{D-1}} \propto \frac{1}{G_{\text{N}} H^{D-2}} \overset{(D=4)}{=} \frac{1}{G_{\text{N}} H^2} \,, \tag{4.70}$$

where we have used (4.68). Of course, the expression (4.70) only makes sense for the de Sitter phases of the evolution. From the relative sizes of the Hubble constants $H_\pm$ we have that

$$c_3^+ \gg c_3^- \,. \tag{4.71}$$

Since the central charge is a measure of the number of degrees of freedom of the theory, this indicates that there are overwhelmingly more degrees of freedom in the late universe than in the early universe. Such an increase of the number of degrees of freedom seems to be at odds with unitary evolution.[¶] In the current context, this can be understood in the following way, again inspired by the AdS analogy [48,59].

For a generic unitary (non-conformal) field theory in two dimensions, Zamolodchikov [146] has proven that there exists a function c_2 that decreases from the UV to the IR along RG flows; this is called the '*c*-theorem'. So far, attempts have failed to generalize this theorem to higher dimensions. Moreover, while the dual boundary theory may not be unitary for de Sitter, unitarity was crucial in the proof given by Zamolodchikov. Nevertheless, by using the bulk theory, Strominger proves that c_3, as defined by (4.70), is an increasing function of time and hence a decreasing function along the RG flow. Indeed, through Einstein's equations, the time derivative of Hubble's constant in asymptotically

[¶]Note that it is only the dual boundary theory that is possibly non-unitary; the bulk theory is unitary. It is important to realize that this is true even though the bulk theory can be reconstructed – at least in principle – from the boundary theory.

de Sitter space in four dimensions can be written as

$$\dot{H} = -4\pi G_{\rm N}(p+\rho)\,. \tag{4.72}$$

Imposing the null energy condition, which requires $(p+\rho) \geqslant 0$ while $\rho > 0$, ensures that the right hand side is non-positive. Hence, H decreases with time and c_3 increases with time. This is an example of how the bulk/boundary duality can be put to use. We will come back to this below.

With time evolution corresponding to inverse RG flow, this suggests the following interpretation [122]. As the universe expands, more and more degrees of freedom become available; they are 'integrated in' in the language of RG flows. Only in the asymptotic future does the universe come into full existence.

The c-function as discussed in [8,122] and reviewed here only applies to spatially flat slicings of de Sitter space. It has been generalized in [87] to include spherical and hyperbolic slicings. Using (4.2), (4.70) can be re-written in terms of the cosmological constant. In [87], this is subsequently generalized by replacing Λ by an effective $\Lambda_{\rm e}$, appropriate for the different slicings, defined by

$$\Lambda_{\rm e} \equiv G_{\mu\nu} n^\mu n^\nu\,. \tag{4.73}$$

Here, $G_{\mu\nu}$ denotes the Einstein tensor and n^μ is the unit normal to the respective slices. Evaluated for flat ($k=0$), spherical ($k=1$) and hyperbolic ($k=-1$) slicings, this becomes [87]

$$\Lambda_{\rm e} = \frac{(D-1)(D-2)}{2}\left[\left(\frac{\dot{a}}{a}\right)^2 + \frac{k}{a^2}\right]. \tag{4.74}$$

The generalized c-function has the form

$$c_{\text{D-1}} \propto \frac{1}{G_{\rm N}\Lambda_{\rm e}^{\frac{D-2}{2}}} \tag{4.75}$$

and a c-theorem is subsequently proven in [87].

4.4.3 Apparent horizon

A nice geometric interpretation of the c-functions defined above is given in [85]. The boundary c-function is identified in the bulk as the area of the apparent horizon, which is a naturally increasing function of time. First, we need to define the apparent horizon. At the end of Section 3.2.1, we briefly mentioned Bousso's [23,24] generalization of the Fischler-Susskind bound to general spacetimes. It associates to a general surface at least two light sheets.

Consider, *e.g.*, a $D-2$-dimensional spherical surface surrounding an observer in de Sitter space. There are four families of radial null rays orthogonal to this surface; corresponding to future/past directed outgoing/ingoing. Let λ be an appropriately chosen affine parameter on one of the four families of null rays. A family is then referred to as a light sheet of the corresponding spherical surface if it has non-positive expansion, $\theta(\lambda) \leqslant 0$. Recall the definition of θ as the expansion of the cross sectional area, $\mathcal{A}$, of neighbouring light rays,

$$\theta \equiv \frac{1}{\mathcal{A}} \frac{d\mathcal{A}}{d\lambda} \,. \tag{2.34}$$

There are at least two such light sheets, which extend until they reach a caustic where the expansion becomes positive. Bousso then identifies three situations. A surface which has both a future directed and a past directed ingoing (outgoing) lightsheet is called normal. Similarly, a surface with two future (past) directed lightsheets, but no past (future) directed ones, is called (anti-)trapped. Spherical surfaces outside the cosmological horizon of an observer in de Sitter space are anti-trapped.

We are now ready to define the apparent horizon as the boundary between normal and (anti-)trapped regions. It is characterized by the fact that at least two light sheets have vanishing expansion, $\theta = 0$, there. For pure de Sitter space, the apparent horizon coincides with the cosmological horizon, but this is no longer the case for general asymptotically de Sitter spaces. However, in a de Sitter phase, the apparent horizon will tend towards the cosmological horizon.

For the class of models with positive Λ considered in [85], including big bang models that tend to de Sitter in the future ,the area of the apparent horizon is

$$A_{\rm ah}(t) = \left(\frac{2\Lambda}{(D-1)(D-2)} \right)^{\frac{D-2}{2}} \left[\left(\frac{\dot{a}}{a} \right)^2 + \frac{k}{a^2} \right]^{-\frac{D-2}{2}} A_{\rm C} \,. \tag{4.76}$$

The time independent area of the cosmological horizon, $A_{\rm C}$, is given in (4.29). Note that $A_{\rm ah} \leqslant A_{\rm C}$ for physical values of the scale factor a and, applying the limit (4.66), we see that

$$A_{\rm ah} \sim A_{\rm C} \qquad (t \to \infty) \,, \tag{4.77}$$

as expected for such models.

Based on the observation that the central charge (4.70) is proportional to the area of the cosmological horizon (4.29), the authors of [85] propose the area of the apparent horizon (4.76) in Planck units as c-function,

$$c_{\text{D-1}} \propto \frac{A_{\rm ah}}{G_{\rm N}} \,. \tag{4.78}$$

This function can be evaluated from local data on any constant time slice. As a first check, we have already shown that it tends to the cosmological horizon in a de Sitter phase. Actually, as observed in [85], the function (4.78) defines the same c-function as (4.75). Indeed, substituting (4.74) into (4.75) and (4.76) into (4.78) one easily sees that both are of the form

$$c_{\text{D-1}} \propto \frac{1}{G_{\text{N}}\left[\left(\frac{\dot{a}}{a}\right)^2 + \frac{k}{a^2}\right]^{\frac{D-2}{2}}} \,. \tag{4.79}$$

This provides a geometric interpretation of the boundary theory c-function in terms of the increase in area of the apparent horizon in a future de Sitter universe.

5

THE ELLIPTIC INTERPRETATION: $dS/\mathbb{Z}_2$

We propose that for every event in de Sitter space, there is a CPT-conjugate event at its antipode. Such a $\mathbb{Z}_2$ identification of de Sitter space provides a concrete realization of observer complementarity: every observer has complete information. It is possible to define the analogue of an S-matrix for quantum gravity in elliptic de Sitter space that is measurable by all observers. In a holographic description, S-matrix elements may be represented by correlation functions of a dual (conformal field) theory that lives on the single boundary sphere. S-matrix elements are de Sitter-invariant, but have different interpretations for different observers. We argue that Hilbert states do not necessarily form representations of the full de Sitter group, but just of the subgroup of rotations. As a result, the Hilbert space can be finite dimensional and still have positive norm. We also discuss this 'elliptic interpretation' of de Sitter space in the context of type IIB* string theory. The discussion is based on [96,111].

5.1 INTRODUCTION

The exponential expansion of space in a de Sitter universe separates spacetime into causally inaccessible regions. This is not just unaesthetic, but conceptually problematic. It suggests, for instance, that pure states could evolve into mixed states, as degrees of freedom disappear across the horizon. For an observer in de Sitter space this would manifest itself as quantum decoherence and a loss of information. Similar issues arose in the study of the information loss problem for black holes. Gedankenexperiments in that context essentially led to the conclusion that unitarity could be preserved for all observers if one allowed for a duplication of information on either side of the horizon. According to this 'principle of black hole complementarity' [80,120,126], the freely-falling observer and the external observer would both be able to perform quantum

mechanics experiments without any loss of coherence, but their interpretation of the physics would be very different.

The arguments that led to black hole complementarity can also be applied to other types of event horizons, in particular to cosmological event horizons. A better name therefore would be 'observer complementarity'. In its strongest form observer complementarity postulates that each observer has complete information and can in principle describe everything that happens within his cosmological horizon using pure states. This information may appear to different observers in different – complementary – guises: one observer may pass smoothly through the horizon, whereas another observer may see there a source of hot radiation. Although these drastically different realities may seem to be inconsistent, it is important to recognize that paradoxes arise only when one takes the unphysical perspective of a global super-observer.

The question is whether observer complementarity can be implemented in de Sitter space. That this is indeed possible was already noticed by Schrödinger [114]. In his 'elliptic interpretation'* of de Sitter space, Schrödinger proposed a simple $\mathbb{Z}_2$ identification of spacetime by declaring antipodes to represent the same event. Schrödinger's motivation was indeed to give every observer complete information about all events and thus in a way he argued already in 1956 in favor of observer complementarity. The current treatise adds charge conjugation, completing the antipodal map to CPT. This ensures that whichever version of an event an observer witnesses, it always has the same probability. We find that elliptic de Sitter space has some rather remarkable properties. Indeed, not only does it lead to a concrete realization of observer complementarity, it also improves the nature of many of the severe theoretical challenges that de Sitter space presents. The main aim of this chapter therefore is to re-discuss, in the context of this elliptic interpretation, the conceptual issues discussed in Chapter 4.

This chapter is organized as follows. In Section 5.2 we motivate the proposed $\mathbb{Z}_2$ identification by discussing several properties of de Sitter space that support it. In Section 5.3, we define Schrödinger's antipodal identification and refine it to include CPT. We then discuss its classical properties and show that elliptic de Sitter space does not suffer from any obvious problems, such as closed timelike curves. Next, in Section 5.4, we consider quantum fields propagating in this space. In particular, we discuss the vacuum state in the Fock space of a free scalar field. As an illustrative example we consider the case of $1+1$-dimensional de Sitter space. In Section 5.5, we consider holography and the S-matrix. It is here that the advantages of the elliptic interpretation are perhaps most evident; conceptually, the holographic theory seems to have a more

*The term 'elliptic' refers to the fact that identified points are related by elliptic, *i.e.*, spacelike generators, as distinct from hyperbolic (timelike) or parabolic (null) generators.

natural interpretation with the $\mathbb{Z}_2$ identification than without. In Section 5.6, we discuss how elliptic de Sitter space might be realized in string theory. We conclude in Section 5.7.

5.2 Mirror Images in de Sitter Space

The characterization of de Sitter space, given in Section 4.1, as the unique solution to the Einstein equations with maximal symmetry and constant positive curvature, leaves free the choice of a global topology. We will use this freedom to impose the proposed identification.

For a given point on de Sitter space at embedding coordinate X, defined in (4.3), we define the 'antipodal point' to be the point obtained by reflection through the origin of Minkowski space, *i.e.*, the point with embedding coordinate $-X$. We then define 'elliptic de Sitter space' to be the spacetime in which for every physical event at any point on de Sitter space there is a CPT-conjugate event at the antipodal point. Hence we are using our freedom of topology to impose a $\mathbb{Z}_2$ identification of de Sitter space. Note that the connected part of the isometry group remains unchanged after the identification; the $\mathbb{Z}_2$ identification mods out by a center of the de Sitter group. The preservation of all local isometries justifies the appellation 'de Sitter space'.

In the remainder of this section we consider various properties of global de Sitter space that suggest that information on one side of the horizon is naturally mirrored on the other side. We do not claim that de Sitter space *must* be antipodally identified; rather, the examples should be seen as circumstantial evidence that elliptic de Sitter space may be more natural than global de Sitter space. In this light, it is interesting that de Sitter himself states [40]:

> "The elliptical space is, however, really the simpler case, and it is preferable to adopt this for the physical world."

5.2.1 Mirror singularities

The great circles, or geodesics, of a sphere are determined by the intersection of the sphere with planes that pass through the origin. Similarly, the spatial geodesics of de Sitter space can be obtained by intersecting its embedding in Minkowski space (depicted in Figure 4.1 on page 64) with spacelike planes through the origin of Minkowski space. It is clear then that *every* spatial geodesic that passes through a point must also pass through its antipode, because if the embedding coordinate X lies in a plane through the origin then so does $-X$. These geodesics form ellipses which are related to each other by de Sitter transformations. If we think of null rays as degenerate spatial geodesics

and we allow them to 'bounce off' null infinity, then all light rays leaving a point converge on the antipodal point. This last fact affects the singularity structure of Green's functions of quantum fields in de Sitter space.

Consider a scalar field in de Sitter space. It is convenient to express de Sitter-invariant equations in terms of a dimensionless de Sitter-invariant variable Z. We can define such a variable by

$$Z(X, Y) \equiv \frac{1}{R^2} X \cdot Y \,, \tag{5.1}$$

where the dot product is given by the Minkowski metric. Obviously, Z is Lorentz-invariant in $D+1$ dimensions and therefore de Sitter-invariant in D dimensions. For points that are connected by geodesics, the geodesic distance is given by $R \arccos Z$. In particular, for any given X, if Y is on the light cone of X, then $Y = X + N$ with $N^2 = 0$. Since X and Y must both lie on the same de Sitter hypersurface, $X^2 = Y^2 = R^2$ and therefore $Z = +1$. On the other hand, if Y is on the light cone of the antipodal point, $Y = -X + N$ and so here Z takes the value -1.

The wave equation for a massive scalar field, written in terms of Z, is

$$\left[(1 - Z^2) \frac{d^2}{dZ^2} - DZ \frac{d}{dZ} - \frac{m^2}{R^2} \right] \phi(Z) = 0 \,. \tag{5.2}$$

The Wightman functions obey this equation. The precise form of the solution, a hypergeometric function, is not relevant for our discussion; the key point is that it is singular at $Z = 1$. This is analogous to the usual short-distance singularity at $\sigma = 0$ that one has in Minkowski space along the light cones. But now the wave equation is symmetric under $Z \to -Z$. Therefore, in de Sitter space, there is a second solution to (5.2) with a singularity at $Z = -1$, *i.e.* on the light cones of the antipode. Hence, we see that in contrast to Minkowski space, singularities of Green's functions in de Sitter space come in pairs. The mirror singularity along the antipodal light cones is our first example of duplication in de Sitter space.

5.2.2 SHOCKWAVES

Following work by Dray and 't Hooft [43], Sfetsos [115] discusses how shock waves can be introduced in de Sitter space. De Sitter space in 4 dimensions, written in terms of Kruskal coordinates, takes the form [118]

$$ds^2 = -\frac{4}{(1 - uv)^2} du dv + r^2 (d\theta^2 + \sin^2\theta \, d\phi^2) \,, \tag{5.3}$$

where

$$r = \frac{1+uv}{1-uv}\,. \tag{5.4}$$

Consider a massless particle located at $u = 0$ and moving with the speed of light in the v-direction. The question is what happens to the geometry. Following [43], as an ansatz is taken that for $u < 0$ the spacetime is described by (5.3) and for $u > 0$ also by (5.3) but with v shifted as $v \to v + f(\theta)$, where $f(\theta)$ is a function to be determined. In the case of de Sitter space, the function $f(\theta)$ is determined in [115] to be of the form (up to constant factors)

$$f(\theta) = \left[1 - \frac{1}{2}\cos\theta\,\ln\left(\cot^2\theta/2\right)\right]. \tag{5.5}$$

This function has poles at $\theta = 0, \pi$, indicating the presence of particles there. Since no particle is a priori placed at the south pole, $\theta = \pi$, the second singularity is considered unphysical in [115]. In order to have a solution that blows up only once, the solution is modified by a heaviside stepfunction, $\Theta(\theta)$, that essentially restricts the solution to the northern hemisphere,

$$\hat{f}(\theta) = \left[1 - \frac{1}{2}\cos\theta\,\ln\left(\cot^2\theta/2\right)\right]\Theta\left(\frac{\pi}{2} - \theta\right). \tag{5.6}$$

Here, we would like to take a different viewpoint and regard the appearance of the second pole as necessary. Indeed, we take the appearance of a second, antipodal singularity in the general solution (5.5) as motivation for our proposal to antipodally identify de Sitter space.

A shockwave configuration can be obtained by boosting a corresponding black hole configuration, in the limit where the kinetic energy of the black holes dominates over their rest energy. It is well known in 2+1-dimensional de Sitter space that black holes appear in antipodal pairs, see for example [118]. This corroborates our suggestion that shockwaves also necessarily appear in pairs, at least in $2+1$ dimensions. In the following section we will show that the fact that black holes appear in antipodal pairs holds in general dimension.

5.2.3 Mirror black holes

We will show that, when the Schwarzschild-de Sitter black hole solution is analytically extended beyond the cosmological horizon, there is a mirror black hole on the antipodal hemisphere of de Sitter space. Recall the Schwarzschild-de Sitter metric,

$$ds^2 \;=\; -F(r)\,dt^2 + F^{-1}(r)\,dr^2 + r^2 d\Omega_{n-1}^2\,, \tag{4.25}$$

$$F(r) \;=\; 1 - \frac{2M}{r^{d-2}} - \frac{r^2}{R^2}\,. \tag{4.26}$$

Let us introduce Kruskal-Szekeres type coordinates and analytically continue the metric beyond the cosmological horizon. Note that, a priori, the coordinates in (4.25) are only valid for $r_{\rm bh} < r < r_{\rm c}$.

In terms of its roots, the function $F(r)$ can be written as

$$F(r) = -\frac{1}{R^2 r^{d-2}}(r - r_{\rm c})(r - r_{\rm bh}) \prod_{n=3}^{d} (r - r_n)\,, \tag{5.7}$$

where $r_{\rm c}$ and $r_{\rm bh}$ are the only real and positive roots. Hence

$$F^{-1}(r) = \frac{c_1}{r - r_{\rm c}} + \frac{c_2}{r - r_{\rm bh}} + \sum_{n=3}^{d} \frac{c_n}{r - r_n}\,, \tag{5.8}$$

for certain constants c_n. Define Eddington-Finkelstein coordinates through

$$dx^{\pm} = dt \pm \frac{dr}{F(r)}\,, \tag{5.9}$$

which, using (5.8), is easily integrated to give

$$x^{\pm} = t \pm \left[c_1 \ln(r - r_{\rm c}) + c_2 \ln(r - r_{\rm bh}) + \sum_{n=3}^{d} c_n \ln(r - r_n) \right]. \tag{5.10}$$

In terms of these coordinates, the metric takes the form

$$ds^2 = -F(r) dx^+ dx^- + r^2 d\Omega_{d-1}^2\,. \tag{5.11}$$

Finally, introduce Kruskal-Szekeres coordinates through

$$\begin{aligned} U &= e^{-\frac{x^-}{2c_1}}\,, \\ V &= -e^{\frac{x^+}{2c_1}}\,, \end{aligned} \tag{5.12}$$

where it is clear that $U > 0$ and $V < 0$. The metric becomes

$$ds^2 = 4c_1^2 \frac{F(r)}{UV} dU dV + r^2(U, V) d\Omega_{d-1}^2\,. \tag{5.13}$$

In terms of these coordinates the metric is regular at $r = r_{\rm c}$ and we can analytically continue (5.13)to the full range $-\infty < U, V < \infty$. Note from (5.10) and (5.12) that $r(U, V) = r(UV)$ and thus $F(r) = F(UV)$. Hence, if $F(UV)$

is zero for certain nonzero values of U and V, *e.g.* at the black hole horizon, then it will also be zero at $-U$ and $-V$. This second horizon is antipodal from the first and thus we find that black holes in de Sitter space come in antipodal pairs. Actually, this is a choice: instead of extending the metric analytically entirely to the other side, we could have replaced the antipodal black hole by a static, spherically symmetric mass distribution with the same total mass.

Now consider adding charge to the de Sitter black hole [107]. De Sitter space cannot support Noether charges because its spatial sections are compact. The total charge has to add up to zero; the antipodal black hole therefore necessarily carries equal, but opposite charge. Moreover, for the same reason there cannot be any net angular momentum. This leads us to propose that the antipodal map must be combined with charge conjugation, C.

5.3 The Elliptic Interpretation

The elliptic interpretation of de Sitter space consists of identifying points that are antipodally related under charge conjugation, C. The antipodal map is most easily expressed in terms of embedding coordinates, defined in (4.3). It takes the form

$$X^I \to -X^I \,, \tag{5.14}$$

with $I = 0, 1, \ldots, D$, *cf.* (4.3). Together with charge conjugation, we will see that this means that particles and events at X^I and $-X^I$ are related by CPT. We thus have an involution, a $\mathbb{Z}_2$ map. The fixed point of the map, $X^I = 0$, is not itself in de Sitter space, so this is a freely-acting symmetry. The quotient space $\mathrm{dS}/\mathbb{Z}_2$ is therefore a homogeneous space with no special points. The embedding equation (4.3) makes manifest that the de Sitter isometry group is the Lorentz group in $D+1$ dimensions, O(1, D). Note that this group has four disconnected components. These are the proper orthochronous Lorentz group and its composition with the discrete symmetries of P and T, *i.e.*, with parity and time-reversal. By parity we will always mean a reflection in a hyperplane of one spatial codimension rather than spatial inversion through the origin of Minkowski space; the discussion is therefore unaffected by whether the spacetime is odd or even dimensional. Note that the antipodal map also inverts the direction of time; see Figure 5.1. For example, recall global coordinates (4.4). The line element can be written

$$ds^2 = -dT^2 + R^2 \cosh^2 T/R \left(d\theta^2 + \sin^2\theta \, d\Omega_{D-2}^2 \right) . \tag{5.15}$$

In these coordinates the antipodal map is given by

$$T \to -T \,, \quad \theta \to \pi - \theta \,, \quad \Omega \to \Omega^A \,, \tag{5.16}$$

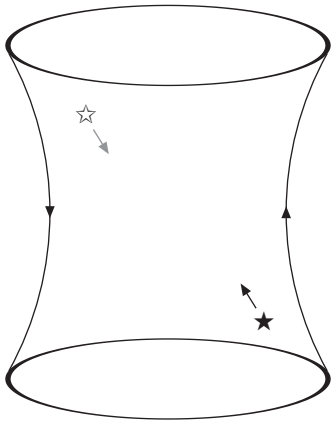

FIGURE 5.1: A star moving forward with respect to the local arrow of time, as well as its antipodal image, are shown. The antipodal map reverses the local arrow of time.

where Ω^A are the angular coordinates of the point antipodal on the $D-2$-dimensional sphere to the point labeled by Ω and time is reversed, $T \to -T$. In the rest of this section, we show that elliptic de Sitter space is nevertheless classically consistent, with no problems of causality or closed timelike curves. We will also demonstrate that the map between a particle and its antipodal image is CPT.

5.3.1 CAUSALITY

The antipodal map identifies points at positive T with points at negative T. Thus, one may wonder whether there are problems with causality or closed timelike curves. That such problems do not arise was explained by Schrödinger [114]. We just give here our version of the argument.

First, let us go to the embedding space. It is easily seen that two antipodal points at X and $-X$ are always spacelike separated, since $X^2 = R^2 > 0$. Moreover, the intersection of the two light cones that start at antipodal points never intersect the de Sitter hypersurface, because if Y is the embedding coordinate of a common point on the light cones emanating from X and $-X$, then

$$(Y + X)^2 = (Y - X)^2 = 0 \Rightarrow Y^2 = -R^2 \,, \tag{5.17}$$

so Y does not lie on the de Sitter hypersurface. This means that the light cones of two antipodal points within de Sitter space do not intersect. Therefore a pair of events that take place at antipodal points cannot both influence the same

event in their past and future. In particular, there are no closed timelike curves after $\mathbb{Z}_2$ identification.

What about closed null curves? A point on $\mathcal{I}^-$ is connected by a lightlike trajectory to its antipodal image on $\mathcal{I}^+$. So at first this appears to give rise to an infinity of closed lightlike trajectories. However, these light rays do not constitute closed trajectories in de Sitter space for three important reasons. First of all, 'points' at $\mathcal{I}^+$ and $\mathcal{I}^-$ are not really points in de Sitter space. They have to be added as points at infinity, and so they are only part of a formal compactification of de Sitter space. De Sitter space itself is non compact and does not include these points. A second, related reason is that the affine parameter along the seemingly closed lightlike trajectory is actually infinite, essentially because the points are at $\mathcal{I}^{\pm}$. Finally, a third reason that the lightlike trajectory is not really closed, is that one cannot continue along the trajectory a second time, third time, etc. without reversing direction each time one is at the endpoints on $\mathcal{I}^+$ or $\mathcal{I}^-$. This is not what happens on a usual closed trajectory, such as on a timelike S^1.

It is also useful to analyse the antipodal identification from the point of view of inertial observers. All points inside the causal diamond of an observer have antipodal points outside the causal diamond. The antipodal points belong to the causal diamond of the antipodal observer and are inaccessible to the first since they lie behind his horizon. Therefore, exactly one of every pair of antipodal events is observable. Which event of each pair is observed depends on the location of the observer; see Figure 5.2. For example, the observer living at the south pole will see precisely all antipodal images of the events that his colleague at the north pole sees. Other observers will see something in between, namely for some part 'northern' events and for the rest 'southern' events, but every event is observed once and no more than once. Identifying antipodal points, we see that all observers will obtain complete information about the spacetime as they approach $\mathcal{I}^+$. Thus observer complementarity is realized by the elliptic interpretation.

What about events that take place outside the causal diamonds of the observer at the south and the north poles? These are the events that take place at the upper and lower parts of the Penrose diagram near past and future infinity. In the elliptic interpretation of de Sitter space these upper and lower regions are identified. The usual square Penrose diagram for de Sitter space is somewhat misleading in the sense that it seems to indicate that all points in the upper region are in the causal future of points of the lower region. But one has to remember that every point represents a $D-2$-dimensional sphere and points that are identified by the antipodal map are on opposite sides of these spheres. A clearer way to see the causal structure of elliptic de Sitter space is to represent the $D-2$-dimensional spheres as two points, each of which is a real projective sphere, as in Figure 5.2. Now one can see that a geodesic that connects two

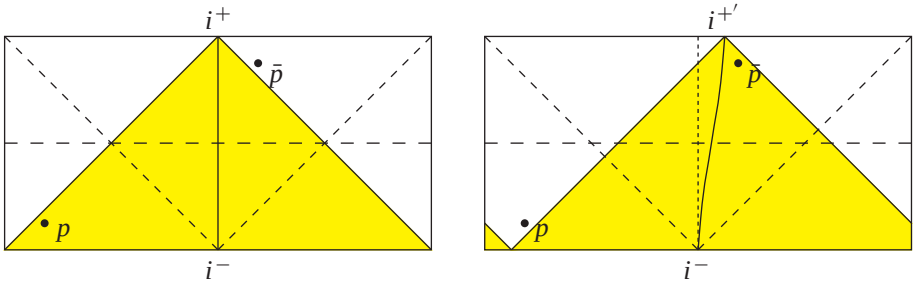

FIGURE 5.2: These Penrose diagrams of de Sitter space have been opened up to make all antipodal points distinct. The left and right edges of a diagram are identified and every point in the interior (except on the central vertical line) now signifies an $\mathbb{R}P^{D-2}$, instead of a S^{D-2}. The antipode of a given point is reached by reflecting about the dashed horizontal line (which corresponds to $T = 0$) and moving horizontally by half the width of the diagram. Two antipodes, marked p and $\bar{p}$, are shown. In (a) an observer traveling from i^- to i^+ has p but not $\bar{p}$ in his causal past (shaded), while in (b) an observer with a different worldline can see $\bar{p}$ but not p. The antipodal image of a shaded region is the unshaded region, giving every observer complete information after the $\mathbb{Z}_2$ identification.

identified points in the upper and lower regions has to travel forward in time, but also has to go around the sphere. Since all antipodal points are spacelike separated, the resulting geodesic is indeed spacelike.

Next consider the horizon itself. Without loss of generality we may consider an observer at the north pole, $\theta = 0$, of the spatial $D-1$-dimensional sphere S^{D-1}. His past and future event horizons are given by

$$\theta = 2 \arg \left(i + e^{\pm \frac{T}{R}} \right) \tag{5.18}$$

and intersect at $T = 0$ at the equator of his $D-1$-dimensional sphere, described by the $D-2$-dimensional sphere at $\theta = \pi/2$. The intersection takes place at the midpoint of the square Penrose diagram. Therefore only by sending a signal at $T = -\infty$ can he contact the equator in time for a signal to come back to him. In fact, such a signal will reach him precisely at $T = \infty$. Hence, if we exclude the points at infinity, there is no way that the observer can communicate (send a question and get a reply) with points on the equator. The antipodes of events that happen right on the equator also lie on the equator. But an observer at the

north (or south) pole only sees these events at $T = \infty$. We conclude that at no finite time can any observer ever directly detect the duplication of events in elliptic de Sitter space.

Finally, note that the asymptotic geometry of elliptic de Sitter space consists of a single S^{D-1}, since the $\mathbb{Z}_2$ identification maps $\mathcal{I}^+$ and $\mathcal{I}^-$ to each other. This property will be useful when we consider the holographic theory.

5.3.2 CPT

Any two antipodal points can be mapped to the north and south poles corresponding to $X^D = \pm R$, $X^k = 0$ for $k = 0, 1, \ldots, D-1$. Without loss of generality, consider a particle with trajectory $X^I(\tau)$, $I = 0, 1, \ldots, D$ in the embedding space passing through the north pole at $\tau = 0$. Its antipodal image is $-X^I(\tau)$ and passes through the south pole. Let us apply time-reversal to the antipodal image:

$$T : -X^I(\tau) \to -X^I(-\tau)\,. \tag{5.19}$$

The relativistic momentum of the particle at the north pole is $p^I = \dot{X}^I$. Note that $p^D = 0$ at $\tau = 0$. At the south pole the momentum is also given by p^I since it is $-X^I(-\tau)$ differentiated with respect to τ at $\tau = 0$. So in the embedding space the momentum is pointing in the same direction. However, in order to compare this to the momentum at the north pole, we have to parallel transport the vector from the south pole to the north pole. There are many ways of doing this because there are an infinite number of spatial geodesics passing through both the north and the south poles. Let us pick one of them, say the one that appears when we intersect de Sitter space with the two-dimensional plane $X^m = 0$ for $m = 0, 1, \ldots, D-2$. This gives as a geodesic $X^{D-1} = R\sin\theta$, $X^D = R\cos\theta$. At $\theta = 0$ we are at the north pole, at $\theta = \pi$ at the south pole. Parallel transport of the momentum p^I along this trajectory gives a momentum $(p')^I$ which satisfies

$$\begin{aligned} (p')^m &= p^m\,, \qquad m = 0, \ldots, D-2 \\ (p')^{D-1} &= -p^{D-1}\,. \end{aligned} \tag{5.20}$$

We see that one of the spatial components of the momentum has changed sign. That is the result of a reflection in a $D-2$ spatial dimensional hyperplane. Thus it corresponds to parity, even though in the embedding space $X^I \to -X^I$ corresponds to an inversion. The plane of reflection in this case is the plane $X^{D-1} = 0$. Had we chosen a different geodesic it would have been another plane. Note that this is consistent, because parallel transport along two different geodesics differs by a rotation, equal to the integrated curvature between the geodesics. This is precisely what one finds if one composes the two reflections in the planes associated with those geodesics.

Therefore, going around from a point in de Sitter space to its antipodal point has the effect of acting on the tangent space by PT. Since our $\mathbb{Z}_2$ map also requires that we act with charge-conjugation, C, the cumulative effect is to relate antipodal points by CPT.

5.3.3 THE ARROW OF TIME

The antipodal map, $X^I \to -X^I$, changes the sign of the time coordinate of the embedding space and also that of the direction of time in de Sitter space. The resulting quotient space $dS/\mathbb{Z}_2$ is as a consequence not time-orientable: although one can locally distinguish past and future, there is no global direction of time. This fact clearly changes many standard notions about space and time that we are accustomed to. For instance, it is impossible to choose a Cauchy surface for elliptic de Sitter space that divides spacetime into a future and a past region.

Since the microscopic laws of physics are generally time-reversible, that is CPT-invariant, there is no problem with time unorientability at a microscopic level. It is more subtle, however, to formulate macroscopic laws of physics on a time unorientable spacetime. For example, the evolution of stars clearly shows a direction of time; one never observes a neutron star turning into a massive star through the enormous implosion of a stellar envelope, yet this is what the antipodal image of a type II supernova would look like.

For sufficiently simple situations, a single observer can always choose a preferred direction of time in the observable part of the universe, consistent with the second law of thermodynamics. Consider an isolated thermodynamic system in configuration A, with antipodal image A', which evolves into system B, with antipodal image B'. If the entropies are such that $S(B) \gg S(A)$, an observer who observed both A and B would say that A preceded B. Since the primed and unprimed systems have the same entropy, this would mean that an observer who observed both A' and B' would say that A' preceded B' and would therefore have time flowing in the opposite direction. Finally, an observer who saw, say, A and B' would see them as two distant, spacelike-separated systems, rather than one system evolving into another. For this observer the choice of the arrow of time is independent of the relative entropies of the two systems. In this simple scenario, no problems arise for any observer.

However, now consider a second thermodynamic system in states C and D. For example, A, B and C, D could describe the configurations before and after two supernova explosions. It is easy to check that if both C and D are outside the past light cone of B, then there is always at least one observer who witnesses a dramatic violation of the second law, irrespective of his choice of time arrow. This is not fatal because, after all, the underlying dynamics do exhibit a CPT symmetry. Rather, the issue is what the allowable initial conditions are. One consistent treatment is to say that there are simply no highly-ordered

systems present. (This would, unfortunately, include realistic observers.) Indeed, there are reasons to believe that our observed macroscopic arrow of time may be related to boundary conditions at cosmological singularities. It would be very interesting to see if there are cosmological scenarios [1] that can be built out of elliptic de Sitter space.

An alternate and quite different viewpoint is to argue that before one can even assign events in spacetime, one should first choose an observer. Indeed, even classically, different observers can have rather different interpretations of local physics, as happens in the membrane paradigm for black holes [126,133]. Then for a given observer one can always arrange events to be consistent with his preferred arrow of time. One only runs into trouble if one tries to consider many observers, who all choose a preferred time direction. But such considerations are against the notion of observer complementarity, which forbids simultaneous consideration of observers on opposite sides of an event horizon.

5.3.4 The $\Lambda \to 0$ limit

An interesting limit of de Sitter space is the limit in which the cosmological constant is sent to zero, so that spacetime locally becomes Minkowski space. This limit has to be treated with care; the quantities of interest should vary smoothly as $\Lambda \to 0$. For elliptic de Sitter space, the $\Lambda \to 0$ limit seems sensible. The causal properties of the $\mathbb{Z}_2$ quotient space for any finite Λ are similar to those of Minkowski space, in the sense that every observer who waits long enough has the chance to observe (and emit signals to) any event in spacetime, just as in Minkowski space. The main difference is that elliptic de Sitter space is not time-orientable. However, as the cosmological constant goes to zero this difference disappears to the null boundaries.

Now, if elliptic de Sitter space goes to Minkowski space in this limit, it seems to imply that global de Sitter, being its two-fold cover, in fact goes to *two* copies of Minkowski space, where the second copy is the CPT-conjugate of the first. The significance of these remarks will be more clear once we discuss the de Sitter analogue of an S-matrix, which as we will argue exists in elliptic de Sitter space but does not appear to exist in global de Sitter space.

5.4 Quantum Field Theory

In this section, we study the quantization properties of a scalar field propagating in elliptic de Sitter space. Some aspects of the quantum field theory of a free scalar field in elliptic de Sitter space have previously been discussed in [51,109,110]. More recently it was discussed, independent of the current work, in [13].

Elliptic de Sitter space is not simply connected; there are closed spacelike curves going from a point to the antipodal point that are noncontractible. Therefore, tensor fields on elliptic de Sitter space can be sections of a twisted bundle over spacetime. Since the first homotopy group is $\pi_1(\mathrm{dS}_n/\mathbb{Z}_2) = \mathbb{Z}_2$, we can essentially choose a sign for the phase of a tensor field as the field is carried around a noncontractible loop. Consider then a complex scalar field. We can choose either periodic or antiperiodic boundary conditions. If we choose periodic conditions, the constraint a complex field must satisfy takes the form

$$\Phi_\pm(\bar{x}) = \pm\Phi^*_\pm(x)\,, \tag{5.21}$$

where $\bar{x}$ denotes the antipodal point to x and the subscript $\pm$ indicates whether we have chosen periodic or anti-periodic boundary conditions. If we write $\Phi_\pm(x) = \Phi_1(x) + i\Phi_2(x)$, then the real and imaginary parts have periodic (antiperiodic) and antiperiodic (periodic) boundary conditions respectively for the plus (minus) subscript.

Globally, one can expand a scalar field in terms of so called Euclidean modes. These are field configurations that satisfy the wave equation, with boundary conditions such that the modes can be analytically continued from the spherical harmonics on a sphere. A property of the Euclidean modes is that they can be chosen to obey

$$\phi^{\mathrm{E}}_n(\bar{x}) = \phi^{\mathrm{E}*}_n(x) \tag{5.22}$$

and we will assume that our modes satisfy this condition. Normally, one expands the field in terms of its modes as

$$\Phi_\pm(x) = \sum_n \left[a_{n,\pm}\,\phi^{\mathrm{E}}_n(x) + a^\dagger_{n,\pm}\,\phi^{\mathrm{E}*}_n(x)\right]. \tag{5.23}$$

In elliptic de Sitter space, however, the field must additionally obey the periodicity condition (5.21). This implies that

$$a^\dagger_{n,\pm} = \pm a_{n,\pm}\,, \tag{5.24}$$

indicating that the global quantization scheme breaks down. As a result, a global Fock space no longer exists; any creation operator acting on a vacuum state would annihilate it. Intuitively, this happens because the identified spacetime is not time-orientable. Creation and annihilation operators create and destroy quanta of positive energy, but if the spacetime is not time-orientable positive energy cannot be defined globally. For essentially the same reason, the inner product of modes over a spatial slice Σ through elliptic de Sitter space always gives zero. This is because the Klein-Gordon inner product

$$(\phi_m, \phi_n) = -i\int_\Sigma (\phi_m\,\partial_t\phi^*_n - \phi^*_n\,\partial_t\phi_m) \tag{5.25}$$

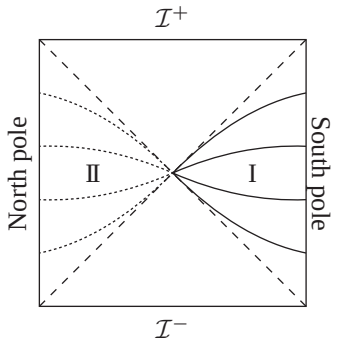

FIGURE 5.3: Penrose diagram of de Sitter space, in which region I (II) corresponds to the static patch of an observer on the south (north) pole. The solid lines indicate equal time slices in the static time; they are Cauchy surfaces for region I. The dotted lines are their antipodal images[‡] and constitute Cauchy surfaces for region II. When a solid line is continued through the horizon, onto its antipodal image, it constitutes a Cauchy surface for the whole space.

vanishes as a consequence of the flipping of the direction of time.

The vanishing of the norm and the lack of a nontrivial Fock space may seem like serious afflictions, but actually in elliptic de Sitter space it is more natural to build a Fock space with oscillators defined on a static patch. To see this, note that under the antipodal identification Cauchy surfaces for the static patch constitute Cauchy surfaces for the whole space, as shown in Figure 5.3. Consider the static patch associated with an observer at the south pole, region I in Figure 5.3. In this region there is a well-defined direction of time, as indicated in Figure 4.4 on page 69, and Fock space operators $a_\omega^{(\dagger)\mathrm{I}}$ can consequently be defined. The vacuum is then constructed in the usual way,

$$a_\omega^{\mathrm{I}}|\mathrm{vac}\rangle = 0 \qquad \forall\omega > 0\,, \tag{5.26}$$

and a Fock space can be constructed. The antipodal map identifies

$$a_\omega^{\mathrm{I(II)}} \leftrightarrow a_\omega^{\dagger\mathrm{II(I)}}\,, \tag{5.27}$$

i.e., creation (annihilation) operators in region I are identified with annihilation (creation) operators in region II, *cf.* (5.24). It would be interesting to work

[‡]Note that, comparing to Figure 4.4, these coincide with the equal time slices in region II. This is, at least from the current viewpoint, coincidence; they simply denote the antipodal images of the time slices in region I.

out the behavior of higher-spin fields and, in particular, fermions in elliptic de Sitter space.

Different observers are related by Bogolubov transformations. These are invertible, mapping pure states onto pure states. We expect no de Sitter-invariant pure states; in particular the vacuum state is not invariant, as is obvious by considering observers that are antipodal to each other. There are nevertheless de Sitter-invariant mixed states. These states correspond to de Sitter-invariant pure states in the global Fock space, traced over the modes behind the horizon. In particular, there is a state that is observed as a thermal state by any observer moving along a timelike geodesic $x(\tau)$. To see this, consider a real scalar field on the identified spacetime, given in terms of a scalar field on the unidentified space as

$$\Phi_{\pm}(x) = \frac{1}{\sqrt{2}}[\Phi(x) \pm \Phi(\bar{x})]\,. \tag{5.28}$$

This field satisfies the condition (5.21) for a real field. The Wightman function takes the form [109]

$$G^0_{\pm}[x(\tau), x(\tau')] = G^0[x(\tau), x(\tau')] \pm G^0[x(\tau), \overline{x(\tau')}]\,, \tag{5.29}$$

where $G^0(x, x')$ is the Euclidean Green's function on the unidentified de Sitter space. In obtaining this we have used the fact that $G(x, x') = G(\bar{x}, \bar{x}')$, which holds because under $x \to \bar{x}$ and $x' \to \bar{x}'$, the de Sitter-invariant quantity Z remains unchanged and $G^0(x, x')$ is a function only of $Z(x, x')$ since the Wightman functions are de Sitter-invariant; see Section 5.2.1. Assuming, without loss of generality, that the observer remains static on the south pole, $Z(x(\tau), x(\tau'))$ is given in terms of static coordinates by $\cosh \tau - \tau'/R$ when τ is the proper time. The Green's function thus takes the form

$$G_{\pm}[x(\tau), x(\tau')] = G^0\left(\cosh \tau - \tau'/R\right) \pm G^0\left(-\cosh \tau - \tau'/R\right)\,. \tag{5.30}$$

This is a thermal Green's function at a temperature $1/2\pi R$. So even though every observer in elliptic de Sitter space has complete information, one still has thermal states at the de Sitter temperature. Unlike the unidentified case, however, there is no frame for which this Green's function corresponds to a pure vacuum state.

As discussed in [28,36,119,132], there is a one-parameter family of de Sitter-invariant Green's functions in unidentified de Sitter space. This family is parametrized by α, with the Euclidean Green function corresponding to $\alpha = 0$.[§] The existence of such a family stems from the fact that on de Sitter space one can add an antipodal source, as we saw in Section 5.2.1. The

[§] We adhere to the conventions of [5].

corresponding modes are related by Bogolubov transformations:

$$\phi_n^\alpha(x) = \cosh\alpha\,\phi_n^{\mathrm{E}}(x) + \sinh\alpha\,\phi_n^{\mathrm{E}}(\bar{x})\,. \tag{5.31}$$

By (5.22), the new modes mix the old positive and negative energy modes and therefore define a new, inequivalent vacuum. The α-vacua, denoted by $|\alpha\rangle$ and called Mottola-Allen states [5,94], form a one-parameter family of de Sitter-invariant vacua. Presumably, they correspond to (nonthermal) de Sitter-invariant states on the elliptically identified space. The α-vacua have Green's functions given by

$$G^\alpha(x,x') = \langle\alpha|\Phi(x)\Phi(x')|\alpha\rangle\,. \tag{5.32}$$

Substituting the mode expansion and the Bogolubov transformation for a field satisfying (5.21), the α-Wightman function on the identified space takes the form [109]

$$G_\pm^\alpha(x,x') = e^{\pm 2\alpha} G_\pm^0(x,x')\,, \tag{5.33}$$

where $G_\pm^0(x,x')$ is given by (5.29), which corresponds to $\alpha = 0$. In elliptic de Sitter space the Green's functions for the different α-vacua differ by an overall normalization (ignoring subtleties involving $i\epsilon$ prescriptions). We regard the Mottola-Allen states for $\alpha \neq 0$ as unphysical, since their Green's functions do not have the short-distance singularities that we expect from Minkowski space. The Green's function on elliptic de Sitter space has singularities on the light cone as well as on the light cone of the antipode, even for $\alpha = 0$. The singularities have equal strength but can have a relative plus or minus sign due to the double-valuedness of the phase.

5.4.1 1+1-DIMENSIONAL DE SITTER SPACE

As an illustrative example, consider the case of $1+1$-dimensional de Sitter space. This simple space allows for definite statements to be made. In the elliptic interpretation every observer has access to all information. Their complementary representations should thus be in one-to-one correspondence. Since two observers in de Sitter space generically accelerate with respect to each other, one expects the transformation between the two perspectives to be a nontrivial Bogolubov transformation. In the following we will explicitly construct this transformation in the case of $1+1$-dimensional de Sitter spacetime.

The $1+1$-dimensional de Sitter metric in global coordinates reads

$$ds^2 = -dT^2 + \cosh^2 T\, d\theta^2\,, \tag{5.34}$$

cf. (4.4). This metric has three Killing vectors,

$$\begin{aligned} \partial_1 &= \cos\theta\,\partial_{\rm T} - \tanh T\ \sin\theta\,\partial_\theta\,, \\ \partial_2 &= \sin\theta\,\partial_{\rm T} + \tanh T\ \cos\theta\,\partial_\theta\,, \\ \partial_3 &= \partial_\theta\,. \end{aligned} \tag{5.35}$$

Of these, ∂_1 is the generalized generator of time translations for an observer at the south pole ($\theta = 0$). Let us construct its eigenmodes. First, recall from Section 4.1.1 that the metric (5.34) is conformal to flat space,

$$ds^2 = \cosh^2 T\,\left(-d\tau^2 + d\theta^2\right)\,, \tag{5.36}$$

where $\tan\tau(T)/2 = \tanh T/2$. The wave equation thus takes the same form as in flat space and has right- and left-moving solutions. In the following we will only consider the right-movers. We are looking for positive frequency eigenmodes, *i.e.* modes that obey

$$\partial_1\phi_\omega(\tau-\theta) = -i\omega\,\phi_\omega(\tau-\theta)\,. \tag{5.37}$$

We have

$$\partial_1\phi_\omega(\tau-\theta) = \phi'_\omega(\tau-\theta)\cos(\tau-\theta)\,. \tag{5.38}$$

From (5.37) and (5.38) we find that the modes take the form

$$\begin{aligned} \phi_\omega(\tau-\theta) &= \left(\frac{1-\tan\tau-\theta/2}{1+\tan\tau-\theta/2}\right)^{i\omega}\,, &(5.39)\\ &\equiv x^{i\omega}\,. &(5.40) \end{aligned}$$

Concentrating on the slice $\tau = 0$, we see that these modes have branch cuts at $x = 0$ and $x = \infty$, corresponding to $\theta = \pm\pi/2$. Using the condition (5.21), which in this case takes the form

$$\phi(\theta+\pi) = \phi^*(\theta) \qquad (\tau = 0)\,, \tag{5.41}$$

these modes are extended to the region $\pi/2 < \theta < 3\pi/2$. We can define new modes that are well defined for the full range $0 < \theta \leqslant 2\pi$, through

$$\tilde\phi_\omega = \frac{1}{\sqrt{\omega}}\,|x|^{-i\omega}\,. \tag{5.42}$$

Note that these modes are still singular at $\theta = \pm\pi/2$, but they do implement the constraint (5.41). These modes are normalized according to

$$\int_0^\infty dx\ |x|^{-i\omega}\frac{\partial}{\partial x}|x|^{i\omega'} = \delta(\omega-\omega')\,. \tag{5.43}$$

After a rotation over an angle φ, they take the form

$$\tilde{\phi}^{\varphi}_{\omega} = \frac{1}{\sqrt{\omega}} \left| \frac{x + \tan \varphi/2}{1 - x \tan \varphi/2} \right|^{-i\omega} . \tag{5.44}$$

And the Bogolubov coefficients take the form

$$A_{0\varphi} = \sqrt{\frac{\omega}{\omega'}} \int_0^{\infty} \frac{dx}{x} x^{-i\omega} \left| \frac{x + \tan \varphi/2}{1 - x \tan \varphi/2} \right|^{i\omega'} , \tag{5.45}$$

where the integral is defined through the principal value.

5.5 Holography in Elliptic de Sitter Space

Now we turn to the theory on the boundary and consider the proposed dS/CFT correspondence, discussed in Section 4.3, from the perspective of elliptic de Sitter space. An immediate consequence of taking a $\mathbb{Z}_2$ quotient is that every observer now has access to all of elliptic de Sitter space. Moreover, the antipodal identification implies that the spacetime now has only a single spacelike boundary. Hence the holographic dual theory is a Euclidean conformal field theory on a *single* sphere. In the spirit of the dS/CFT correspondence we shall consider first the general features of the holographic CFT, independent of the details of the theory. The discussion does not need the corresponding bulk fields to be free; indeed, it applies also to gravity. We find that the holographic properties of elliptic de Sitter space are very good, with satisfying implications for observer complementarity, the existence of an S-matrix and a possible explanation of the finiteness of the de Sitter entropy.

5.5.1 Holographic time evolution

Even though we do not know what the interior of quantum de Sitter space looks like, we can still say the following. Classically, the past and future light cones of an observer intersect the $D-1$-dimensional spheres at asymptotic infinity on $D-2$-dimensional spheres. In fact, after identification both light cones intersect the *same* sphere. The polar angle at which the light cones emanating from time T (at the north pole) intersect the S^{D-2} at $\mathcal{I}^{\pm}$ is given by

$$\theta(T) = 2 \arctan \left(\tanh T/2\right) + \frac{\pi}{2} . \tag{5.46}$$

At $T = -\infty$ this is zero, at $T = 0$, $\theta = \pi/2$ and at $T = \infty$ it is π. So by choosing an S^{D-2} at a certain radius on $\mathcal{I}^{\pm}$ we are basically taking the point of view of an observer who is in the middle of de Sitter space at a certain

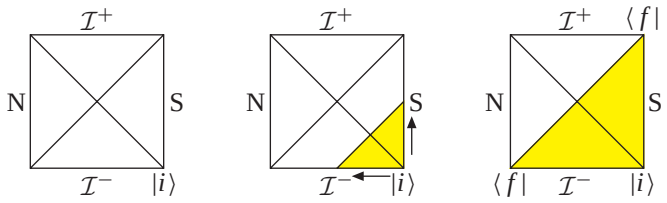

FIGURE 5.4: In the far past, an observer at the south pole might describe the state of the world by an initial state $|i\rangle$ on $\mathcal{I}^-$. The observer evolves in time until he reaches his final state $\langle f|$ on $\mathcal{I}^+$. The antipodal map relates this again to a state on $\mathcal{I}^-$. In- and out-states are therefore associated with a single surface, as in a conventional CFT.

time T. This is holography at work: we do not need to go to the interior of de Sitter space to describe time evolution, we do it at the boundary. Even in the quantum theory, since the metric near the boundary still looks like classical de Sitter space and we have the SO(1, D) de Sitter group acting, we can use the global time T to measure the distance from the scris to the poles.

Now, time translations increase the distance with respect to the north pole and decrease the distance to the south pole. In fact, this is precisely what scale transformations do. To see this, map the north pole patch to flat Euclidean space and similarly for a neighborhood of the south pole. Then the transition function that glues the two together is inversion, $\vec{x} \to \vec{y} = \vec{x}/|\vec{x}|^2$, which is a conformal transformation. But now note that scaling up in x is equivalent to scaling down in y, exactly like time translations in the bulk.

That time evolution in the bulk leads to scale transformations in the boundary was already emphasized by Strominger [121]. In planar coordinates covering, say, the causal past, the line element reads

$$ds^2 = -dt^2 + e^{-\frac{2t}{R}} dx^2 \tag{5.47}$$

and it follows that

$$t \to t + \lambda\,, \quad x \to e^{\frac{\lambda}{R}} x \tag{5.48}$$

is an isometry of the metric. Alternatively, one can use static coordinates in the upper or lower region of the Penrose diagram. The line element is

$$ds^2 = \left(\frac{r^2}{R^2} - 1\right) dt_s^2 - \frac{dr^2}{\frac{r^2}{R^2} - 1} + r^2 d\Omega_{D-2}^2 \tag{5.49}$$

and the 'Hamiltonian' $\partial/\partial t_s$ manifestly constitutes a Killing vector. In fact, it generates the same isometry as (5.48), as can be seen by transforming to

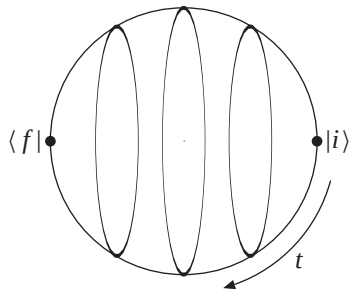

FIGURE 5.5: Radial quantization on an S^{D-1}. In-states and out-states are at antipodal points. The Hamiltonian is the dilation operator. Each surface corresponding to constant time for the observer in the bulk is an S^{D-2}.

$r = |\vec{x}| \exp(-t/R)$ and $t_s = t + \frac{1}{2}R \ln (r^2/R^2 - 1)$. From the metric it is clear that this is a spacelike vector, as indeed it should be since it now corresponds to dilations of the boundary sphere. We note that there is, however, an important difference between the patches covered by these coordinates and elliptic de Sitter space: the boundary of the inflationary patch has the topology $\mathbb{R}^{D-1}$, while elliptic de Sitter space has an S^{D-1}, which contains an extra point.

This leads to a nice picture of how an observer would view the CFT. Consider an observer in elliptic de Sitter space. By means of de Sitter transformations, the worldline of any inertial observer can be mapped to the time axis, say at the south pole. In the far past, such an observer would characterize the world by an in-state, $|i\rangle$. As in conventional CFT with radial quantization, we would like to assign incoming states to the origin. Here we choose the origin as the point where the observer's worldline intersects $\mathcal{I}^-$. Correspondingly, we insert the in-state at the south pole of the boundary sphere. As time passes, the observer moves vertically up the Penrose diagram. As we have seen this corresponds to a dilation on the sphere. Finally, in the far future, the observer describes the world by an out-state, $\langle f|$. This is where the elliptic interpretation comes in: the out-state is mapped to the antipodal point on the same S^{D-1} as the in-state; see Figure 5.4. For an inertial observer, the out-state is inserted precisely at the extra point (the north pole) that S^{D-1} has compared with $\mathbb{R}^{D-1}$. In a stereographic projection of the sphere to flat Euclidean space, the outgoing state would be at infinity. The corresponding situation on the boundary is depicted in Figure 5.5.

In conclusion, the $\mathbb{Z}_2$ identification implies that the holographic CFT is simply a theory with conventional radial quantization on an ordinary sphere. We will see, however, that the Hermiticity conditions of the theory are somewhat unusual.

5.5.2 THE EXISTENCE OF AN S-MATRIX AND HOLOGRAPHY

Defining an S-matrix for quantum gravity in global de Sitter space is tricky. The problem is that, having defined in- and out-states on two disconnected surfaces ($\mathcal{I}^-$ and $\mathcal{I}^+$), the only available pairing between them, CPT, is used merely to define an inner product [142]. Since in quantum gravity the spacetime between these two boundaries fluctuates, there does not seem to be another way to map states on $\mathcal{I}^-$ to $\mathcal{I}^+$. Hence it is not obvious how to define an S-matrix. If we consider only the quantum field theory of matter (and neglect back-reaction) with the geometry fixed, then we are able to define an S-matrix, but even then its matrix elements are not physically measurable, since no observer can determine the state at both $\mathcal{I}^-$ and $\mathcal{I}^+$, not even in the far future.

In elliptic de Sitter space the situation is different. The past and future asymptotic regions have been identified, so initial and final states can be defined in the same asymptotic region, where the fluctuations of the metric are set to zero. It is useful to think about the initial and final states in terms of the asymptotic boundary conditions of various fields, including the metric, in this single asymptotic region. As discussed in Section 5.5.1, an observer positioned at the south pole will use the asymptotic data on the southern hemisphere to define the in-state and the data on the northern hemisphere to define the out-state. First, to define an inner product one can use the canonical map from the south to the north pole which associates to a state $|\Psi_i\rangle$ its CPT conjugate state $\langle\Psi_i|$. Next, to define the S-matrix one uses the combined asymptotic data provided in the in- and out-states, $|\Psi_i\rangle$ and $\langle\Psi_f|$, as boundary conditions for the 'functional integral' over all fields in the bulk of the quantum de Sitter space. This produces a number that can then be identified with the S-matrix element $\langle\Psi_f|\Psi_i\rangle$.

We will now discuss how these S-matrix elements would possibly be described in a holographic description of de Sitter space. So let us suppose that elliptic de Sitter space allows a holographic description in terms of a dual theory, which for concreteness we assume to be a conformal field theory. Since there is only one asymptotic region one is dealing with a single Euclidean CFT living on a $D-1$-sphere, which one can think of as the S^{D-1} at $\mathcal{I}^+$ or $\mathcal{I}^-$. In a CFT, states can be defined using radial quantization. They are created by the action of some (local) operator at the origin:

$$|j\rangle = \mathcal{O}_j(0)|\text{vac}\rangle\,, \tag{5.50}$$

where we have used the operator-state correspondence. The state $|\text{vac}\rangle$ is the 'vacuum', by which we mean not necessarily a state of lowest energy (since energy is difficult to define in de Sitter space), but rather a de Sitter-invariant state. Similarly, we can define a final state as

$$\langle j| = \langle\text{vac}|\mathcal{O}_j^*(\infty)\,. \tag{5.51}$$

Notice that this also involves complex conjugation, since our $\mathbb{Z}_2$ map includes charge conjugation, C. Now we can define an inner product via

$$\langle \mathcal{O}_i^*(\infty)\mathcal{O}_j(0)\rangle_{S^{D-1}} \equiv \delta_{ij} \,. \tag{5.52}$$

This pairing of an operator with its CPT conjugate provides an inner product in the sense of being a map $\mathcal{H} \times \mathcal{H} \to \mathbb{C}$ that is linear in one argument and anti-linear in the other.

If indeed there is a CFT dual of (elliptic) de Sitter space, then intuitively one expects that interactions (and hence S-matrix elements) are encoded in the correlation functions and the operator product expansion. It is important to note that a CFT by itself does not have an S-matrix. Therefore, instead of studying just the asymptotic states, let us consider operator insertions at points other than the origin and infinity. There are an infinite number of such operators since we can associate an operator with every point on the sphere. So in principle one could define an infinite set of in-states by considering strings of operators acting on the in-vacuum,

$$|\Psi_i\rangle = \mathcal{O}_{j_1}(x_1)\ldots\mathcal{O}_{j_n}(x_n)|\text{vac}\rangle \,, \tag{5.53}$$

and similarly for the out-states. S-matrix elements are then expressed as correlation functions where part of the operators, those on the northern hemisphere, represent the in-state, while the operators on the southern hemisphere represent the out-state. Note, however, that not all of these states are independent, because there are operator product relations. For example, two operators $\mathcal{O}_i$ and $\mathcal{O}_j$ inserted at different points have an operator product relation of the form

$$\mathcal{O}_i(x_i)\mathcal{O}_j(x_j) = \sum_k \frac{c_{ij}^k}{|x_i - x_j|^{\Delta_i+\Delta_j-\Delta_k}}\mathcal{O}_k(x_j) \,. \tag{5.54}$$

Here, the sum on the right hand side includes (quasi-)primary operators as well as their descendants. If one allows descendants of arbitrary conformal dimension, then all operators can be moved to one preferred point by simply using the Taylor expansion. One natural way to reduce the redundancy in the states is to consider only quasi-primary operators. Note that since the conformal dimension of an operator corresponds to the energy as seen by an observer in de Sitter space, it is physically reasonable to consider only operators with conformal dimensions that are below a certain threshold. The number of (quasi-)primary fields below a certain conformal dimension is finite. It is natural to conjecture that this fact is related to the finiteness of the de Sitter entropy. However, note that when one allows the operators to be inserted at arbitrary points on the sphere, this still would give an infinite number of states. It may very well be that there are additional requirements that one has to impose, but without

a more definite and concrete theoretical foundation one can only guess what these requirements could be.

The most specific proposal that we have for the de Sitter 'S-matrix' is that it is given by the overlap of the initial and final states:

$$S_{fi} = \langle \Psi_f | \Psi_i \rangle \,, \tag{5.55}$$

where both $|\Psi_i\rangle$ and $\langle \Psi_f|$ are expressed, as in (5.53), in terms of (quasi-)primary operators with restricted conformal dimensions. Hence the S-matrix elements are simply given by the correlation functions of the boundary conformal field theory. This proposal is truly holographic, since the correlation function are computed in terms of the CFT at the boundary.

5.5.3 Observer complementarity

How do different observer interpret these S-matrix elements? In fact, the same operator insertions at the boundary are interpreted differently by different observers in the bulk. This is because the physical states defined above depend on the choice of origin. For any observer, the incoming states are those that correspond to insertions made on the hemisphere of which his origin forms the pole, while outgoing states are created by operator insertions on the opposite hemisphere. Different observers have different origins so this leads to different interpretations of a given set of operator insertions, *i.e.*, they divide them up differently into incoming and outgoing; this is observer complementarity.

Consider, for example, the situation indicated in Figure 5.6. A south pole observer would describe this as pair annihilation: an electron and a positron come in and annihilate to give a photon. On the other hand, a north pole observer, being antipodal to the south pole observer, would see the same events happening in a CPT mirror. In this case, it would describe the CPT-conjugate process of pair creation: an incoming photon decays into an electron and a positron. A third observer in between these two poles would see yet another situation, for example an incoming electron emitting a photon. It is important to realize that all these processes have the same amplitude.

5.5.4 A little group theory

A striking consequence of the preceding discussion is that, although the S-matrix is de Sitter-invariant, the in-states are not. De Sitter transformations that take one observer into another generically transform in-states into out-states and vice versa. Hence the asymptotic Hilbert space does not decompose into irreducible representations of the de Sitter group. This is important because there is a well-known theorem which states that (nontrivial) unitary

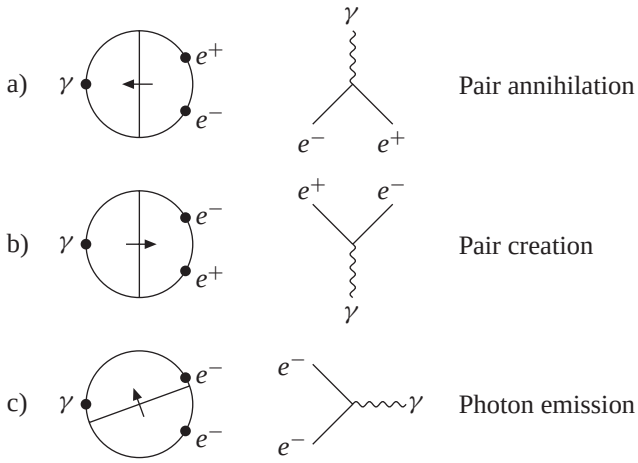

FIGURE 5.6: Complementarity in action: the same correlation function as interpreted by an observer (a) at the south pole, (b) at the north pole and (c) at an intermediate point. The circle denotes the sphere on which the dual theory lives, the dots are operator insertions, the arrow indicates the observer's direction of time and the equator divides the in-states from the out-states. On the right are the corresponding processes in spacetime.

representations of non compact groups must be infinite-dimensional. This theorem is in tension with the finiteness of the de Sitter entropy. If the de Sitter entropy enumerates the microscopic degrees of freedom underlying a quantum description of de Sitter space, then we would expect it to form a (possibly reducible) representation of some group. Were that group to be the non compact de Sitter group, $O(1, D)$, then the holographic theory could not be unitary. For elliptic de Sitter space, the entropy is presumably also given by the Bekenstein-Hawking formula:

$$S = \frac{A}{4} = \frac{\pi^{\frac{D-1}{2}} R^{D-2}}{4\Gamma\left(\frac{D-1}{2}\right)}, \tag{5.56}$$

where the 'area', A, is the volume of the horizon, which is now a $D-2$-dimensional real projective sphere, $\mathbb{R}P^{D-2}$. The important point is that this is again finite. But as we saw, the states in elliptic de Sitter space do not transform under representations of the full de Sitter group. Instead, they only transform under the subgroup that preserves the asymptotic position of an observer. Since in the asymptotic past an observer defines a point on a $D-1$-dimensional sphere and in the future a possibly different point on the same sphere, the relevant group

is actually SO($D-1$). We propose that the entropy of de Sitter space is related to representations of this compact group.

Another way to make the same point is the following. The Bekenstein-Hawking entropy refers to the area of a holographic screen bounding a given region of spacetime. For de Sitter space, a horizon is actually the holographic screen of a particular observer in the far future. But the screen accessible to any single observer must furnish a representation of the *little group* of that observer. This is precisely the rotation group SO($D-1$).

A given physical state is therefore labeled by its conformal weight, its angular momenta and the quantum numbers of any internal symmetries. Nevertheless it is still a great challenge to show that the number of such states is precisely $\exp A/4$. In principle, the conformal weights and angular momenta could be arbitrarily high, leading to representations that would be too big. One possibility might be to restrict the maximum scaling dimension

$$\Delta_i \leqslant \Delta_{\max} \tag{5.57}$$

of any state $|i\rangle$. Here the idea is that the scaling weight is the eigenvalue of the CFT Hamiltonian, but we know that energy in de Sitter space is bounded by the mass of the largest black hole that can fit within the de Sitter horizon. This suggests that we should only consider those states which have scaling dimension below some maximum.

5.6 On a String Realization

Our discussion of the elliptic interpretation of de Sitter space and its holographic implementation has been rather intuitive. Clearly, to make things more precise one needs a concrete realization of these ideas in a working theory of quantum gravity, such as string theory (or perhaps loop gravity [117]). It has been surprisingly hard to find a realization of de Sitter space in string theory. One obstacle to a satisfactory string-theoretic description of de Sitter space is the lack of supersymmetry. Intuitively, de Sitter space cannot be supersymmetric because it is thermal; at finite temperature bosons and fermions have different statistics. More formally, there is no superalgebra that contains the de Sitter isometry group and is represented by Hermitian supercharges. The known super-extensions of the de Sitter isometry group [99] involve nonpositive quadratic forms and have no unitary representations. This difficulty can be traced back to the fact that there is no globally-defined timelike Killing vector in de Sitter space and hence there is no positive-definite Hamiltonian, H. This same non-positive-definite nature shows up in attempts to construct de Sitter space using timelike T-duality and compactifications on non compact Euclidean manifolds [73,74]. The resulting gauged supergravity theories allow

de Sitter space as a solution but have ghosts, *i.e.*, fields with kinetic terms of the wrong sign.

The nature of these problems changes in elliptic de Sitter space, mainly because it is not a time-orientable space. In fact, we would like to believe that the only possible realization of de Sitter space in string theory is in its elliptic form. The cause of the failure to find a de Sitter solution in string theory, at least so far, may well be that one should perhaps have been looking at string backgrounds that are not time-orientable. Clearly, time-unorientability poses new challenges for string theory and it is not immediately obvious how it can be defined consistently [9]. In this respect, it is interesting that de Sitter space arises in type IIB* string theory [73,74], obtained from the usual IIB theory by a timelike T-duality, which can be thought of as a change of sign of the left- (or right-) moving part of the worldsheet scalar X^0, corresponding to time. Hence, after a T-duality it is as if the right- (or left-) movers go forward in time, while the left- (or right-) movers go backward in time. Perhaps this means that type IIB* string theory has to be quantized in a different way so that worldsheets and the spacetime background have to be time-unorientable. This may change the problem of ghost-like fields and perhaps solve it.

Now let us make some observations on the candidate conformal field theory dual of five-dimensional elliptic de Sitter space as suggested by its realization in IIB* string theory. The low-energy limit of IIB* theory is IIB* supergravity which has Dirichlet brane solutions that have purely spatial extent; they are called Ep-branes when their worldvolume is p-dimensional. Following Hull, we consider the near-horizon geometry of a stack of N E4-branes, which are the Euclidean analogues of the D3-branes of type IIB theory. The metric resembles that of the D3-brane,

$$ds^2 = H^{-\frac{1}{2}}(\rho) dx_\parallel^2 + H^{\frac{1}{2}}(\rho) dx_\perp^2 \,, \tag{5.58}$$

where $H(\rho)$ is the usual harmonic function,

$$H(\rho) = 1 + \frac{4\pi\alpha'^2 g N}{\rho^4} \,, \tag{5.59}$$

except that, because the branes are Euclidean, the transverse 'radius' also includes time:

$$\rho^2 = x_\perp^2 = \vec{x}^2 - t^2 \,. \tag{5.60}$$

The horizon is at $\rho = 0$. Now we would like to take the near-horizon limit. Since ρ depends on time, there are two ways we can approach the horizon, where ρ is timelike and where ρ is spacelike. For spacelike ρ the transverse geometry is

$$dx_\perp^2 = -dt^2 + d\vec{x}^2 = d\rho^2 + \rho^2 ds^2_{\mathrm{dS}_5} \,, \tag{5.61}$$

where $ds^2_{\mathrm{dS}_5}$ is the line element of five-dimensional de Sitter space. For timelike ρ we get instead

$$dx_\perp^2 = -d\rho^2 + \rho^2 ds^2_{H^5}\,, \tag{5.62}$$

where H^5 is the five-dimensional hyperbolic Lobachevsky plane (Euclidean anti-de Sitter space). In the near-horizon limit we drop the 1 in $H(\rho)$ to obtain, for spacelike ρ,

$$ds^2 = \left(\sqrt{4\pi\alpha'^2 gN}\,\frac{d\rho^2}{\rho^2} + \frac{\rho^2}{\sqrt{4\pi\alpha'^2 gN}}dx_\parallel^2\right) + \sqrt{4\pi\alpha'^2 gN}\,ds^2_{\mathrm{dS}_5}\,. \tag{5.63}$$

The geometry is therefore locally that of $H^5 \times \mathrm{dS}_5$. For timelike ρ we obtain

$$ds^2 = \left(\sqrt{4\pi\alpha'^2 gN}\,\frac{-d\rho^2}{\rho^2} + \frac{\rho^2}{\sqrt{4\pi\alpha'^2 gN}}dx_\parallel^2\right) + \sqrt{4\pi\alpha'^2 gN}\,ds^2_{H^5}\,. \tag{5.64}$$

This too is $\mathrm{dS}_5 \times H^5$. So again we get the same local geometry. However, there are some important differences between the two. For spacelike ρ, the branes are part of H^5 and de Sitter space is part of the transverse space; that is not what we want. For timelike ρ, the branes are part of de Sitter space and H^5 is transverse. So we should choose ρ to be timelike. The E4-branes are now on the boundary of de Sitter space, at $\mathcal{I}^\pm$. But note that there are two disconnected branches because in foliating Minkowski space into spacelike slices (which corresponds to timelike ρ) one can have $t > 0$ or $t < 0$. In order to have a connected geometry, we should really identify these two branches by making a $\mathbb{Z}_2$ identification. In that case the metric that we just described must be modded out by a $\mathbb{Z}_2$ that maps $t \to -t$. Since the line element on de Sitter space in (5.64) covers one inflationary patch, an identification of t and $-t$ suggests that the near-horizon geometry becomes $\mathrm{edS}_5 \times H^5$, elliptic de Sitter space times a hyperbolic five-plane. A $\mathbb{Z}_2$ identification of the transverse geometry implies that the E4-branes are on a T-orientifold, the purely spatial counterpart of a conventional orientifold. Indeed, elliptic de Sitter space is the analytic continuation of the $\mathbb{R}P^5$ that arises (instead of an S^5) in the transverse geometry of D3-branes on an orientifold plane.

The theory on the worldvolume of the E4-brane is Euclidean $\mathcal{N} = 4$ SYM. This theory is obtained from $\mathcal{N} = 1$ SYM in $D = 9+1$ by dimensional reduction, where one of the compactification directions is time. So one of the six scalars in the E4 worldvolume theory comes from the timelike component of the $9+1$-dimensional gauge field. This becomes a scalar with the wrong sign kinetic operator and therefore we are dealing with a conformal field theory with a ghost. In fact, there are several reasons to expect such ghost fields to

be present in a CFT dual to de Sitter space. First, the six scalars form a vector $(\phi_0, \vec{\phi})$ of the SO(1, 5) R-symmetry of the Euclidean theory; invariance under the R-symmetry already implies that one scalar has the wrong sign kinetic term. A second reason is the following.

Just as in the AdS/CFT correspondence, one expects the holographic direction to correspond to the RG-scale of the dual field theory. But unlike in AdS/CFT, the holographic direction is timelike in de Sitter space, as discussed in Section 4.4. This timelike nature of the RG-scale is directly related to the presence of the ghost scalar. Namely, the energy scale μ of the theory can be defined in terms of the values of the scalar fields as

$$\langle \vec{\phi}^2 - \phi_0^2 \rangle = \pm \mu^2 \,. \tag{5.65}$$

Let us now fix the energy scale μ. The scalar fields are then restricted to a five-dimensional scalar manifold. Here we have a choice: for the $-$ sign the resulting scalar manifold is the Lobachevsky plane, while for the $+$ sign it is de Sitter space. If we take the $+$ sign the ϕ_0 field still has fluctuations with the wrong sign. However, if we take the $-$ sign, all the fluctuations of the scalar field have the correct sign in their kinetic terms.

The parameter μ becomes the renormalization group scale and in fact is the same as the holographic time coordinate ρ: together with the four Euclidean coordinates on the E4-brane, it leads to de Sitter space. As we noted, the scalar manifold has two disconnected branches, corresponding to $\phi_0 > 0$ and $\phi_0 < 0$. Now here there is a difference between $U(N)$ and SO(N) SYM. In the latter case one can use the gauge symmetry to map ϕ to $-\phi$. This identifies the two branches of the scalar manifold. An SO(N) gauge group arises if we put N coincident E4-branes on top of a T-orientifold plane. This is precisely what we argued for earlier. In the near-horizon limit we get antipodally-identified de Sitter space. So finally, we come to the following conjecture: the large-N limit of SO(N) SYM theory, with conformal group SO(1, 5) and R-symmetry group SO(1, 5), in the phase described by the $-$ sign in the scalar equation is the holographic dual of edS$_5 \times H^5$. There is now only one boundary, an S^4, and that is the boundary on which the CFT lives.

5.7 Conclusion

In this chapter we studied de Sitter space in its elliptic interpretation with antipodal points identified. We discussed several conceptual issues in the context of the elliptic interpretation, especially questions regarding holography and the definition of an S-matrix. Our conclusions support the view that the antipodal identification does make sense and in fact may even be required to arrive at a consistent description of de Sitter quantum gravity. The arguments presented

in favor of the antipodal identification range from suggestive to rather compelling; they are not yet sufficient to claim that antipodal identification is the only way to view quantum de Sitter space.

From our point of view, the two most convincing arguments supporting the elliptic de Sitter space are the following. Firstly, the implementation of observer complementarity: all observers have complete information, but have different interpretations. And secondly, the realization of holography: for every observer time-evolution and the S-matrix are naturally described in terms of a dual theory on a single boundary. The most serious challenge elliptic de Sitter space will have to withstand is the issue of possible closed timelike curves after including backreaction. Once gravitational backreaction is taken into account, the Penrose diagram of perturbed de Sitter space becomes a 'tall' rectangle; see Section 4.1.1. This implies that certain antipodal points come into causal contact. The resulting closed timelike curves are contained in the bulk of de Sitter space and therefore it is not immediately obvious how it would affect the theory on the boundary. One point of view is that the perturbation of de Sitter space should be described by an appropriately perturbed CFT, for which the holographic reconstruction breaks down at some point in the bulk. The prescriptions for the time evolution of a single observer and for his observable S-matrix are defined purely in terms of the boundary and could still make sense. Clearly this issue needs further study.

Finally, the most pressing open issue is whether one can find a consistent description of de Sitter space in string theory, or perhaps in some other working theory of quantum gravity. There are many reasons to believe that such a description would be holographic and will incorporate a version of observer complementarity. We are hopeful that the ideas presented here will then be realized in some form.

REFERENCES

[1] A. Aguirre and S. Gratton, *Steady-state eternal inflation*, Phys. Rev. **D65** (2002) 083507, astro-ph/0111191.

[2] O. Aharony, S. S. Gubser, J. M. Maldacena, H. Ooguri, and Y. Oz, *Large N field theories, string theory and gravity*, Phys. Rept. **323** (2000) 183, hep-th/9905111.

[3] K. Akama, *An early proposal of 'brane world'*, Lect. Notes Phys. **176** (1982) 267, hep-th/0001113.

[4] A. Albrecht and P. J. Steinhardt, *Cosmology for grand unified theories with radiatively induced symmetry breaking*, Phys. Rev. Lett. **48** (1982) 1220.

[5] B. Allen, *Vacuum states in de sitter space*, Phys. Rev. **D32** (1985) 3136.

[6] E. Alvarez and C. Gomez, *Geometric holography, the renormalization group and the c- theorem*, Nucl. Phys. **B541** (1999) 441, hep-th/9807226.

[7] I. Aref'eva, *On the holographic S-matrix*, (1999), hep-th/9902106.

[8] V. Balasubramanian, J. de Boer, and D. Minic, *Mass, entropy and holography in asymptotically de Sitter spaces*, Phys. Rev. **D65** (2002) 123508, hep-th/0110108.

[9] V. Balasubramanian, S. F. Hassan, E. Keski-Vakkuri, and A. Naqvi, *A space-time orbifold: A toy model for a cosmological singularity*, Phys. Rev. **D67** (2003) 026003, hep-th/0202187.

[10] V. Balasubramanian, P. Horava, and D. Minic, *Deconstructing de Sitter*, JHEP **05** (2001) 043, hep-th/0103171.

[11] V. Balasubramanian and P. Kraus, *Spacetime and the holographic renormalization group*, Phys. Rev. Lett. **83** (1999) 3605, hep-th/9903190.

[12] T. Banks, *Cosmological breaking of supersymmetry or little Lambda goes back to the future. II*, (2000), hep-th/0007146.

[13] T. Banks and L. Mannelli, *De Sitter vacua, renormalization and locality*, (2002), hep-th/0209113.

[14] J. M. Bardeen, B. Carter, and S. W. Hawking, *The Four laws of black hole mechanics*, Commun. Math. Phys. **31** (1973) 161.

[15] J. D. Bekenstein, *Black holes and the second law*, Nuovo Cim. Lett. **4** (1972) 737.

[16] J. D. Bekenstein, *Black holes and entropy*, Phys. Rev. **D7** (1973) 2333.

[17] J. D. Bekenstein, *Generalized second law of thermodynamics in black hole physics*, Phys. Rev. **D9** (1974) 3292.

[18] J. D. Bekenstein, *A universal upper bound on the entropy to energy ratio for bounded systems*, Phys. Rev. **D23** (1981) 287.

[19] J. D. Bekenstein, *Is the cosmological singularity thermodynamically possible?*, Int. J. Theor. Phys. **28** (1989) 967.

[20] J. D. Bekenstein, *Entropy bounds and black hole remnants*, Phys. Rev. **D49** (1994) 1912, gr-qc/9307035.

[21] D. Bigatti and L. Susskind, *TASI lectures on the holographic principle*, (1999), hep-th/0002044.

[22] R. Blumenhagen, B. Kors, D. Lust, and T. Ott, *The standard model from stable intersecting brane world orbifolds*, Nucl. Phys. **B616** (2001) 3, hep-th/0107138.

[23] R. Bousso, *A covariant entropy conjecture*, JHEP **07** (1999) 004, hep-th/9905177.

[24] R. Bousso, *Holography in general space-times*, JHEP **06** (1999) 028, hep-th/9906022.

[25] R. Bousso, *Positive vacuum energy and the N-bound*, JHEP **11** (2000) 038, hep-th/0010252.

[26] R. Bousso, *Bekenstein bounds in de sitter and flat space*, JHEP **104** (2001) 35.

[27] R. Bousso, *The holographic principle*, Rev. Mod. Phys. **74** (2002) 825, hep-th/0203101.

[28] R. Bousso, A. Maloney, and A. Strominger, *Conformal vacua and entropy in de Sitter space*, Phys. Rev. **D65** (2002) 104039, hep-th/0112218.

[29] J. D. Brown and M. Henneaux, *Central charges in the canonical realization of asymptotic symmetries: an example from three-dimensional gravity*, Commun. Math. Phys. **104** (1986) 207.

[30] J. D. Brown and J. W. York, *Quasilocal energy and conserved charges derived from the gravitational action*, Phys. Rev. **D47** (1993) 1407.

[31] S. M. Carroll, *The cosmological constant*, Living Rev. Rel. **4** (2001) 1, astro-ph/0004075.

[32] B. Carter, *An axisymmetric black hole has only two degrees of freedom*, Phys. Rev. Lett. **26** (1970) 331.

[33] H. B. G. Casimir, *On the attraction between two perfectly conducting plates*, Kon. Ned. Akad. Wetensch. Proc. **51** (1948) 793.

[34] G. Chalmers, H. Nastase, K. Schalm, and R. Siebelink, *R-current correlators in N = 4 super Yang-Mills theory from anti-de Sitter supergravity*, Nucl. Phys. **B540** (1999) 247, hep-th/9805105.

[35] A. Chamblin and N. D. Lambert, *de Sitter space from M-theory*, Phys. Lett. **B508** (2001) 369, hep-th/0102159.

[36] N. A. Chernikov and E. A. Tagirov, *Quantum theory of scalar fields in de Sitter space-time*, Annales Poincare Phys. Theor. **A9** (1968) 109.

[37] M. Cvetic, G. Shiu, and A. M. Uranga, *Three-family supersymmetric standard like models from intersecting brane worlds*, Phys. Rev. Lett. **87** (2001) 201801, hep-th/0107143.

[38] S. R. Das and S. D. Mathur, *Excitations of D-strings, Entropy and Duality*, Phys. Lett. **B375** (1996) 103, hep-th/9601152.

[39] J. de Boer, E. Verlinde, and H. Verlinde, *On the holographic renormalization group*, JHEP **08** (2000) 003, hep-th/9912012.

[40] W. de Sitter, *On Einstein's theory of gravitation, and its astronomical consequences*, MNRAS **78**, no. 1 (1917).

[41] R. Dick, *Brane worlds*, Class. Quant. Grav. **18** (2001) R1, hep-th/0105320.

[42] M. R. Douglas, *Branes within branes*, (1995), hep-th/9512077.

[43] T. Dray and G. 't Hooft, *The gravitational shock wave of a massless particle*, Nucl. Phys. **B253** (1985) 173.

[44] W. Fischler, A. Kashani-Poor, R. McNees, and S. Paban, *The acceleration of the universe, a challenge for string theory*, JHEP **07** (2001) 003, hep-th/0104181.

[45] W. Fischler and L. Susskind, *Holography and cosmology*, (1998), hep-th/9806039.

[46] E. E. Flanagan, D. Marolf, and R. M. Wald, *Proof of classical versions of the Bousso entropy bound and of the generalized second law*, Phys. Rev. **D62** (2000) 084035, hep-th/9908070.

[47] S. Forste, *Strings, branes and extra dimensions*, Fortsch. Phys. **50** (2002) 221, hep-th/0110055.

[48] D. Z. Freedman, S. S. Gubser, K. Pilch, and N. P. Warner, *Renormalization group flows from holography supersymmetry and a c-theorem*, Adv. Theor. Math. Phys. **3** (1999) 363, hep-th/9904017.

[49] D. Z. Freedman, S. D. Mathur, A. Matusis, and L. Rastelli, *Correlation functions in the CFT(d)/AdS(d + 1) correspondence*, Nucl. Phys. **B546** (1999) 96, hep-th/9804058.

[50] S. Gao and R. M. Wald, *Theorems on gravitational time delay and related issues*, Class. Quant. Grav. **17** (2000) 4999, gr-qc/0007021.

[51] G. W. Gibbons, *The elliptic interpretation of black holes and quantum mechanics*, Nucl. Phys. **B271** (1986) 497.

[52] G. W. Gibbons and S. W. Hawking, *Action integrals and partition functions in quantum gravity*, Phys. Rev. **D15** (1977) 2752.

[53] G. W. Gibbons and S. W. Hawking, *Cosmological event horizons, thermodynamics, and particle creation*, Phys. Rev. **D15** (1977) 2738.

[54] W. D. Goldberger and M. B. Wise, *Modulus stabilization with bulk fields*, Phys. Rev. Lett. **83** (1999) 4922, `hep-ph/9907447`.

[55] M. B. Green, J. H. Schwarz, and E. Witten, *Superstring theory*, Cambridge University Press, Cambridge, UK, 1987 (2 vols).

[56] B. R. Greene, *The elegant universe: superstrings, hidden dimensions, and the quest of the ultimate theory*, Norton, New York, USA, 1999.

[57] D. J. Gross, *Two-dimensional QCD as a string theory*, Nucl. Phys. **B400** (1993) 161, `hep-th/9212149`.

[58] D. J. Gross and I. Taylor, Washington, *Two-dimensional QCD is a string theory*, Nucl. Phys. **B400** (1993) 181, `hep-th/9301068`.

[59] S. S. Gubser, *Non-conformal examples of AdS/CFT*, Class. Quant. Grav. **17** (2000) 1081, `hep-th/9910117`.

[60] S. S. Gubser, *AdS/CFT and gravity*, Phys. Rev. **D63** (2001) 084017, `hep-th/9912001`.

[61] S. S. Gubser, I. R. Klebanov, and A. M. Polyakov, *Gauge theory correlators from non-critical string theory*, Phys. Lett. **B428** (1998) 105, `hep-th/9802109`.

[62] S. S. Gubser, I. R. Klebanov, and A. A. Tseytlin, *String theory and classical absorption by three-branes*, Nucl. Phys. **B499** (1997) 217, `hep-th/9703040`.

[63] A. H. Guth, *The inflationary universe: a possible solution to the horizon and flatness problems*, Phys. Rev. **D23** (1981) 347.

[64] S. W. Hawking, *Gravitational radiation from colliding black holes*, Phys. Rev. Lett. **26** (1971) 1344.

[65] S. W. Hawking, *Particle creation by black holes*, Commun. Math. Phys. **43** (1975) 199.

[66] S. W. Hawking, *A brief history of time*, Bantam, New York USA, 1988.

[67] S. W. Hawking and G. F. R. Ellis, *The large scale structure of space-time*, Cambridge University Press, Cambridge, UK, 1973.

[68] S. W. Hawking and D. N. Page, *Thermodynamics of black holes in Anti-de Sitter space*, Commun. Math. Phys. **87** (1983) 577.

[69] S. Hellerman, N. Kaloper, and L. Susskind, *String theory and quintessence*, JHEP **06** (2001) 003, `hep-th/0104180`.

[70] M. Henningson and K. Skenderis, *The holographic Weyl anomaly*, JHEP **07** (1998) 023, `hep-th/9806087`.

[71] G. T. Horowitz and A. Strominger, *Black strings and P-branes*, Nucl. Phys. **B360** (1991) 197.

[72] C. D. Hoyle et al., *Sub-millimeter tests of the gravitational inverse-square law: A search for large extra dimensions*, Phys. Rev. Lett. **86** (2001) 1418, hep-ph/0011014.

[73] C. M. Hull, *Timelike T-duality, de Sitter space, large N gauge theories and topological field theory*, JHEP **07** (1998) 21, hep-th/9806146.

[74] C. M. Hull, *de Sitter space in supergravity and M theory*, JHEP **11** (2001) 012, hep-th/0109213.

[75] W. Israel, *Singular hypersurfaces and thin shells in general relativity*, Nuovo Cim. **B44S10** (1966) 1.

[76] W. Israel, *Event horizons in static vacuum space-times*, Phys. Rev. **164** (1967) 1776–1779.

[77] T. Jacobson, *Thermodynamics of space-time: The Einstein equation of state*, Phys. Rev. Lett. **75** (1995) 1260, gr-qc/9504004.

[78] Z. Kakushadze and S. H. H. Tye, *Brane world*, Nucl. Phys. **B548** (1999) 180, hep-th/9809147.

[79] N. Kaloper and A. D. Linde, *Cosmology vs. holography*, Phys. Rev. **D60** (1999) 103509, hep-th/9904120.

[80] Y. Kiem, H. Verlinde, and E. Verlinde, *Black hole horizons and complementarity*, Phys. Rev. **D52** (1995) 7053, hep-th/9502074.

[81] I. R. Klebanov, *World-volume approach to absorption by non-dilatonic branes*, Nucl. Phys. **B496** (1997) 231, hep-th/9702076.

[82] I. R. Klebanov, *TASI lectures: Introduction to the AdS/CFT correspondence*, (2000), hep-th/0009139.

[83] D. Klemm, *Some aspects of the de Sitter/CFT correspondence*, Nucl. Phys. **B625** (2002) 295, hep-th/0106247.

[84] E. W. Kolb and M. S. Turner, *The early universe*, Number 69 in Frontiers in physics. Addison-Wesley, Redwood City, USA, 1990.

[85] K. R. Kristjansson and L. Thorlacius, *Cosmological models and renormalization group flow*, JHEP **05** (2002) 011, hep-th/0204058.

[86] F. Larsen, J. P. van der Schaar, and R. G. Leigh, *de Sitter holography and the cosmic microwave background*, JHEP **04** (2002) 047, hep-th/0202127.

[87] F. Leblond, D. Marolf, and R. C. Myers, *Tall tales from de Sitter space. I: Renormalization group flows*, JHEP **06** (2002) 052, hep-th/0202094.

[88] A. D. Linde, *A new inflationary universe scenario: a possible solution of the horizon, flatness, homogeneity, isotropy and primordial monopole problems*, Phys. Lett. **B108** (1982) 389.

[89] K. Maeda, T. Koike, M. Narita, and A. Ishibashi, *Upper bound for entropy in asymptotically de Sitter space- time*, Phys. Rev. **D57** (1998) 3503, gr-qc/9712029.

[90] J. Maldacena, *The large N limit of superconformal field theories and supergravity*, Adv. Theor. Math. Phys. **2** (1998) 231, hep-th/9711200.

[91] J. M. Maldacena and C. Nunez, *Supergravity description of field theories on curved manifolds and a no go theorem*, Int. J. Mod. Phys. **A16** (2001) 822–855, hep-th/0007018.

[92] J. M. Maldacena and A. Strominger, *Statistical Entropy of Four-Dimensional Extremal Black Holes*, Phys. Rev. Lett. **77** (1996) 428, hep-th/9603060.

[93] B. McInnes, *Exploring the similarities of the dS/CFT and AdS/CFT correspondences*, Nucl. Phys. **B627** (2002) 311, hep-th/0110062.

[94] E. Mottola, *Particle creation in de Sitter space*, Phys. Rev. **D31** (1985) 754.

[95] S. G. Naculich, H. A. Riggs, and H. J. Schnitzer, *Two-dimensional Yang-Mills theories are string theories*, Mod. Phys. Lett. **A8** (1993) 2223, hep-th/9305097.

[96] M. Parikh, I. Savonije, and E. Verlinde, *Elliptic de Sitter space:* $dS/\mathbb{Z}_2$, Phys. Rev. **D67** (2003) 064006, hep-th/0209120.

[97] M. Perez-Victoria, *Randall-Sundrum models and the regularized AdS/CFT correspondence*, JHEP **05** (2001) 064, hep-th/0105048.

[98] S. Perlmutter et al., *Measurements of omega and lambda from 42 high-redshift supernovae*, Astrophys. J. **517** (1999) 565, astro-ph/9812133.

[99] K. Pilch, P. van Nieuwenhuizen, and M. F. Sohnius, *De Sitter superalgebras and supergravity*, Commun. Math. Phys. **98** (1985) 105.

[100] J. Polchinski, *Dirichlet-branes and Ramond-Ramond charges*, Phys. Rev. Lett. **75** (1995) 4724, hep-th/9510017.

[101] J. Polchinski, *String theory*, Cambridge University Press, Cambridge, UK, 1998 (2 vols).

[102] J. Polchinski, *S-matrices from AdS spacetime*, (1999).

[103] L. Randall and R. Sundrum, *An alternative to compactification*, Phys. Rev. Lett. **83** (1999) 4690, hep-th/9906064.

[104] L. Randall and R. Sundrum, *A large mass hierarchy from a small extra dimension*, Phys. Rev. Lett. **83** (1999) 3370, hep-ph/9905221.

[105] R. Rattazzi and A. Zaffaroni, *Comments on the holographic picture of the Randall-Sundrum model*, JHEP **04** (2001) 021, hep-th/0012248.

[106] A. G. Riess et al., *Observational evidence from supernovae for an accelerating universe and a cosmological constant*, Astron. J. **116** (1998) 1009, astro-ph/9805201.

[107] L. J. Romans, *Supersymmetric, cold and lukewarm black holes in cosmological Einstein-Maxwell theory*, Nucl. Phys. **B383** (1992) 395.

[108] V. A. Rubakov and M. E. Shaposhnikov, *Do we live inside a domain wall?*, Phys. Lett. **B125** (1983) 136.

[109] N. Sanchez, *Quantum field theory and the 'elliptic interpretation' of de Sitter space-time*, Nucl. Phys. **B294** (1987) 1111.

[110] N. Sanchez and B. F. Whiting, *Quantum field theory and the antipodal identification of black holes*, Nucl. Phys. **B283** (1987) 605.

[111] I. Savonije, *Observer complementarity in de Sitter space*, In *Proceedings of NATO advanced study institute*, Cargèse, 2002.

[112] I. Savonije and E. Verlinde, *CFT and entropy on the brane*, Phys. Lett. **B507** (2001) 305, hep-th/0102042.

[113] B. P. Schmidt et al., *The high-Z supernova search: measuring cosmic deceleration and global curvature of the universe using type Ia supernovae*, Astrophys. J. **507** (1998) 46, astro-ph/9805200.

[114] E. Schrödinger, *Expanding universes*, Cambridge University Press, Cambridge, UK, 1957.

[115] K. Sfetsos, *On gravitational shock waves in curved space-times*, Nucl. Phys. **B436** (1995) 721.

[116] E. Silverstein, *(A)dS backgrounds from asymmetric orientifolds*, (2001), hep-th/0106209.

[117] L. Smolin, *Quantum gravity with a positive cosmological constant*, (2002), hep-th/0209079.

[118] M. Spradlin, A. Strominger, and A. Volovich, *Les Houches lectures on de Sitter space*, hep-th/0110007.

[119] M. Spradlin and A. Volovich, *Vacuum states and the S-matrix in dS/CFT*, Phys. Rev. **D65** (2002) 104037, hep-th/0112223.

[120] C. R. Stephens, G. 't Hooft, and B. F. Whiting, *Black hole evaporation without information loss*, Class. Quant. Grav. **11** (1994) 621, gr-qc/9310006.

[121] A. Strominger, *The dS/CFT correspondence*, JHEP **10** (2001) 34, hep-th/0106113.

[122] A. Strominger, *Inflation and the dS/CFT correspondence*, JHEP **11** (2001) 049, hep-th/0110087.

[123] A. Strominger and C. Vafa, *Microscopic Origin of the Bekenstein-Hawking Entropy*, Phys. Lett. **B379** (1996) 99, hep-th/9601029.

[124] R. Sundrum, *Effective field theory for a three-brane universe*, Phys. Rev. **D59** (1999) 085009, hep-ph/9805471.

[125] L. Susskind, *The world as a hologram*, J. Math. Phys. **36** (1995) 6377, hep-th/9409089.

[126] L. Susskind, L. Thorlacius, and J. Uglum, *The Stretched horizon and black hole complementarity*, Phys. Rev. **D48** (1993) 3743, hep-th/9306069.

[127] L. Susskind and E. Witten, *The holographic bound in anti-de Sitter space*, (1998), hep-th/9805114.

[128] G. 't Hooft, *A planar diagram theory for strong interactions*, Nucl. Phys. **B72** (1974) 461.

[129] G. 't Hooft, *On the quantum structure of a black hole*, Nucl. Phys. **B256** (1985) 727.

[130] G. 't Hooft, *The black hole interpretation of string theory*, Nucl. Phys. **B335** (1990) 138.

[131] G. 't Hooft, *Dimensional reduction in quantum gravity*, (1993), gr-qc/9310026.

[132] E. A. Tagirov, *Consequences of field quantization in de Sitter type cosmological models*, Ann. Phys. **76** (1973) 561.

[133] K. Thorne, R. Price, and D. Macdonald, editors, *Black holes: the membrane paradigm*, Yale University Press, 1986, New Haven, USA.

[134] W. G. Unruh, *Notes on black hole evaporation*, Phys. Rev. **D14** (1976) 870.

[135] G. Veneziano, *Pre-bangian origin of our entropy and time arrow*, Phys. Lett. **B454** (1999) 22, hep-th/9902126.

[136] E. Verlinde, *Fusion rules and modular transformations in 2-D conformal field theory*, Nucl. Phys. **B300** (1988) 360.

[137] E. Verlinde, *On the holographic principle in a radiation dominated universe*, (2000), hep-th/0008140.

[138] E. Verlinde and H. Verlinde, *RG-flow, gravity and the cosmological constant*, JHEP **05** (2000) 034, hep-th/9912018.

[139] H. Verlinde, *Holography and compactification*, Nucl. Phys. **B580** (2000) 264, hep-th/9906182.

[140] S. Weinberg, *Gravitation and cosmology*, Wiley, 1972.

[141] S. Weinberg, *The cosmological constant problem*, Rev. Mod. Phys. **61** (1989) 1.

[142] E. Witten, *Quantum gravity in de Sitter space*, hep-th/0106109.

[143] E. Witten, *Bound states of strings and p-branes*, Nucl. Phys. **B460** (1996) 335, hep-th/9510135.

[144] E. Witten, *Anti-de Sitter space and holography*, Adv. Theor. Math. Phys. **2** (1998) 253, hep-th/9802150.

[145] E. Witten, *Anti-de Sitter space, thermal phase transition, and confinement in gauge theories*, Adv. Theor. Math. Phys. **2** (1998) 505, hep-th/9803131.

[146] A. B. Zamolodchikov, *Irreversibility of the flux of the renormalization group in a 2-D field theory*, JETP Lett. **43** (1986) 730.

SAMENVATTING

(Summary in Dutch)

De specialisatie binnen theoretische natuurkunde waartoe het in dit proefschrift beschreven onderzoek behoort is de hoge energie fysica. We beginnen deze samenvatting met een uitleg van wat hoge energie fysica is en hoe zij verschilt van de natuurkunde bij lagere energieën. Vervolgens gaan we in op het onderwerp dat momenteel de meeste aandacht trekt binnen de theoretische hoge energie fysica en welk het kader vormt voor het in dit proefschrift beschreven onderzoek, namelijk quantumgravitatie. De belangrijkste kandidaat voor een theorie van quantumgravitatie is de snaartheorie; we zullen deze theorie kort beschrijven. Tenslotte behandelen we het holografische principe en geven een korte samenvatting van het onderzoek dat in dit proefschrift wordt gepresenteerd. Uitgebreide introducties voor een breed publiek tot hoge energie fysica, en de snaartheorie in het bijzonder, worden gegeven in [56,66].

HOGE ENERGIE FYSICA

Zoals de naam al zegt houdt hoge energie fysica zich bezig met processen die met hoge energieën gepaard gaan. Dergelijke processen zijn onder te verdelen in drie categorieën. De eerste categorie wordt gevormd door processen tussen deeltjes die heel snel bewegen. We spreken dan van deeltjes met een hoge kinetische energie.

De tweede categorie omvat alle processen die op heel kleine afstandsschaal plaatsvinden. De relatie tussen kleine afstanden en hoge energieën is niet zo makkelijk uit te leggen. Om een idee te krijgen, kun je denken aan lichtdeeltjes, de zogenaamde fotonen. Deze fotonen kun je beschouwen als een trilling, waarbij de golflengte van de trilling korter wordt naarmate de kleur van het licht meer naar blauw neigt. Dit is uitgebeeld in Figuur S.1. Daarbij is het zo dat blauw licht een hogere energie heeft dan rood licht. We zien dus dat trillingen op een kleine afstandsschaal corresponderen met hoge energieën.

De derde en laatste categorie wordt gevormd door processen waarbij grote massa's een rol spelen. De relatie tussen massa en energie is gelegd door Einstein, middels zijn beroemde formule

$$E = M \cdot c^2 \,. \tag{1}$$

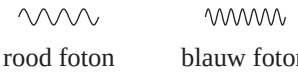

FIGUUR S.1: Links een rood foton en rechts een blauw foton. Het blauwe foton heeft een hogere energie en corresponderende kortere golflengte.

Deze formule, waarin c staat voor de lichtsnelheid, geeft aan dat massa en energie in feite hetzelfde zijn. Een grote massa correspondeert dus met hoge energie.

Al in de zeventiende eeuw is door Newton een theorie opgesteld om de beweging van objecten te beschrijven. Deze theorie is bijzonder nauwkeurig in het beschrijven van dynamica zoals die zich in het dagelijks leven voordoet. Hierbij kun je denken aan de beweging van een fiets of het opendoen van een deur. We noemen deze theorie de Newtoniaanse mechanica. Lange tijd werd aangenomen dat deze theorie ook geldig zou blijven bij heel hoge snelheden, of in het algemeen bij hoge energieën. Dit blijkt echter niet zo te zijn. In alle drie genoemde hoge energie regimes treden correcties op. Het feit dat de natuurkundige wetten afhankelijk zijn van het energieniveau vormt een belangrijk thema binnen de hedendaagse natuurkunde. De correcties die optreden zijn vaak tegen-intuïtief en dit maakt de moderne theorieën ingewikkeld.

Ter illustratie van de correcties die optreden bij hoge snelheden zullen we een auto vergelijken met een zeer snel bewegende raket. Stel, iemand loopt met een snelheid $v_{\text{voetganger}} = 5\,\text{km/uur}$ in de richting van een tegemoetkomende auto met een snelheid $v_{\text{auto}} = 60\,\text{km/uur}$, zoals weergegeven in Figuur S.2.

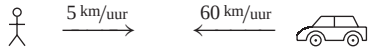

FIGUUR S.2: Voetganger en tegemoetkomende auto.

Als de voetganger de snelheid meet waarmee de auto op hem afkomt, wat we noemen de *relatieve* snelheid, vindt hij

$$v_{\text{relatief}} = v_{\text{voetganger}} + v_{\text{auto}} \tag{2}$$
$$= 5\,\text{km/uur} + 60\,\text{km/uur} = 65\,\text{km/uur}\,. \tag{3}$$

Deze uitkomst zal niemand verrassen. Beschouw nu eens het geval waar het in plaats van een auto een raket betreft. En niet zomaar een raket, maar eentje die met maar liefst 500.000.000 km/uur beweegt, ongeveer de helft van de lichtsnelheid; deze situatie is weergegeven in Figuur S.3. Op basis van onze intuïtie zouden we verwachten dat de relatieve snelheid in dit geval wederom simpelweg de som van de twee snelheden is. Dit is echter niet het geval. De juiste

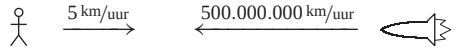

FIGUUR S.3: Voetganger en tegemoetkomende raket.

formule is afgeleid door Einstein en heeft de vorm

$$v_{\text{relatief}} = \frac{v_{\text{voetganger}} + v_{\text{raket}}}{1 + \frac{v_{\text{voetganger}} \cdot v_{\text{raket}}}{c^2}} \,. \tag{4}$$

Als we de waarde van de lichtsnelheid, $c = 1.079.252.849\,\text{km/uur}$, invullen, vinden we

$$\begin{aligned} v_{\text{relatief}} &= 500.000.003,93\,\text{km/uur} && (5)\\ &= 500.000.005\,\text{km/uur} - 1,07\,\text{km/uur}\,. && (6) \end{aligned}$$

Er is dus een kleine, maar daarom niet minder verrassende, correctie opgetreden waardoor het antwoord iets lager uitvalt dan verwacht. Nu is het helemaal niet mogelijk om raketten dergelijke enorme snelheden te geven, maar met bijvoorbeeld protonen is dit wel mogelijk. Het is belangrijk te benadrukken dat effecten zoals deze experimenteel zijn waargenomen. Blijkbaar gelden er bij hoge snelheden andere regels dan bij lage snelheden. Dit is een vaststelling waar weinig aan valt te begrijpen; het is een experimenteel feit. Het doel van de natuurkunde is om dit zo nauwkeuring mogelijk te beschrijven.

Einstein's beschrijving van processen bij extreem hoge snelheden heet speciale relativiteitstheorie. Deze theorie is uitgebreid getest en telkens weer blijken de uitkomsten die de theorie voorspelt, heel nauwkeurig overeen te komen met experimentele waarnemingen. De relatie van deze theorie met de Newtoniaanse mechanica wordt duidelijk als we het sommetje van de voetganger en de auto nogmaals uitvoeren, maar nu met de optelformule (4). De uitkomst die we vinden,

$$v_{\text{relatief}} = 65\,\text{km/uur} - 0,000000000000017\,\text{km/uur}\,, \tag{7}$$

wijkt zo weinig af van het Newtoniaanse resultaat (3) dat het verschil experimenteel niet vast te stellen is. Bij lage snelheden geeft speciale relativiteitstheorie dus dezelfde antwoorden als de Newtoniaanse mechanica. In deze zin is speciale relativiteitstheorie een *uitbreiding* van de Newtoniaanse mechanica die geldig blijft bij hoge snelheden. In het algemeen duiden we theorieën die geldig blijven bij hoge snelheden aan als 'relativistische' theorieën.

We hebben nu gezien dat er correcties optreden bij hoge snelheden. Dit gebeurt ook als we kijken naar heel korte afstanden. Er is bijvoorbeeld een groot verschil tussen hoe een elektron om een atoomkern draait en hoe de aarde om

de zon draait. De theorie die processen op de allerkleinste afstandsschalen beschrijft heet quantummechanica. De parameter van deze theorie die een vergelijkbare rol speelt als de lichtsnelheid, c, in relativiteitstheorie is de constante van Planck, die wordt aangegeven met $\hbar$.*

Bij grote massa's, tenslotte, treden correcties op doordat de zwaartekracht belangrijk wordt. De zwaartekracht is een relatief zwakke kracht, vergeleken met de andere natuurkrachten. Vergelijk bijvoorbeeld hoe moeilijk het kan zijn om twee magneetjes, die bijeen worden gehouden door de elektromagnetische kracht, uit elkaar te trekken met hoe makkelijk het is om die magneten op te tillen. En dat terwijl de hele aarde aan de magneten trekt via de zwaartekracht. Doordat de zwaartekracht zo zwak is kun je bij het beschrijven van een elektron dat rond een atoomkern draait de zwaartekracht buiten beschouwing laten. Natuurlijk trekken het elektron en de kern wel aan elkaar middels de zwaartekracht, maar deze kracht is zoveel kleiner dan de andere krachten die een rol spelen dat de invloed ervan te verwaarlozen is. Bij heel grote massa's, zoals die van de aarde en de zon, wordt de zwaartekracht wel belangrijk.† Newton heeft zijn theorie van de mechanica zelf gecombineerd met de zwaartekracht, resulterend in de zogeheten Newtoniaanse zwaartekrachtstheorie. De parameter die we met zwaartekracht associëren, de zogeheten constante van Newton, wordt aangegeven met G_{N}.

Nadat er aldus theorieën waren opgesteld die elk in één van de drie extreme regimes geldig blijven, probeerde men deze theorieën te combineren en zo te komen tot theorieën die in twee of zelfs alle drie regimes geldig blijven. Dit heeft geleid tot een totaal van acht theorieën. De relaties tussen deze theorieën kunnen handig worden weergegeven in een diagram met de vorm van een kubus, zoals in Figuur S.4. Op elke hoek van de kubus staat een theorie en langs de assen van de kubus wordt het geldigheidsbereik van de theorieën uitgebreid danwel beperkt.

Zoals gezegd, worden theorieën die geldig blijven bij hoge snelheden aangeduid met het woord 'relativiteit', het zijn zogenaamde relativistische theorieën. Theorieën die tot op de kleinste afstandsschalen werken duiden we aan met het woord 'quantum'. Beginnend bij de Newtoniaanse mechanica in Figuur S.4 kunnen we naar voren bewegen. De c geeft aan dat we dan belanden bij een relativistische theorie, namelijk de speciale relativiteitstheorie. Vervolgens naar rechts bewegen, brengt ons bij de algemene relativiteitstheorie, een theorie die niet alleen relativistisch is, maar ook de zwaartekracht beschrijft, aangegeven met G_{N}. Als we tenslotte naar boven bewegen, geeft de $\hbar$ aan dat we terecht komen bij een theorie die bovendien tot op de kleinste afstandsschalen geldig

*Spreek uit: h-streep.

†Hierbij speelt mee dat de aarde en de zon heel ver van elkaar verwijderd zijn. De zwaartekracht valt namelijk veel minder snel in kracht af bij grotere afstand tussen de objecten dan de overige krachten.

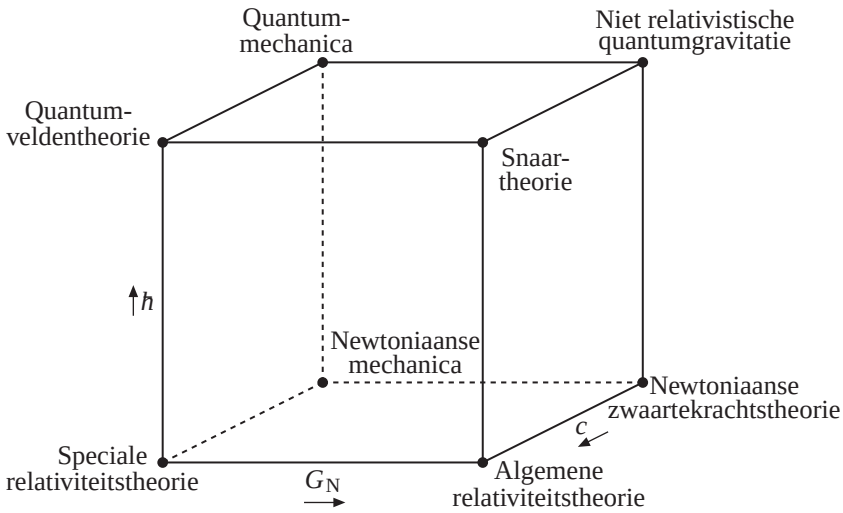

FIGUUR S.4: Aangegeven zijn de relaties tussen de verschillende natuurkundige theorieën. Naar voren bewegen in het diagram leidt naar een relativistische theorie die ook bij hoge snelheden nog correct blijft. Naar rechts bewegen voegt gravitatie, ofwel zwaartekracht, toe aan de theorie. Naar boven bewegen, tenslotte, leidt naar een quantum theorie die tot op zeer kleine afstandschalen geldig blijft.

blijft. Deze theorie, die alle drie de extreme regimes combineert, noemen we snaartheorie. Op deze theorie gaan we in het vervolg uitgebreider in.

QUANTUMGRAVITATIE

De snaartheorie verschilt op een aantal punten fundamenteel van de overige theorieën in Figuur S.4. Voordat we bespreken op welke manier de snaartheorie precies verschilt, bekijken we eerst de reden waarom het nodig was een geheel nieuwe theorie op te stellen.

Toen in de jaren twintig van de vorige eeuw de quantummechanica en de algemene relativiteitstheorie voldoende ontwikkeld waren, ging men op zoek naar een theorie van relativistische quantumgravitatie die op de plek zou moeten komen waar nu de snaartheorie staat in Figuur S.4. Hiertoe probeerde men de quantummechanica en de algemene relativiteitstheorie met elkaar te combineren. Bij deze pogingen stuitte men op fundamentele problemen, die we met een voorbeeld zullen proberen te illustreren.

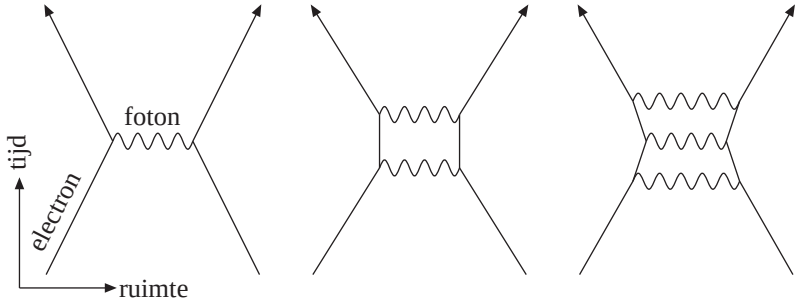

FIGUUR S.5: Twee elektronen stoten elkaar af door uitwisseling van één of meer fotonen.

Beschouw twee elektronen, deeltjes met een minieme massa en een negatieve elektrische lading. Als de elektronen dicht bij elkaar komen, stoten ze elkaar af via de elektromagnetische kracht. Volgens de quantummechanica kan deze interactie worden beschreven in termen van het quantum van de elektromagnetische kracht: het lichtdeeltje ofwel foton. Dit is de kleinst mogelijke drager van de elektromagnetische kracht. De elektronen kunnen één foton uitwisselen, maar ook meerdere, zoals aangegeven in Figuur S.5. Om uit te rekenen hoe de elektronen elkaar afstoten, schrijft de quantummechanica voor dat de bijdragen van elk van deze processen bij elkaar worden opgeteld. Nu kunnen de elektronen een of twee fotonen uitwisselen, maar ook tienduizend of honderdduizend. Om al deze verschillende bijdragen bij elkaar op te tellen is ondoenlijk. Gelukkig blijkt dat voor dit proces de bijdrage heel snel afneemt als er meer fotonen worden uitgewisseld. Het neemt zelfs zo snel af dat als je de eerste drie bijdragen bij elkaar optelt, je al heel dicht bij het werkelijke antwoord komt. Om de afstoting tussen twee elektronen uit te rekenen, is het daarom in de praktijk voldoende om slechts de uitwisseling van een paar fotonen te beschouwen.

Om de quantummechanica en de zwaartekracht met elkaar te verenigen, moeten we een nieuw quantumdeeltje invoeren: het graviton, het quantum van de zwaartekracht. Zoals de twee elektronen elkaar afstoten via de elektromagnetische kracht, trekken twee neutronen (deeltjes met massa, maar zonder elektrische lading) elkaar aan via de zwaartekracht. Dit proces kan op dezelfde manier worden beschreven als de afstoting van de elektronen, maar nu is het uitgewisselde quantum een graviton; zie Figuur S.6. Wederom schrijft de quantummechanica voor dat de bijdragen van de verschillende processen, waarbij een of meerdere gravitonen worden uitgewisseld, bij elkaar worden opgeteld. Tot zover lijkt er niets aan de hand. Het blijkt echter dat in dit geval de bijdrage niet afneemt als er meerdere gravitonen worden uitgewisseld. Inte-

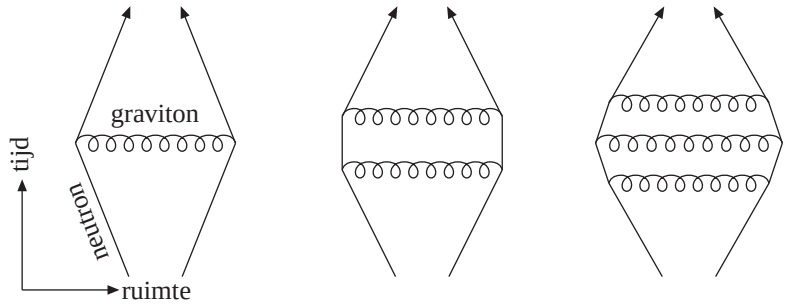

FIGUUR S.6: Twee neutronen trekken elkaar aan door uitwisseling van een of meer gravitonen.

gendeel, de bijdrage neemt alleen maar toe. Als je alle bijdragen op zou tellen krijg je oneindig. Het is duidelijk dat dit geen bruikbaar antwoord is. Dit is in essentie de reden waarom de quantummechanica en de zwaartekracht niet met elkaar te verenigen zijn.

Er bestaan dus twee theorieën, waarvan een (quantummechanica) processen op zeer kleine schaal beschrijft en de ander (algemene relativiteitstheorie) processen op zeer grote schaal. Beide theorieën werken bijzonder goed op het betreffende gebied. Pas als je probeert de ene theorie uit te breiden naar het terrein van de ander gaat het mis. Is er dan wel een noodzaak om op zoek te gaan naar een nieuwe theorie die beide verenigt? Dat die noodzaak wel degelijk bestaat komt doordat er situaties bestaan waar beide theorieën op natuurlijke wijze bij elkaar komen. Dit is met name het geval bij zwarte gaten. Zwarte gaten zijn zeer massieve objecten die ontstaan als de massadichtheid een bepaalde kritische grens overscheid; we komen hier later op terug. Door de enorme massa van zwarte gaten is de zwaartekracht heel sterk. Materie in de buurt van een zwart gat wordt daardoor sterk aangetrokken en zal naar het zwarte gat toe vallen. Zwarte gaten zijn zo zwaar dat zelfs licht er naartoe valt. Een zwart gat kan dan ook geen licht uitstralen; het zou terugvallen naar het zwarte gat. Vergelijk dit met een voetbal die, nadat je hem omhoog hebt geschoten, terugvalt naar de aarde. Dit alles tezamen leidt tot de naam ‘zwart gat’.[‡] Een gevolg van de sterke zwaartekracht is dat het zwarte gat zelf sterk wordt samengeperst, waardoor het heel kleine objecten zijn. Deze combinatie van een heel sterke zwaartekracht en een heel klein object zorgt ervoor dat zowel de quantummechanica

[‡]Hoewel een volledige, quantummechanische beschrijving van zwarte gaten nog niet gevonden is, hebben de pogingen daartoe al verrassende resultaten opgeleverd. Zo is gebleken dat het voor zwarte gaten quantummechanisch wel degelijk mogelijk is om straling uit te zenden. Deze, naar de ontdekker ervan vernoemde, Hawking straling zorgt ervoor dat een zwart gat niet helemaal zwart is; er wordt wel gesproken van ‘grijs-factoren’.

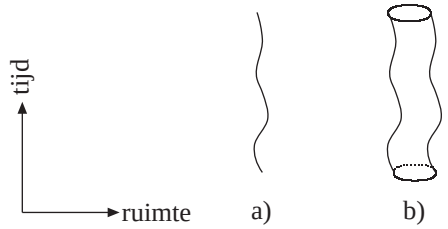

FIGUUR S.7: Een puntdeeltje tekent een lijn uit in een ruimte-tijd diagram, zoals bij (a). Een gesloten snaar tekent een cylinder uit, zoals bij (b).

als de zwaartekracht beiden een rol spelen. Maar, zoals we gezien hebben, gaat dit niet. Voor een goede beschrijving van zwarte gaten is daarom een theorie nodig die de quantummechanica en de zwaartekracht met elkaar verenigt. Zo'n theorie wordt een theorie van quantumgravitatie genoemd.

SNAARTHEORIE

De meest veelbelovende kandidaat voor een theorie van quantumgravitatie is de snaartheorie. Deze theorie is in de jaren zestig van de vorige eeuw ontwikkeld en verschilt fundamenteel van de andere theorieën. Het grote verschil ligt in de fundamentele bouwstenen van de theorie. Bij conventionele theorieën zijn dit 0-dimensionale puntdeeltjes, bij de snaartheorie 1-dimensionale objecten: de snaren waaraan de theorie zijn naam ontleent. Deze snaren kunnen zowel 'open' zijn, als korte touwtjes, of 'gesloten', als lusjes. We zullen ons hier beperken tot gesloten snaren. Het pad van een puntdeeltje en van een snaar in de ruimte-tijd zijn aangegeven in Figuur S.7. De theorie van deze snaren verenigt op een natuurlijke manier de zwaartekracht met de quantummechanica. Bovendien is het ook een relativistische theorie, die geldig blijft bij hoge snelheden. De snaartheorie geeft dus een beschrijving van de natuurwetten in alle drie extreme regimes, het wordt daarom wel een 'theorie van alles' genoemd. De correcties die door de snaartheorie voorspeld worden zijn klein en treden alleen op in extreme situaties, zodat het erg moeilijk is de theorie experimenteel te toetsen. Wiskundig vormt de snaartheorie echter een zó ingenieus bouwwerk, dat veel mensen die aan de theorie werken, ondanks het gebrek aan experimentele verificatie, geloven op de juiste weg te zijn.

De snaartheorie kent slechts één fundamentele bouwsteen: de snaar. Dit in tegenstelling tot de quantumveldentheorie, waar gebruik gemaakt wordt van een hele verzameling elementaire deeltjes, zoals elektronen, protonen en ga zo maar door. De rol van al deze deeltjes wordt binnen de snaartheorie gespeeld

door verschillende trillingstoestanden van de snaar. Hoe sneller de snaar trilt, des te zwaarder het corresponderende deeltje.

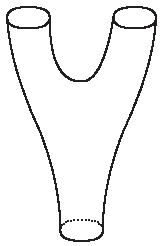

FIGUUR S.8: Splitsende snaar.

Dit leidt tot een sterk geünificeerde beschrijving van de natuur, waarbij er niet alleen slechts één fundamentele bouwsteen bestaat, maar tevens slechts één fundamentele interactie. Deze interactie behelst het opsplitsen van één snaar in twee snaren (of het omgekeerde proces, waarbij twee snaren samensmelten), zoals weergegeven in Figuur S.8. Zo reduceren de verschillende interacties tussen elektronen, neutronen, fotonen en gravitonen, weergegeven in Figuren S.5 en S.6, allemaal tot snaarinteracties. De geünificeerde beschrijving van interacties is een van de redenen dat de snaartheorie wiskundig heel mooi te beschrijven is. Het cruciale punt is dat het bij een snaarinteractie, zoals in Figuur S.8, niet mogelijk is exact aan te geven waar de interactie heeft plaatsgevonden. Eerst is er één snaar en tenslotte zijn er twee, maar deze overgang vindt niet plaats op één punt, zoals bij de interacties tussen fotonen en elektronen, of tussen gravitonen en neutronen. Dit 'uitsmeren' van de interactie zorgt er voor dat de uitkomsten van de snaartheorie niet oneindig worden, zoals we eerder zagen bij een theorie van quantumgravitatie die met puntdeeltjes werkt.

HET HOLOGRAFISCHE PRINCIPE

Een belangrijk concept binnen de snaartheorie is het holografische principe. Dit principe, dat oorspronkelijk een idee is van Gerard 't Hooft, speelt een hoofdrol binnen het in dit proefschrift beschreven onderzoek. Het beperkt zich niet tot de snaartheorie maar is noodzakelijkerwijs een onderdeel van elke theorie van quantumgravitatie.

Het holografische principe stelt dat er een limiet is op de hoeveelheid materie die past in een bepaald volume. De oorsprong hiervan is alsvolgt te begrijpen. Stel je een bolvormig volume voor, zoals de inhoud van een voetbal. Nu kun je proberen zoveel mogelijk materie in dit volume te stoppen. Op een gegeven moment, als je steeds maar meer materie toevoegt, zal zich een zwart gat vormen dat precies zo groot is als de voetbal. Als je vervolgens materie toevoegt aan dit zwarte gat, zal het groeien en daarmee groter worden dan de voetbal. Er past dus maar een bepaalde hoeveelheid materie in de voetbal. Dit betekent dat je materie niet onbeperkt samen kunt persen: er is een grens op de maximale materiedichtheid. Hiermee is er ook een grens op de hoeveelheid 'informatie' die de voetbal kan bevatten. Of, omgekeerd, er is maar een bepaalde, eindige hoeveelheid informatie nodig om de toestand van de voetbal te beschrijven.

Stel nu dat we de straal van de voetbal verdubbelen. Het volume van de voetbal neemt dan acht maal toe ($2^3 = 8$), terwijl het oppervlak van de voetbal vier keer zo groot wordt ($2^2 = 4$). Het bijzondere is dat de maximale hoeveelheid materie die in de grotere voetbal past vier keer zo groot is en dus groeit als het oppervlak en niet als het volume, zoals wel het geval is bij lage dichtheden. Dit is een voorbeeld van een correctie die optreedt bij grote massa. Een gevolg is dat alle informatie die nodig is om de toestand van de materie in de voetbal te beschrijven ook groeit als het oppervlak van de voetbal. In zekere zin kun je dan stellen dat je de toestand van de materie in de voetbal kunt beschrijven *op het oppervlak* van de voetbal. Dit is vergelijkbaar met een hologram waarbij op een 2-dimensionaal plaatje, 3-dimensionale informatie staat. Je kunt namelijk, door het hologram te draaien, zien welke objecten op de voorgrond staan en welke op de achtergrond.

Het doel van het in dit proefschrift beschreven onderzoek is om het holografische principe te gebruiken als toets voor kosmologische modellen. Er bestaan veel verschillende kosmologische modellen, die elk pogen de evolutie van het heelal te beschrijven. Op dit moment weten we niet welk model het beste is. Omdat het holografische principe een eigenschap is van iedere theorie van quantumgravitatie, zal het kosmologische model dat uiteindelijk het juiste blijkt te zijn, ermee verenigbaar moeten zijn. Door de huidige modellen hierop te toetsen kunnen we wellicht bepaalde modellen uitsluiten en aanwijzingen vinden in de richting van het juiste model.

Het proefschrift is alsvolgt opgebouwd. In Hoofdstuk 2 introduceren we het holografische principe in detail. Vervolgens passen we het in Hoofdstuk 3 toe op een specifiek geval van wat het standaard model van de kosmologie wordt genoemd. Dit is het Friendmann-Robertson-Walker (FRW) model. In het geval dat we beschouwen wordt de dynamica van het model uitsluitend gedreven door de aanwezige straling. Andere vormen van materie en energie worden buiten beschouwing gelaten, om het model zo simpel mogelijk te houden. Er treedt een verrassende unificatie op tussen enerzijds de formules die de energie beschrijven, in dit geval straling, en anderzijds de formules die de kosmologische evolutie beschrijven. We bestuderen deze unificatie nader binnen een zogeheten wereldbraan-model, waarin het universum wordt beschreven als een 4-dimensionaal oppervlak in een 5-dimensionale ruimte. In dit geval bevindt zich een zwart gat in de 5-dimensionale ruimte waarbinnen de wereldbraan beweegt. De unificatie blijkt een natuurlijke interpretatie te hebben in dit model. Hoewel de momenten waarop de unificatie plaatsvindt niet bijzonder lijken te zijn in de 4-dimensionale ruimte, zijn ze wel bijzonder in de 5-dimensionale ruimte. Het zijn namelijk precies de momenten waarop de wereldbraan het 5-dimensionale zwarte gat raakt.

In Hoofdstuk 4 richten we ons op een geheel ander kosmologisch model, namelijk het zogeheten de Sitter model. We richten ons met name op de vraag

hoe het holografische principe in dit model tot uiting komt. Er is de laatste tijd veel aandacht voor het de Sitter model omdat recente waarnemingen door astronomen erop duiden dat het heelal zich momenteel ontwikkelt in de richting van een de Sitter universum. Een groot probleem is dat het vooralsnog niet gelukt is om dit model binnen de snaartheorie te construeren.

In Hoofdstuk 5 presenteren we een voorstel voor een andere kijk op het de Sitter model binnen de snaartheorie. Het voorstel behelst om niet de gehele de Sitter ruimte te beschouwen maar slechts een deel, het zogeheten elliptische de Sitter. We tonen aan dat dit model zelf-consistent is. Daarbij is het vooral belangrijk te laten zien dat dingen die later gebeuren geen invloed kunnen hebben op gebeurtenissen eerder, het zogeheten causaliteitsprincipe. Binnen de elliptische de Sitter ruimte beschouwen we opnieuw de formulering van het holografische principe. Tevens beschouwen we de mogelijkheden om dit gereduceerde model te construeren binnen de snaartheorie. De belangrijkste conclusies van dit hoofdstuk zijn dat het holografische principe op een meer natuurlijke manier tot uiting komt in de elliptische de Sitter en dat veel van de problemen die zich voordoen bij het construeren van een de Sitter model binnen de snaartheorie verzacht worden. Het vinden van een complete snaarbeschrijving van de de Sitter ruimte blijft een openstaand probleem.

DANKWOORD

Alvorens dit proefschrift te besluiten zou ik graag diegenen bedanken die hebben bijgedragen aan de totstandkoming ervan. Ten eerste Erik, mijn promotor. Bedankt voor je begeleiding en voor de vele kansen die je mij hebt geboden. Het is leuk en ontzettend leerzaam om met je te werken. Daarbij wil ik jou en Mariëtte bedanken voor jullie gastvrijheid tijdens mijn bezoeken aan Princeton.

I would like to thank the Physics department at Princeton University for its hospitality. The periods I spent there were both interesting and enjoyable. Especially, I would like to thank Chang, Sameer and Marcus for discussing physics and other interesting subjects.

Also, I would like to thank Yang for a careful reading of the introduction to this thesis en Jelle voor een even zorgvuldige correctie van de Nederlandse samenvatting.

Dichter bij huis, zou ik de aio's van het Spinoza Instituut willen bedanken en met name mijn kamergenoten in het afgelopen jaar: Marijn en Jeroen.

Dank aan mijn ouders, mijn zus en mijn vrienden voor de getoonde interesse. En, tenslotte, aan Anneroos voor de steun en het geduld in de afgelopen vier jaar. Aan jou draag ik dit proefschrift op.

Utrecht, maart 2003

CURRICULUM VITAE

Ik ben geboren op 6 april 1975, te Haarlem. Na het behalen van het Gymnasium diploma aan het Stedelijk Gymnasium aldaar, ben ik in 1993 natuurkunde gaan studeren in Utrecht. In 1994 behaalde ik de propaedeutische examens natuurkunde en wiskunde. Vervolgens ben ik in 1998 afgestudeerd in de theoretische natuurkunde met het schrijven van een scriptie over zwarte gaten binnen de snaartheorie, onder begeleiding van Prof. Gerard 't Hooft. In de daaropvolgende vierenhalf jaar heb ik als promovendus onder begeleiding van Prof. Erik Verlinde aan het Spinoza Instituut onderzoek gedaan resulterend in dit proefschrift. In verband met Erik's vertrek naar Princeton heb ik in totaal ruim een jaar daar doorgebracht. Daarnaast heb ik conferenties en scholen bezocht in onder andere Berlijn, Cargèse, Corfu, Leuven, Mumbai, Parijs, Potsdam, Santa Barbara en Triëste en voordrachten gehouden over mijn werk in Amsterdam, Cargèse, Groningen en Princeton.